

Supplementary Information

Supported-amine Catalyzed Cascade Synthesis of Spiro-Thiazolone-Tetrahydrothiophenes: Assessing HSA Activity

Anshul Jain,^a Vinay K. Yadav,^b Akanksha Kumari,^a Suman K. Saha,^a Ramesh K. Metre,^a Sudipta Bhattacharyya,^{*,b} Nirmal K. Rana,^{*,a}

^aDepartment of Chemistry, Indian Institute of Technology Jodhpur, Rajasthan-342030, India

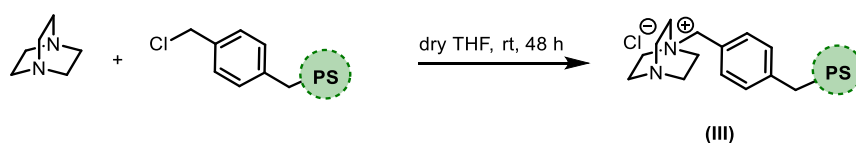
^bDepartment of Bioscience and Bioengineering, Indian Institute of Technology Jodhpur, Rajasthan-342030, India

Sr No.	Table of Contents	Page No.
1.	General information	S2
2.	Synthesis of polymer supported DABCO (PS-DABCO) catalyst	S3
3.	Optimization of reaction solvent	S3
4.	General procedure for diethylaminomethyl-polystyrene catalysed cascade thia-Michael/aldol/esterification of α,β -unsaturated thiazolones 3a-v	S4-8
5.	General procedure of synthetic transformation 4a , and 5a	S8-9
6.	Characterization data of compounds 3a-v , 4a , and, 5a	S9-16
7.	¹ H, and ¹³ C NMR spectra	S17-41
8.	X-ray crystal structure of 3f	S42
9.	Bio-study of spirothiazolono-THTs	S43-47
10.	References	S48

1. General Information

Unless otherwise noted, all reactions were carried out in closed vial. ^1H NMR spectra was recorded on a 500 MHz spectrometer (125 MHz for ^{13}C NMR). The following abbreviations were used to designate chemical shift multiplicities: s = singlet, d = doublet, t = triplet, q = quartet, m = multiplet. TLC was performed with silica gel GF₂₅₄ precoated on aluminium plates and spots were visualized with UV. Flash column chromatography was performed on silica gel with the use of CombiFlash. IR spectra were recorded on a FT-IR spectrometer and only major peaks were reported in cm^{-1} . High resolution mass spectra (HRMS) were obtained by the ESI-TOF method. Melting points were recorded on a digital melting point apparatus. 2-aryl-5-(arylmethylene)thiazol-4(5*H*)-one **1** derivatives were prepared according to the reported methods.¹ All the other reagents were purchased from commercial sources and used as received, unless specified. The polystyrene supported catalyst **I** (4-(dimethylamino)pyridine, polymer-bound); extent of labelling: ~3.0 mmol/g DMAP loading, matrix crosslinked with 2% DVB purchased from Sigma Aldrich. The polystyrene supported catalyst **II** (1,8-diazabicyclo[5.4.0]undec-7-ene, polymer-bound, 100-200 mesh); extent of labelling: 1.5-2.5 mmol/g loading, 1 % cross-linked with divinylbenzene purchased from Sigma Aldrich. The supported catalyst **IV** (diethylaminomethyl-polystyrene, 200 - 400 mesh); extent of labelling: ~3.2 mmol/g loading, purchased from Sigma Aldrich. The polystyrene supported catalyst **V** (diisopropylamine, polymer-bound 100-200 mesh); extent of labelling: 2.0-3.5 mmol/g loading, 1% cross-linked with divinylbenzene purchased from Sigma Aldrich. Chloromethyl Polystyrene Resin cross-linked with 1% DVB (100-200 mesh) (2.0-3.0mmol/g) purchased from TCI chemicals.

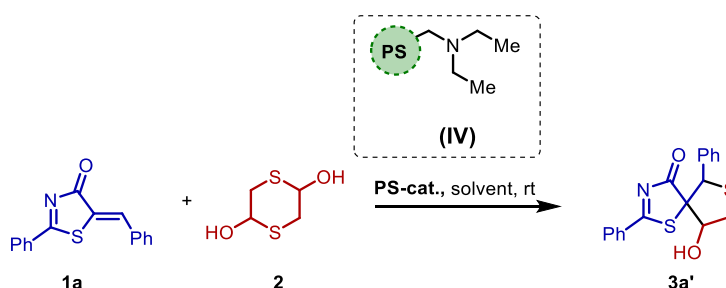
2. Synthesis of polymer-supported DABCO (PS-DABCO) catalyst



Merrifield resin (2.5 mmol, 1 g; 2.5 mmol/g Cl-content) was added slowly in the solution of DABCO (12.5 mmol, 1.35 g) in dry THF under inert atmosphere. The reaction was monitored by TLC. After the complete consumption of DABCO, solid was filtered and washed with acetone to afford PS-DABCO catalyst. [Elemental analysis of **III** (%) = C 73.69, H 8.41, N 4.67; $f = 1.67$ mmol/g]

3. Optimization of reaction solvent

Table S1 Initial optimization of cascade thia-Michael/aldol reaction^a



entry	solvent	time (h)	yield ^b (%)	dr ^c
1	toluene	12	97	80:20
2	EtOAc	10	95	77:23
3	CH ₂ Cl ₂	14	75	66:34
4	H ₂ O	48	65	71:29
5	CH ₃ CN	7	70	77:23
6	<i>m</i> -xylene	48	25	50:50
7	Methanol	48	Not formed	-
8	DMF	48	55	-
9	DMSO	48	50	-
10 ^d	toluene	6	89%	73:27

^aReaction conditions: **1a** (0.1061 g, 0.4 mmol), **2** (0.0365 g, 0.24 mmol), **PS-cat.** (0.02 mmol), toluene (2 mL), unless specified. ^bIsolated yield. ^cDiastereomeric ratio for all entries were determined by ¹H NMR analysis of crude reaction mixture. ^dthe reaction was carried out at 50 °C.

(which is the supported catalyst **IV**) was filtered and the residue was washed with EtOAc (20 mL) and CH₂Cl₂ (20 mL). The combined filtrate was concentrated under a vacuum to get the crude product. The crude mixture was then purified by flash chromatography on silica support (hexane/ethyl acetate = 5:1) to afford the pure product **3** (1.41 gm, 98%, >20:1 dr).

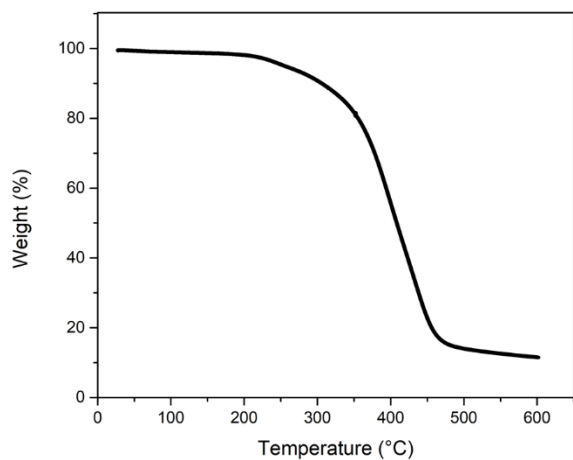
The recovered supported-amine catalyst **IV** was washed with water (3x10 ml), acetone (3x10 ml), hexane (3x10 ml), CH₂Cl₂ (3x10 ml), acetone (3x10 ml) respectively and dried under vacuum to give light brown beads and reused for the next cycle.

Table S2: Recycling of diethylaminomethyl-polystyrene **IV for the synthesis of **3a****

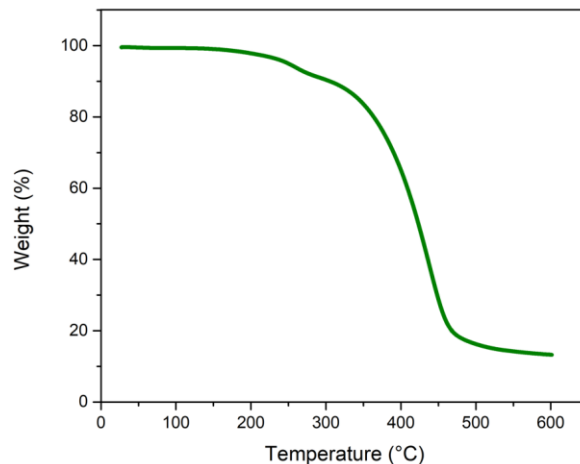
Cycle	Weight of Product 3aa (g)	Yield (%)	Polymer Weight (mg)	Polymer Loss (mg)	% Recovery of Polymer
1	1.419	98	353.4	1.2	99.7
2	1.415	98	352.2	1.4	99.6
3	1.392	96	350.8	1.7	99.5
4	1.381	95	349.1	2.2	99.4
5	1.365	94	346.9	1.4	99.6
6	1.350	93	345.5	2.1	99.4
7	1.346	93	343.4	1.2	99.7
8	1.342	93	342.2	1.1	99.7
9	1.319	91	341.1	1.5	99.6
10	1.315	91	339.6	1.4	99.6
11	1.312	91	338.2	1.9	99.4
12	1.300	90	336.3	2.1	99.4
13	1.281	89	334.2	1.4	99.6
14	1.265	88	332.8	1.7	99.5
15	1.262	87	331.1	2.0	99.4
16	1.258	87	329.1	0.9	99.7
17	1.250	86	328.2	1.8	99.5
18	1.246	86	326.4	1.4	99.6
19	1.246	86	325.0	1.7	99.5
20	1.242	86	323.3	1.3	99.6
21	1.239	86	322.0	1.9	99.4

^a% of recovered polymer = (Polymer Weight – Polymer loss) / Polymer Weight.

Thermogravimetric analysis (TGA) of diethylaminomethyl-polystyrene IV



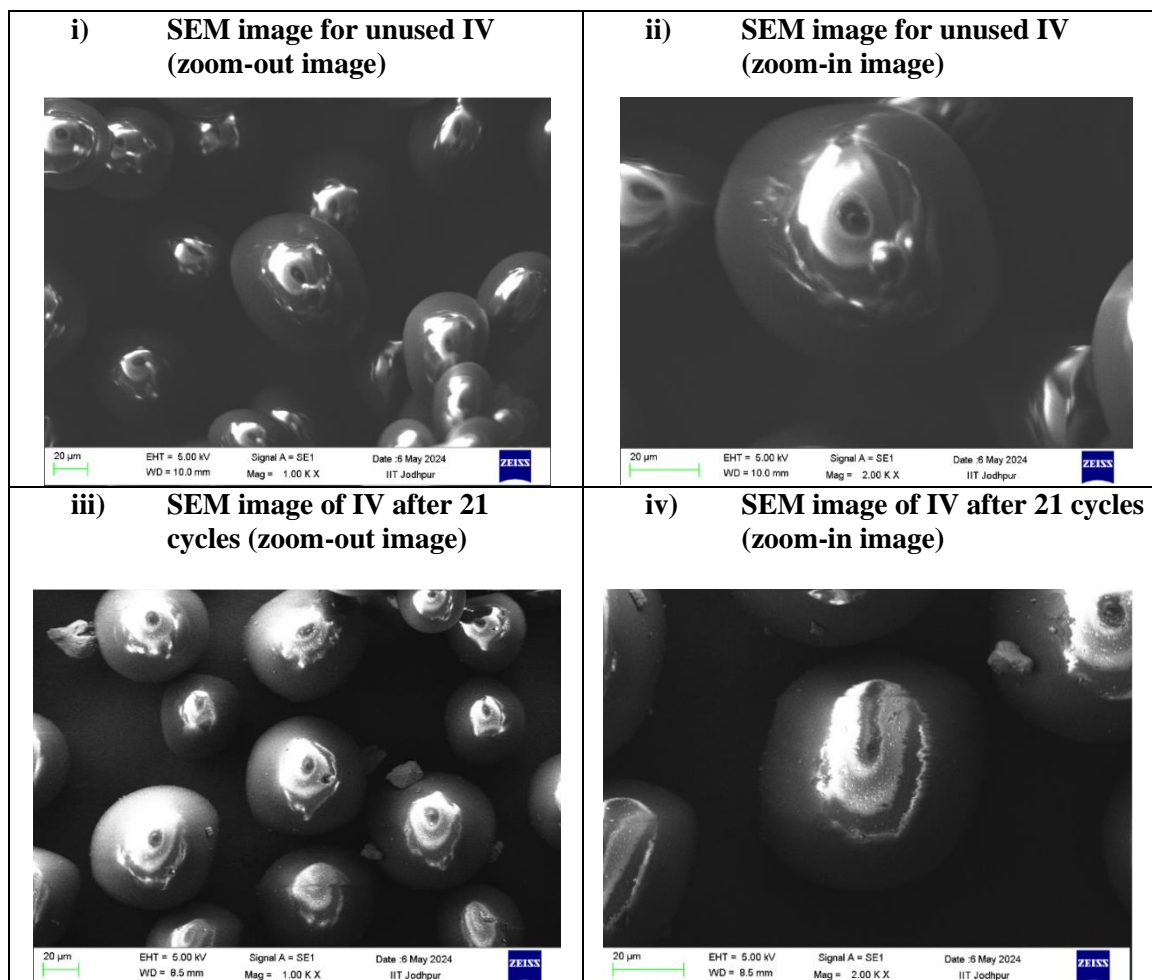
a) TGA graph for unused IV



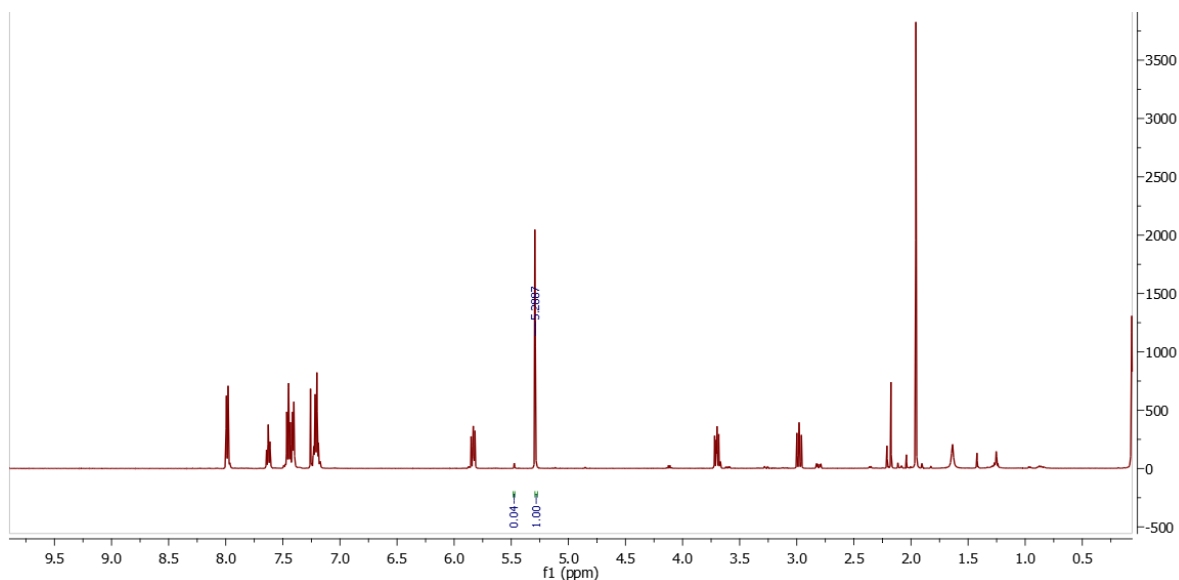
b) TGA graph of IV after used in 21 cycles

TGA analysis of diethylaminomethyl-polystyrene IV reveals that the polymer thermal stability has not been affected even after used in 21 cycles for the reaction to construct sTTHT 3a

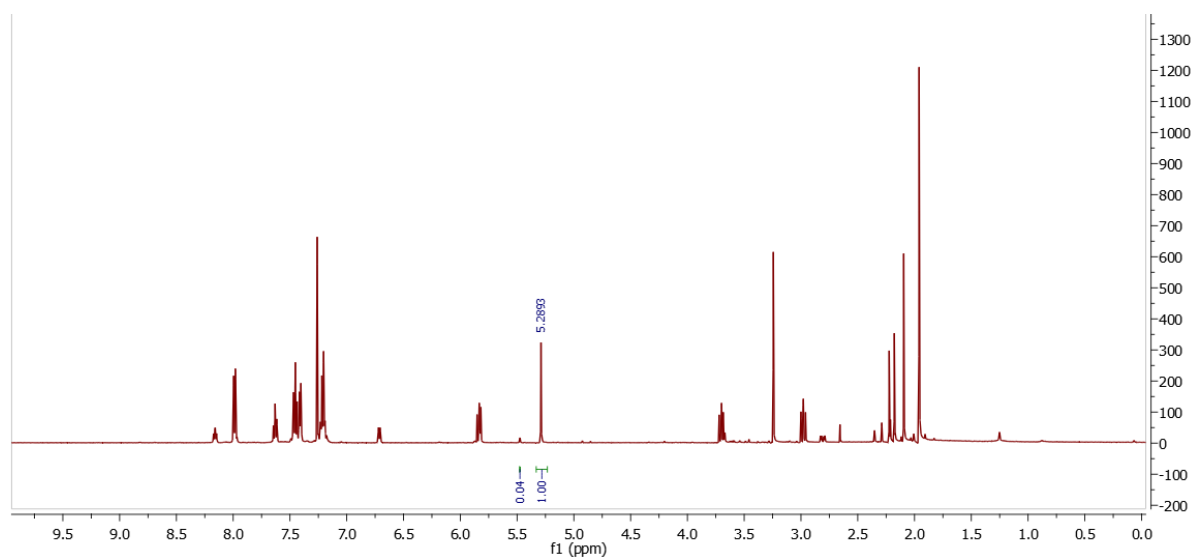
Scanning Electron Microscope (SEM) images of diethylaminomethyl-polystyrene IV



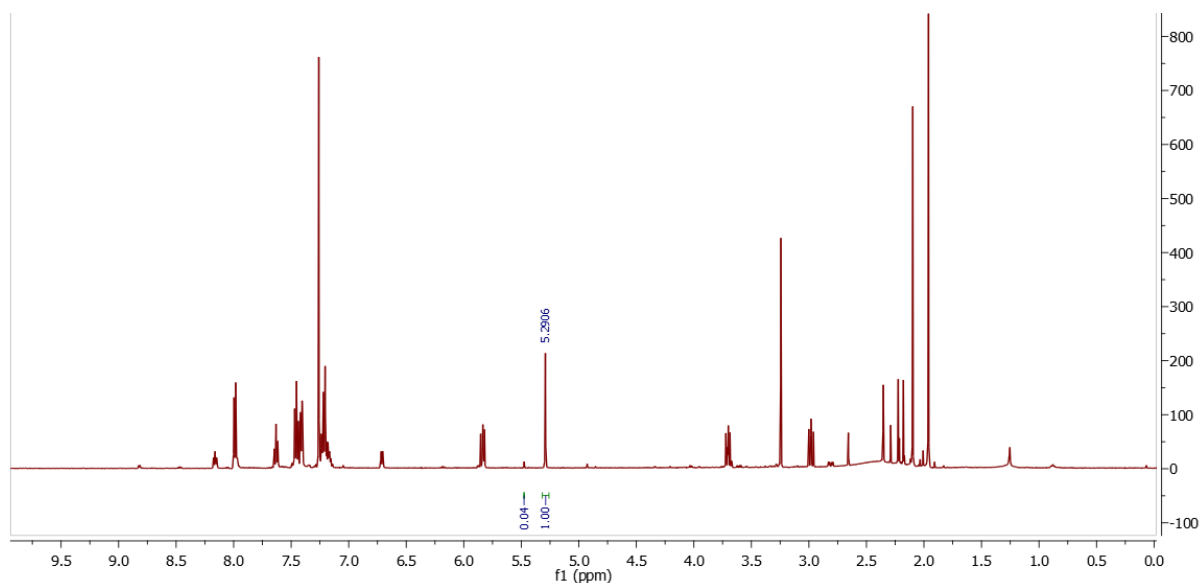
SEM images (i) and (ii) are the SEM images taken for the unused polystyrene supported catalyst **IV** while (iii) and (iv) represent the recovered base catalyst after the 21st cycle. It can be seen that there are no significant changes occur at the surface of the catalyst after 21 cycles represented here. However, after performing several reaction cycles, there are some minor impurities attached to the surface of the catalyst. This may be attributed to the regular use of the same polymer for several times. Although the efficiency has not been compromised after 21 cycles. The diastereomeric ratio has been unchanged as shown in the ¹H NMR spectra of crude reaction mixture of **3a** below. The crude reaction mixture was taken after filtration of supported catalyst **IV**. The attached ¹H NMR spectra of crude reaction mixture support the evidence of the reusability and efficiency of the catalyst **IV**.



Cycle 1: 500 MHz ¹H NMR of crude reaction mixture of **3a** (>20:1 dr)



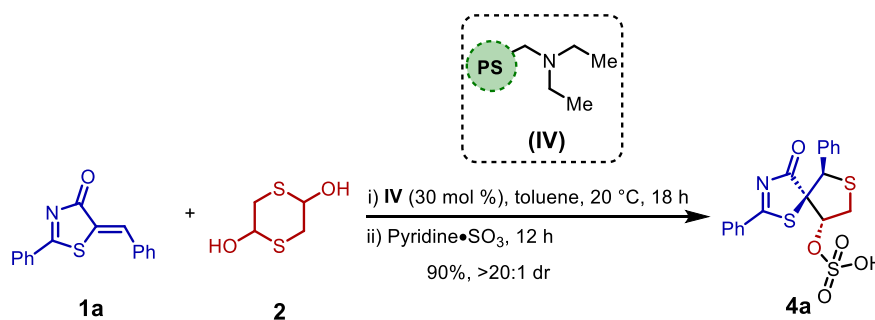
Cycle 10: 500 MHz ¹H NMR of crude reaction mixture of **3a** (>20:1 dr)



Cycle 21: 500 MHz ^1H NMR of crude reaction mixture of **3a** (>20:1 dr)

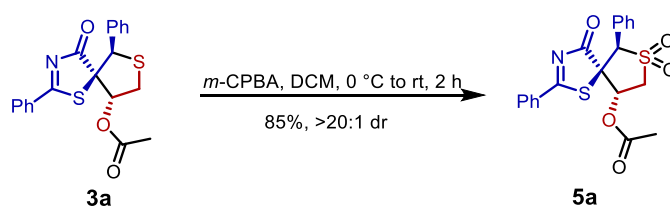
5. General procedure of synthetic transformation **4a**, and **5a**

Synthesis of 4-oxo-2,6-diphenyl-1,7-dithia-3-azaspiro[4.4]non-2-en-9-yl hydrogen sulfate **4a**:



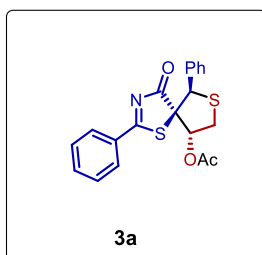
1,4-Dithiane-2,5-diol (0.24 mmol, 36.5 mg) **2** and diethylaminomethyl-polystyrene (N-content 3.2 mmol/gm) **IV** (30 mol %, 0.12 mmol, 37.5 mg) were added in the solution of 5-benzylidene-2-phenylthiazol-4(5*H*)-one **1a** (0.4 mmol) in dry toluene (2 mL). The reaction mixture was stirred at 20 °C and reaction was monitored by TLC. After the reaction was completed, pyridine sulphur trioxide complex (0.6 mmol, 95.5 mg) was added to reaction mixture and stirred for 12 h. After the filtration concentrated under reduced pressure and crystallized with ethanol and water. The desired product **4a** was obtained in 90% yield (151.7 mg).

Synthesis of 7,7-dioxido-4-oxo-2,6-diphenyl-1,7-dithia-3-azaspiro[4.4]non-2-en-9-yl acetate **5a**:



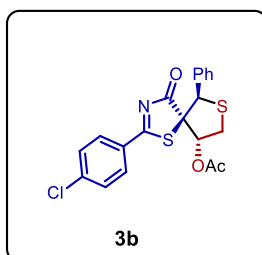
Substituted spiro thiazolono/tetrahydrothiophene **3a** (0.4 mmol, 153.4 mg) was dissolved into CH₂Cl₂ at 0 °C and *m*-CPBA (70% purity, 0.88 mmol, 217.0 mg) was added. The ice-bath was removed and the mixture was stirred for 2 h at room temperature. The mixture was diluted with CH₂Cl₂ and washed with a mixed aqueous solution of NaHCO₃ and Na₂SO₃. The organic layer was separated, dried over Na₂SO₄, and concentrated under reduced pressure and purified by silica gel column to afford compound **5a** as a white solid, yield 85%, (141.3 mg).

6. Characterization data of compounds **3a-v**, **4a**, and **5a**



4-oxo-2,6-diphenyl-1,7-dithia-3-azaspiro[4.4]non-2-en-9-yl acetate (**3a**):

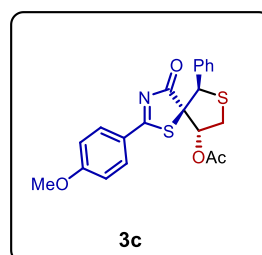
White solid, Yield = 98% (150.3 mg); ¹H NMR (500 MHz, CDCl₃) δ 7.99 (dd, *J* = 8.3, 1.1 Hz, 2H), 7.63 (t, *J* = 7.5 Hz, 1H), 7.46 – 7.42 (m, 4H), 7.25 – 7.15 (m, 3H), 5.83 (dd, *J* = 9.5, 7.3 Hz, 1H), 5.29 (s, 1H), 3.70 (dd, *J* = 10.6, 7.3 Hz, 1H), 3.02 – 2.93 (m, 1H), 1.96 (s, 3H); ¹³C NMR (125 MHz, CDCl₃) δ 196.21, 190.00, 169.52, 135.53, 133.30, 131.94, 129.28, 129.12, 129.03, 128.95, 128.29, 81.00, 80.16, 54.24, 32.83, 20.76; IR (ATR): ν 3060, 3028, 2924, 2855, 1750, 1715, 1600, 1506, 1482, 1447, 1372, 1313, 1251, 1211, 1176, 1117, 1058 cm⁻¹; HRMS (ES⁺) calc. for C₂₀H₁₈NO₃S₂ [M+H]⁺: 384.0723, found: 384.0713; M.P. 111-113 °C



4-oxo-6-phenyl-2-(4-(chloro)phenyl)-1,7-dithia-3-azaspiro[4.4]non-2-en-9-yl acetate (**3b**):

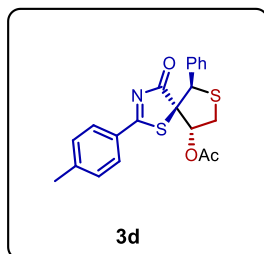
White solid, Yield = 90% (150.5 mg); ¹H NMR (500 MHz, CDCl₃) δ 7.93 – 7.85 (m, 2H), 7.50 – 7.47 (m, 2H), 7.43 – 7.40 (m, 2H), 7.27 – 7.20 (m, 3H), 5.87 (dd, *J* = 5.1, 1.9 Hz, 1H), 5.47 (s, 1H), 3.60 (dd, *J* = 12.4, 5.1 Hz, 1H), 3.27 (dd, *J* = 12.4, 2.0 Hz, 1H), 2.21 (s, 3H); ¹³C NMR (125 MHz, CDCl₃) δ 191.86, 187.80, 169.85, 142.11, 133.87, 130.24, 130.14, 129.69, 129.51, 128.86, 128.48, 81.49, 80.37, 55.56, 36.58, 21.07; IR (ATR): ν 3061, 2989, 2945, 2887, 1755, 1723, 1594, 1509, 1484, 1404, 1262, 1219, 1179, 1093, 1061 cm⁻¹; HRMS (ES⁺) calc. for C₂₀H₁₇ClNO₃S₂ [M+H]⁺: 418.0333, found: 418.0335; M.P. 202-204 °C.

2-(4-methoxyphenyl)-4-oxo-6-phenyl-1,7-dithia-3-azaspiro[4.4]non-2-en-9-yl acetate (**3c**):

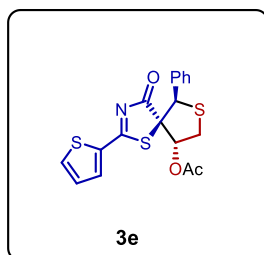


White solid, Yield = 89% (147.2 mg); ¹H NMR (500 MHz, CDCl₃) δ 7.97 (d, *J* = 8.9 Hz, 2H), 7.47 – 7.34 (m, 2H), 7.24 – 7.10 (m, 3H), 6.92 (d, *J* = 8.9 Hz, 2H), 5.82 (dd, *J* = 9.5, 7.3 Hz, 1H), 5.28 (s, 1H), 3.87 (s, 3H), 3.69 (dd, *J* = 10.5, 7.3 Hz, 1H), 3.02 – 2.91 (m, 1H), 1.96 (s, 3H); ¹³C NMR (125 MHz, CDCl₃) δ 194.52, 189.87, 169.57, 165.87, 133.55, 131.56, 129.35, 128.85, 128.25, 124.66, 114.51, 80.91, 80.11, 55.90, 54.10, 32.81, 20.80; IR (ATR):

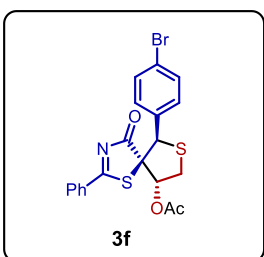
ν 3066, 3031, 2932, 2852, 1753, 1710, 1603, 1519, 1479, 1423, 1369, 1308, 1254, 1213, 1163, 117, 1058 cm^{-1} ; HRMS (ES+) calc. for $\text{C}_{21}\text{H}_{20}\text{NO}_4\text{S}_2$ $[\text{M}+\text{H}]^+$: 414.0828, found: 414.0830; M.P. 153-155 $^\circ\text{C}$.



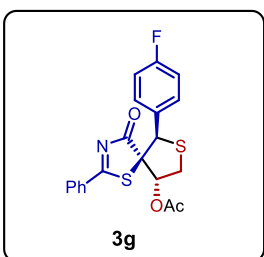
4-oxo-6-phenyl-2-(*p*-tolyl)-1,7-dithia-3-azaspiro[4.4]non-2-en-9-yl acetate (3d): White solid, Yield = 92% (146.3 mg); ^1H NMR (500 MHz, CDCl_3) δ 7.94 – 7.82 (m, 2H), 7.46 – 7.35 (m, 2H), 7.27 – 7.16 (m, 5H), 5.82 (dd, J = 9.5, 7.3 Hz, 1H), 5.28 (s, 1H), 3.69 (dd, J = 10.5, 7.3 Hz, 1H), 2.97 (dd, J = 10.3, 9.7 Hz, 1H), 2.41 (s, 3H), 1.95 (s, 3H); ^{13}C NMR (125 MHz, CDCl_3) δ 195.83, 190.04, 169.54, 147.17, 133.40, 129.84, 129.38, 129.29, 129.14, 128.89, 128.25, 80.83, 80.12, 54.18, 32.82, 22.08, 20.75; IR (ATR): ν 3066, 3031, 2967, 2935, 1750, 1718, 1605, 1519, 1490, 1452, 1409, 1372, 1315, 1216, 1182, 1061, 1023 cm^{-1} ; HRMS (ES+) calc. for $\text{C}_{21}\text{H}_{20}\text{NO}_3\text{S}_2$ $[\text{M}+\text{H}]^+$: 398.0879, found: 398.0885; M.P. 147-149 $^\circ\text{C}$.



4-oxo-6-phenyl-2-(thiophen-2-yl)-1,7-dithia-3-azaspiro[4.4]non-2-en-9-yl acetate (3e): White solid, Yield = 88% (137.1 mg); ^1H NMR (500 MHz, CDCl_3) δ 7.80 (dd, J = 37.6, 4.4 Hz, 2H), 7.40 (d, J = 7.3 Hz, 2H), 7.25 – 7.09 (m, 4H), 5.89 – 5.70 (m, 1H), 5.27 (s, 1H), 3.68 (dd, J = 10.4, 7.5 Hz, 1H), 2.94 (t, J = 10.0 Hz, 1H), 1.97 (s, 3H); ^{13}C NMR (125 MHz, CDCl_3) δ 189.07, 187.05, 169.47, 137.03, 136.26, 134.52, 133.35, 129.28, 129.14, 128.89, 128.28, 81.73, 80.06, 54.00, 32.64, 20.74; IR (ATR): ν 3095, 3031, 2934, 2849, 1753, 1710, 1533, 1471, 1415, 1372, 1216, 1166, 1055 cm^{-1} ; HRMS (ES+) calc. for $\text{C}_{18}\text{H}_{16}\text{NO}_3\text{S}_3$ $[\text{M}+\text{H}]^+$: 390.0287, found: 390.0280; M.P. 143-145 $^\circ\text{C}$.

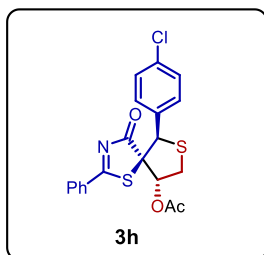


6-(4-bromophenyl)-4-oxo-2-phenyl-1,7-dithia-3-azaspiro[4.4]non-2-en-9-yl acetate (3f): White solid, Yield = 92% (170.2 mg); ^1H NMR (500 MHz, CDCl_3) δ 7.98 (d, J = 7.9 Hz, 2H), 7.64 (t, J = 7.4 Hz, 1H), 7.46 (t, J = 7.6 Hz, 2H), 7.37 (s, 4H), 5.86 (d, J = 4.5 Hz, 1H), 5.44 (s, 1H), 3.61 (dd, J = 12.4, 4.9 Hz, 1H), 3.26 (d, J = 12.5 Hz, 1H), 2.22 (s, 3H); ^{13}C NMR (125 MHz, CDCl_3) δ 193.12, 187.78, 169.76, 135.70, 132.89, 131.61, 131.54, 131.40, 129.18, 129.15, 122.89, 81.52, 79.78, 54.95, 36.90, 21.06; IR (ATR): ν 3066, 3034, 2967, 2935, 2846, 1753, 1720, 1595, 1514, 1487, 1447, 1401, 1372, 1315, 1217, 1176, 1141 cm^{-1} ; HRMS (ES+) calc. for $\text{C}_{20}\text{H}_{17}\text{BrNO}_3\text{S}_2$ $[\text{M}+\text{H}]^+$: 461.9828 & 463.9808, found: 461.9824 & 463.9800; M.P. 170-172 $^\circ\text{C}$.

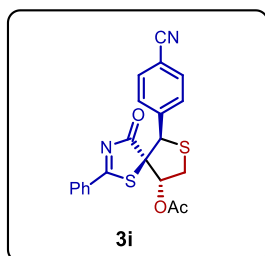


6-(4-fluorophenyl)-4-oxo-2-phenyl-1,7-dithia-3-azaspiro[4.4]non-2-en-9-yl acetate (3g): White solid, Yield = 88% (141.3 mg); ^1H NMR (500 MHz, CDCl_3) δ 7.98 (d, J = 7.4 Hz, 2H), 7.63 (t, J = 7.4 Hz, 1H), 7.46 (dd, J =

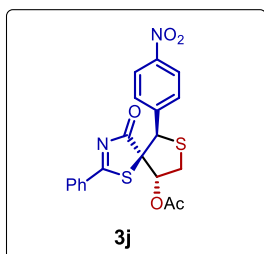
15.2, 8.0 Hz, 4H), 6.93 (t, $J = 8.6$ Hz, 2H), 5.96 – 5.79 (m, 1H), 5.47 (s, 1H), 3.61 (dd, $J = 12.5, 5.0$ Hz, 1H), 3.25 (dd, $J = 12.5, 1.4$ Hz, 1H), 2.22 (s, 3H); ^{13}C NMR (125 MHz, CDCl_3) δ 193.13, 187.85, 169.78, 163.80, 161.83, 135.63, 131.61, 131.50, 131.44, 129.42, 129.39, 129.16, 129.08, 115.47, 115.30, 81.43, 80.00, 54.90, 36.90, 21.06; IR (ATR): ν 3069, 3039, 2975, 2943, 2884, 1750, 1718, 1600, 1509, 1485, 1450, 1370, 1316, 1222, 1182, 1160 cm^{-1} ; HRMS (ES⁺) calc. for $\text{C}_{20}\text{H}_{17}\text{FNO}_3\text{S}_2$ $[\text{M}+\text{H}]^+$: 402.0628, found: 402.0624, M.P. 155-157 °C.



6-(4-chlorophenyl)-4-oxo-2-phenyl-1,7-dithia-3-azaspiro[4.4]non-2-en-9-yl acetate (3h): White solid, Yield = 98% (163.8 mg); ^1H NMR (500 MHz, CDCl_3) δ 8.04 – 7.92 (m, 2H), 7.65 (t, $J = 7.5$ Hz, 1H), 7.53 – 7.39 (m, 4H), 7.22 (d, $J = 8.5$ Hz, 2H), 5.86 (d, $J = 3.7$ Hz, 1H), 5.46 (s, 1H), 3.61 (dd, $J = 12.5, 4.9$ Hz, 1H), 3.26 (dd, $J = 12.5, 1.2$ Hz, 1H), 2.22 (s, 3H); ^{13}C NMR (125 MHz, CDCl_3) δ 193.15, 187.79, 169.79, 135.70, 134.66, 132.35, 131.61, 131.09, 129.20, 129.15, 128.66, 81.52, 76.91, 54.93, 36.92, 21.07; IR (ATR): ν 3069, 3031, 2970, 2938, 1750, 1718, 1600, 1514, 1487, 1447, 1410, 1372, 1313, 1214, 1182, 1144, 1021 cm^{-1} ; HRMS (ES⁺) calc. for $\text{C}_{20}\text{H}_{17}\text{ClNO}_3\text{S}_2$ $[\text{M}+\text{H}]^+$: 418.0333, found: 418.0328; M.P. 159-161 °C.



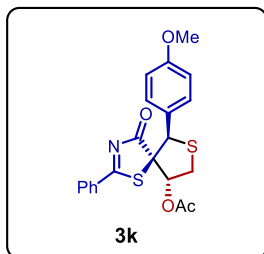
6-(4-cyanophenyl)-4-oxo-2-phenyl-1,7-dithia-3-azaspiro[4.4]non-2-en-9-yl acetate (3i): White solid, Yield = 89% (145.4 mg); ^1H NMR (500 MHz, CDCl_3) δ 8.00 – 7.91 (m, 2H), 7.69 – 7.58 (m, 3H), 7.56 – 7.50 (m, 2H), 7.46 (t, $J = 7.9$ Hz, 2H), 5.87 (dd, $J = 4.8, 1.4$ Hz, 1H), 5.52 (s, 1H), 3.64 (dd, $J = 12.5, 4.9$ Hz, 1H), 3.28 (dd, $J = 12.5, 1.5$ Hz, 1H), 2.22 (s, 3H); ^{13}C NMR (125 MHz, CDCl_3) δ 192.96, 187.49, 169.68, 139.35, 135.91, 132.19, 131.38, 130.59, 129.24, 129.14, 118.42, 112.69, 81.49, 79.61, 55.12, 37.18, 21.02; IR (ATR): ν 3064, 2932, 2857, 2233, 1753, 1718, 1603, 1509, 1487, 1450, 1375, 1308, 1273, 1223, 1189, 1150 cm^{-1} ; HRMS (ES⁺) calc. for $\text{C}_{21}\text{H}_{17}\text{N}_2\text{O}_3\text{S}_2$ $[\text{M}+\text{H}]^+$: 409.0678, found: 409.0675; M.P. 219-221 °C.



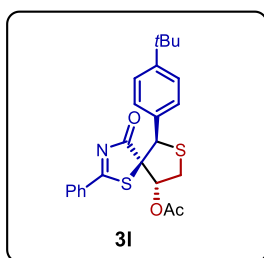
6-(4-nitrophenyl)-4-oxo-2-phenyl-1,7-dithia-3-azaspiro[4.4]non-2-en-9-yl acetate (3j): White solid, Yield = 85% (145.7 mg); ^1H NMR (500 MHz, CDCl_3) δ 8.17 – 8.05 (m, 2H), 7.97 (dd, $J = 8.4, 1.1$ Hz, 2H), 7.73 – 7.59 (m, 3H), 7.46 (t, $J = 7.9$ Hz, 2H), 5.88 (dd, $J = 4.8, 1.3$ Hz, 1H), 5.58 (s, 1H), 3.67 (dd, $J = 12.5, 4.9$ Hz, 1H), 3.30 (dd, $J = 12.5, 1.4$ Hz, 1H), 2.24 (s, 3H); ^{13}C NMR (125 MHz, CDCl_3) δ 192.95, 187.45, 169.70, 148.10, 141.32, 135.97, 131.36, 130.84, 129.27, 129.19, 123.58, 81.53, 79.64, 54.89, 37.33, 21.04; IR (ATR): ν 3064, 2964, 2927, 2852, 1753, 1723, 1595, 1525, 1485, 1444, 1372, 1348, 1313, 1217, 1182, 1147, 1064,

1024 cm^{-1} ; HRMS (ES+) calc. for $\text{C}_{20}\text{H}_{17}\text{N}_2\text{O}_5\text{S}_2$ $[\text{M}+\text{H}]^+$: 429.0573, found : 429.0544; M.P. 197-199 $^{\circ}\text{C}$.

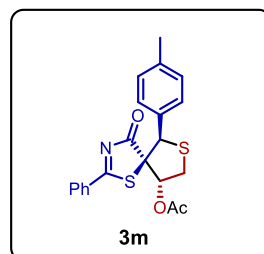
6-(4-methoxyphenyl)-4-oxo-2-phenyl-1,7-dithia-3-azaspiro[4.4]non-2-en-9-yl acetate (3k): White



solid, Yield = 92% (152.2 mg); ^1H NMR (500 MHz, CDCl_3) δ 8.03 – 7.90 (m, 2H), 7.67 – 7.56 (m, 1H), 7.53 – 7.35 (m, 4H), 6.82 – 6.69 (m, 2H), 5.86 (dd, J = 5.0, 1.8 Hz, 1H), 5.44 (s, 1H), 3.72 (s, 3H), 3.59 (dd, J = 12.4, 5.1 Hz, 1H), 3.25 (dd, J = 12.4, 1.9 Hz, 1H), 2.21 (s, 3H); ^{13}C NMR (125 MHz, CDCl_3) δ 193.25, 188.10, 169.83, 159.79, 135.47, 131.75, 130.87, 129.10, 129.06, 125.62, 113.74, 81.45, 80.19, 55.29, 55.10, 36.64, 21.08; IR (ATR): ν 3067, 3034, 2999, 2959, 2929, 2851, 2838, 1747, 1718, 1608, 1595, 1584, 1509, 1487, 1447, 1372, 1302, 1275, 1217, 1173 cm^{-1} ; HRMS (ES+) calc. for $\text{C}_{21}\text{H}_{19}\text{NO}_4\text{S}_2$ $[\text{M}]^+$: 436.0648, found : 436.0628; M.P. 128-131 $^{\circ}\text{C}$.

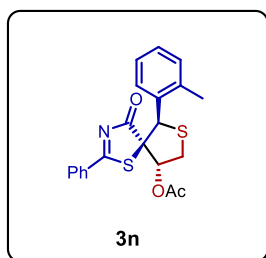


6-(4-(tert-butyl)phenyl)-4-oxo-2-phenyl-1,7-dithia-3-azaspiro[4.4]non-2-en-9-yl acetate (3l): White solid, Yield = 89% (156.5 mg); ^1H NMR (500 MHz, CDCl_3) δ 8.03 – 7.94 (m, 18H), 7.63 (t, J = 7.5 Hz, 9H), 7.46 (t, J = 7.8 Hz, 18H), 7.40 (d, J = 8.4 Hz, 16H), 7.33 (d, J = 8.5 Hz, 2H), 7.26 (d, J = 8.4 Hz, 21H), 7.22 (d, J = 8.4 Hz, 2H), 5.86 (dd, J = 5.0, 1.9 Hz, 8H), 5.83 – 5.79 (m, 1H), 5.45 (s, 8H), 5.26 (s, 1H), 3.69 (dd, J = 10.5, 7.3 Hz, 1H), 3.60 (dd, J = 12.4, 5.1 Hz, 8H), 3.25 (dd, J = 12.4, 1.9 Hz, 8H), 2.99 – 2.93 (m, 1H), 2.21 (s, 24H), 1.96 (s, 3H), 1.23 (s, 72H), 1.19 (s, 10H); ^{13}C NMR (125 MHz, CDCl_3) δ 193.31, 188.07, 169.89, 151.69, 135.46, 131.86, 130.85, 129.45, 129.13, 129.09, 125.44, 81.67, 80.05, 55.01, 36.47, 34.66, 31.32, 21.11; IR (ATR): ν 3069, 3031, 2968, 2908, 2865, 1747, 1718, 1597, 1514, 1485, 1447, 1415, 1372, 1313, 1273, 1214, 1015 cm^{-1} ; HRMS (ES+) calc. for $\text{C}_{24}\text{H}_{26}\text{NO}_3\text{S}_2$ $[\text{M}+\text{H}]^+$: 440.1349, found : 440.1346; M.P. 140-142 $^{\circ}\text{C}$.



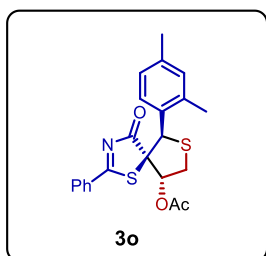
6-(4-methyl)-4-oxo-2-phenyl-1,7-dithia-3-azaspiro[4.4]non-2-en-9-yl acetate (3m): White solid, Yield = 91% (144.7 mg); ^1H NMR (500 MHz, CDCl_3) δ 7.99 (dd, J = 8.3, 0.9 Hz, 2H), 7.63 (t, J = 7.5 Hz, 1H), 7.45 (t, J = 7.9 Hz, 2H), 7.37 (d, J = 8.1 Hz, 2H), 7.05 (d, J = 8.1 Hz, 2H), 5.86 (dd, J = 5.0, 1.9 Hz, 1H), 5.45 (s, 1H), 3.60 (dd, J = 12.4, 5.1 Hz, 1H), 3.26 (dd, J = 12.4, 2.0 Hz, 1H), 2.25 (s, 3H), 2.21 (s, 3H); ^{13}C NMR (125 MHz, CDCl_3) δ 193.30, 188.11, 169.89, 138.63, 135.48, 131.80, 130.98, 130.92, 129.58, 129.18, 129.12, 81.59, 80.02, 55.26, 36.52, 21.23, 21.11; IR (ATR): ν 3069, 3031, 2956, 2934, 2860, 1747, 1718, 1600, 1509, 1485, 1450, 1366, 1313, 1211, 1144 cm^{-1} ; HRMS (ES+) calc. for $\text{C}_{21}\text{H}_{20}\text{NO}_3\text{S}_2$ $[\text{M}+\text{H}]^+$: 398.0879, found : 398.0861; M.P. 128-131 $^{\circ}\text{C}$.

6-(2-methyl)-4-oxo-2-phenyl-1,7-dithia-3-azaspiro[4.4]non-2-en-9-yl acetate (3n): White solid,



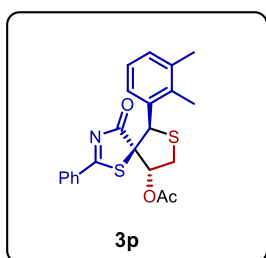
Yield = 87% (138.3 mg); ^1H NMR (500 MHz, CDCl_3) δ 8.06 – 7.97 (m, 2H), 7.84 (dd, J = 7.8, 1.0 Hz, 1H), 7.65 (t, J = 7.5 Hz, 1H), 7.47 (t, J = 7.9 Hz, 2H), 7.23 – 7.06 (m, 3H), 5.86 (t, J = 5.8 Hz, 1H), 5.56 (s, 1H), 3.52 (dd, J = 11.5, 5.7 Hz, 1H), 3.43 (dd, J = 11.5, 5.8 Hz, 1H), 2.32 (s, 3H), 2.09 (s, 3H); ^{13}C NMR (125 MHz, CDCl_3) δ 194.11, 189.78, 169.96, 137.60, 135.56, 135.30, 131.72, 130.74, 129.92, 129.17, 129.04, 128.44, 126.14, 81.03, 78.00, 49.03, 33.62, 20.99, 20.24; IR (ATR): ν 3061, 3023, 2938, 2852, 1747, 1715, 1597, 1514, 1485, 1449, 1367, 1318, 1214, 1144, 1024 cm^{-1} ; HRMS (ES⁺) calc. for $\text{C}_{21}\text{H}_{20}\text{NO}_3\text{S}_2$ $[\text{M}+\text{H}]^+$: 398.0879, found : 398.0885; M.P. 165-167 °C.

6-(2,4-dimethylphenyl)-4-oxo-2-phenyl-1,7-dithia-3-azaspiro[4.4]non-2-en-9-yl acetate (3o):

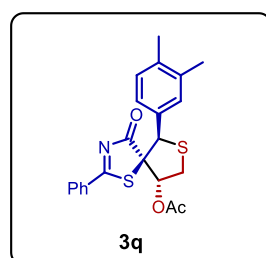


White solid, Yield = 86% (141.6 mg); ^1H NMR (500 MHz, CDCl_3) δ 8.10 – 7.98 (m, 2H), 7.73 (d, J = 8.1 Hz, 1H), 7.65 (t, J = 7.5 Hz, 1H), 7.48 (t, J = 7.8 Hz, 2H), 6.92 (d, J = 8.1 Hz, 1H), 6.84 (s, 1H), 5.84 (dd, J = 8.9, 7.0 Hz, 1H), 5.60 (s, 1H), 3.71 (dd, J = 10.7, 7.0 Hz, 1H), 3.02 (dd, J = 10.7, 9.0 Hz, 1H), 2.29 (s, 3H), 2.19 (s, 3H), 1.98 (s, 3H); ^{13}C NMR (126 MHz, CDCl_3) δ 195.99, 190.37, 169.49, 138.30, 137.53, 135.50, 132.09, 131.45, 131.23, 129.15, 129.10, 128.92, 126.06, 80.73, 80.17, 49.06, 33.41, 21.11, 20.84, 19.96; IR (ATR): ν 3066, 3015, 2954, 2924, 2857, 1750, 1723, 1616, 1600, 1506, 1482, 1444, 1377, 1313, 1216, 1179, 1050 cm^{-1} ; HRMS (ES⁺) calc. for $\text{C}_{22}\text{H}_{22}\text{NO}_3\text{S}_2$ $[\text{M}+\text{H}]^+$: 412.1036, found : 412.1032; M.P. 124-126 °C.

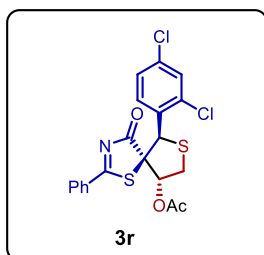
6-(2,3-dimethylphenyl)-4-oxo-2-phenyl-1,7-dithia-3-azaspiro[4.4]non-2-en-9-yl acetate (3p): White solid, Yield = 90% (148.2 mg); ^1H NMR (500 MHz, CDCl_3) δ 8.02 (dd, J = 8.4, 1.1 Hz, 2H), 7.74 (d, J = 7.7 Hz, 1H), 7.70 – 7.59 (m, 1H), 7.53 – 7.41 (m, 2H), 7.12 – 6.91 (m, 2H), 5.86 (dd, J = 8.9, 6.9 Hz, 1H), 5.76 (s, 1H), 3.72 (dd, J = 10.7, 6.9 Hz, 1H), 3.04 (dd, J = 10.7, 8.9 Hz, 1H), 2.22 (s, 3H), 2.18 (s, 3H), 1.98 (s, 3H); ^{13}C NMR (125 MHz, CDCl_3) δ 196.04, 190.31, 169.49, 137.09, 136.37, 135.50, 132.03, 131.79, 130.27, 130.17, 129.14, 129.05, 124.53, 80.79, 80.18, 49.30, 33.43, 21.30, 20.83, 15.50; IR (ATR): ν 3066, 3034, 2970, 2927, 2849, 1747, 1715, 1595, 1506, 1485, 1444, 1369, 1317, 1216, 1179, 1050 cm^{-1} ; HRMS (ES⁺) calc. for $\text{C}_{22}\text{H}_{22}\text{NO}_3\text{S}_2$ $[\text{M}+\text{H}]^+$: 412.1036, found : 412.1032; M.P. 123-125 °C.



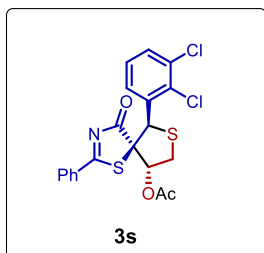
6-(3,4-dimethylphenyl)-4-oxo-2-phenyl-1,7-dithia-3-azaspiro[4.4]non-2-en-9-yl acetate (3q): White solid, Yield = 89% (146.5 mg); ^1H NMR (500 MHz, CDCl_3) δ 8.00 (dd, J = 8.4, 1.2 Hz, 2H), 7.66 – 7.59 (m, 1H), 7.45 (t, J = 7.9 Hz, 2H), 7.25 – 7.16 (m, 2H), 7.00 (d, J = 7.7 Hz, 1H), 5.86 (dd, J = 5.1, 2.1 Hz, 1H), 5.41 (s, 1H), 3.59 (dd, J = 12.3, 5.1 Hz, 1H), 3.25 (dd, J =



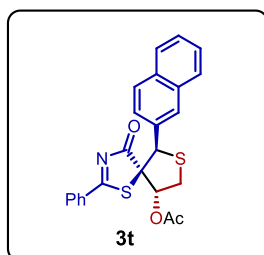
12.4, 2.2 Hz, 1H), 2.20 (s, 3H), 2.18 (s, 3H), 2.16 (s, 3H); ^{13}C NMR (125 MHz, CDCl_3) δ 193.31, 188.18, 169.87, 137.29, 136.69, 135.43, 131.86, 131.42, 130.83, 129.66, 129.33, 129.10, 127.05, 81.69, 79.94, 55.11, 36.34, 21.09, 19.94, 19.56; IR (ATR): ν 3069, 3061, 3018, 2968, 2940, 2924, 2859, 1753, 1715, 1602, 1508, 1482, 1448, 1372, 1310, 1220, 1181, 1149, 1052, 1023 cm^{-1} ; HRMS (ES⁺) calc. for $\text{C}_{22}\text{H}_{22}\text{NO}_3\text{S}_2$ [M+H]⁺ : 412.1036, found : 412.1039; M.P. 145-147 °C.



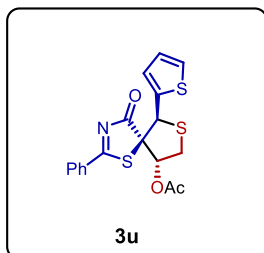
6-(2,4-dichlorophenyl)-4-oxo-2-phenyl-1,7-dithia-3-azaspiro[4.4]non-2-en-9-yl acetate (3r): White solid, Yield = 86% (155.6 mg); ^1H NMR (500 MHz, CDCl_3) δ 8.02 (dd, J = 8.4, 1.2 Hz, 2H), 7.86 (d, J = 8.5 Hz, 1H), 7.68 (t, J = 7.5 Hz, 1H), 7.50 (t, J = 7.9 Hz, 2H), 7.38 – 7.28 (m, 2H), 5.73 (dd, J = 8.3, 6.1 Hz, 1H), 5.61 (s, 1H), 3.57 (dd, J = 10.9, 8.3 Hz, 1H), 3.43 (dd, J = 10.9, 6.1 Hz, 1H), 2.01 (s, 3H); ^{13}C NMR (125 MHz, CDCl_3) δ 194.20, 190.19, 170.00, 136.21, 135.68, 135.25, 134.93, 131.85, 131.54, 129.46, 129.23, 129.07, 127.55, 80.17, 75.73, 48.60, 31.63, 20.87; IR (ATR): ν 3058, 2959, 2932, 2851, 1755, 1729, 1591, 1522, 1487, 1465, 1452, 1369, 1313, 1219, 1170, 1045 cm^{-1} ; HRMS (ES⁺) calc. for $\text{C}_{20}\text{H}_{16}\text{Cl}_2\text{NO}_3\text{S}_2$ [M+H]⁺ : 451.9943, found : 451.9939; M.P. 130-132 °C.



6-(2,3-dichlorophenyl)-4-oxo-2-phenyl-1,7-dithia-3-azaspiro[4.4]non-2-en-9-yl acetate (3s): White solid, Yield = 84% (152.0 mg); ^1H NMR (500 MHz, CDCl_3) δ 8.01 (dd, J = 8.3, 1.1 Hz, 2H), 7.86 (dd, J = 7.9, 1.5 Hz, 1H), 7.67 (t, J = 7.5 Hz, 1H), 7.49 (t, J = 7.9 Hz, 2H), 7.42 (dd, J = 8.0, 1.5 Hz, 1H), 7.28 (d, J = 8.0 Hz, 1H), 5.74 (dd, J = 8.8, 6.1 Hz, 1H), 5.67 (s, 1H), 3.60 (dd, J = 10.8, 8.8 Hz, 1H), 3.42 (dd, J = 10.8, 6.1 Hz, 1H), 2.00 (s, 3H); ^{13}C NMR (125 MHz, CDCl_3) δ 194.50, 190.59, 170.10, 139.43, 135.70, 134.04, 133.57, 131.63, 130.62, 129.26, 129.13, 129.06, 127.54, 80.20, 75.50, 49.59, 31.14, 20.91; IR (ATR): ν 2959, 1753, 1726, 1597, 1519, 1487, 1447, 1420, 1369, 1310, 1216, 1157, 1146, 1042 cm^{-1} ; HRMS (ES⁺) calc. for $\text{C}_{20}\text{H}_{16}\text{Cl}_2\text{NO}_3\text{S}_2$ [M+H]⁺ : 451.9943, found : 451.9935; M.P. 150-152 °C.

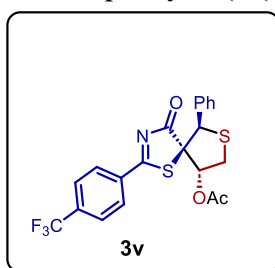


6-(naphthalen-2-yl)-4-oxo-2-phenyl-1,7-dithia-3-azaspiro[4.4]non-2-en-9-yl acetate (3t): White solid, Yield = 92% (159.5 mg); ^1H NMR (500 MHz, CDCl_3) δ 7.99 – 7.89 (m, 3H), 7.84 – 7.69 (m, 3H), 7.67 – 7.55 (m, 2H), 7.46 – 7.39 (m, 4H), 5.91 (dd, J = 5.0, 2.2 Hz, 1H), 5.66 (s, 1H), 3.66 (dd, J = 12.3, 5.0 Hz, 1H), 3.33 (dd, J = 12.3, 2.2 Hz, 1H), 2.24 (s, 3H); ^{13}C NMR (125 MHz, CDCl_3) δ 193.30, 188.21, 169.90, 135.52, 133.44, 133.02, 131.77, 131.64, 129.26, 129.11, 129.07, 128.34, 128.15, 127.67, 127.00, 126.58, 126.37, 81.74, 79.89, 55.60, 36.58, 21.11; IR (ATR): ν 3052, 3024, 2970, 2930, 2855, 1745, 1712, 1597, 1509, 1485, 1450, 1370, 1313, 1211, 1176, 1144, 1023 cm^{-1} ; HRMS (ES⁺) calc. for $\text{C}_{24}\text{H}_{20}\text{NO}_3\text{S}_2$ [M+H]⁺ : 434.0879, found : 434.0898; M.P. 175-177 °C.

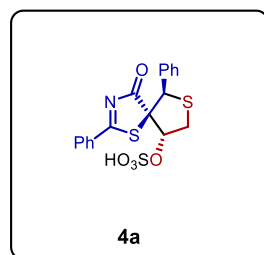


4-oxo-2-phenyl-6-(thiophen-2-yl)-1,7-dithia-3-azaspiro[4.4]non-2-en-9-yl acetate (3u): White solid, Yield = 90% (155.8 mg); ^1H NMR (500 MHz, CDCl_3) δ 8.15 – 8.01 (m, 2H), 7.67 (t, J = 7.5 Hz, 1H), 7.50 (t, J = 7.9 Hz, 2H), 7.17 (dd, J = 5.1, 0.8 Hz, 1H), 7.01 (d, J = 3.6 Hz, 1H), 6.84 (dd, J = 5.0, 3.7 Hz, 1H), 5.77 (dd, J = 9.5, 7.3 Hz, 1H), 5.50 (s, 1H), 3.69 (dd, J = 10.5, 7.3 Hz, 1H), 3.04 – 2.94 (m, 1H), 1.97 (s, 3H); ^{13}C NMR (126 MHz, CDCl_3) δ 196.44, 189.67, 169.47, 137.22, 135.67, 132.00, 129.21, 129.17, 127.94, 126.93, 126.54, 80.97, 79.55, 49.62, 33.23, 20.74; IR (ATR): ν 3109, 3058, 2977, 2956, 2924, 1750, 1715, 1600, 1509, 1487, 1447, 1372, 1316, 1251, 1216, 1176, 1061 cm^{-1} ; HRMS (ES⁺) calc. for $\text{C}_{18}\text{H}_{16}\text{NO}_3\text{S}_3$ $[\text{M}+\text{H}]^+$: 390.0287, found: 390.0285; M.P. 128-130 °C.

4-oxo-6-phenyl-2-(4-(trifluoromethyl)phenyl)-1,7-dithia-3-azaspiro[4.4]non-2-en-9-yl acetate (3v):

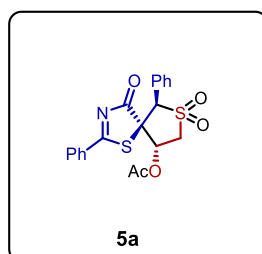


(3v): Yellow semi liquid, Yield = 58% (104.7 mg); ^1H NMR (500 MHz, CDCl_3) δ 8.08 (d, J = 8.2 Hz, 2H), 7.71 (d, J = 8.3 Hz, 2H), 7.43 – 7.37 (m, 2H), 7.21 (t, J = 5.6 Hz, 3H), 5.86 (dd, J = 9.3, 7.5 Hz, 1H), 5.29 (s, 1H), 3.72 (dd, J = 10.7, 7.4 Hz, 1H), 3.02 – 2.94 (m, 1H), 1.97 (s, 3H); ^{13}C NMR (125 MHz, CDCl_3) δ 194.81, 189.72, 169.42, 136.53, 136.27, 134.87, 133.04, 129.23, 129.12, 128.88, 128.36, 126.15 (q, $J_{\text{C-F}}$ = 3.75 Hz), 81.76, 80.20, 54.55, 32.91, 20.70; IR (ATR): ν 3109, 3089, 2992, 1720, 1690, 1644, 1565, 1544, 1488, 1451, 1250 cm^{-1} ; HRMS (ES⁺) calc. for $\text{C}_{21}\text{H}_{16}\text{F}_3\text{NO}_3\text{S}_2$ $[\text{M}+\text{H}]^+$: 452.0596, found: 452.0611.



4-oxo-2,6-diphenyl-1,7-dithia-3-azaspiro[4.4]non-2-en-9-yl hydrogen sulfate (4a): Light yellow solid, Yield = 90% (151.7 mg); ^1H NMR (500 MHz, CDCl_3) δ 7.93 (d, J = 8.2 Hz, 4H), 7.56 (t, J = 7.4 Hz, 2H), 7.39 (dt, J = 15.5, 4.7 Hz, 8H), 7.25 – 7.09 (m, 7H), 5.33 (s, 2H), 5.11 (dt, J = 10.0, 7.5 Hz, 2H), 3.47 (dd, J = 10.7, 7.2 Hz, 2H), 3.25 – 3.15 (m, 2H), 3.03 (t, J = 10.4 Hz, 2H); ^{13}C NMR (125 MHz, CDCl_3) δ 197.53, 192.08, 135.31, 134.46, 131.63, 129.10, 128.96, 128.85, 128.64, 128.28, 84.42, 81.21, 54.06, 35.27; IR (ATR): ν 3088, 3064, 3037, 2962, 2924, 2855, 1712, 1597, 1583, 1532, 1493, 1455, 1377, 1313, 1267, 1216, 1179, 1112, 1024 cm^{-1} ; HRMS (ES⁺) calc. for $\text{C}_{18}\text{H}_{15}\text{NO}_5\text{S}_3$ $[\text{M}]^+$: 421.0107, found: 421.0102; M.P. 163-165 °C.

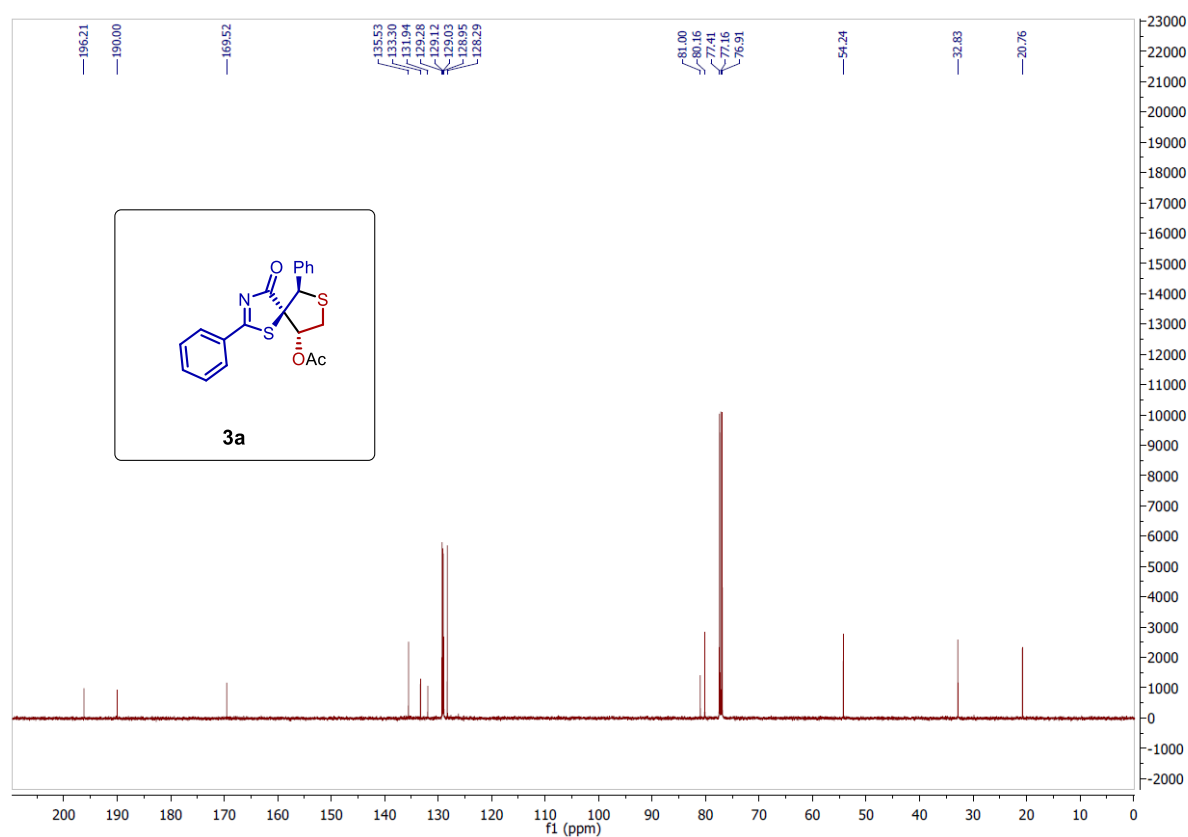
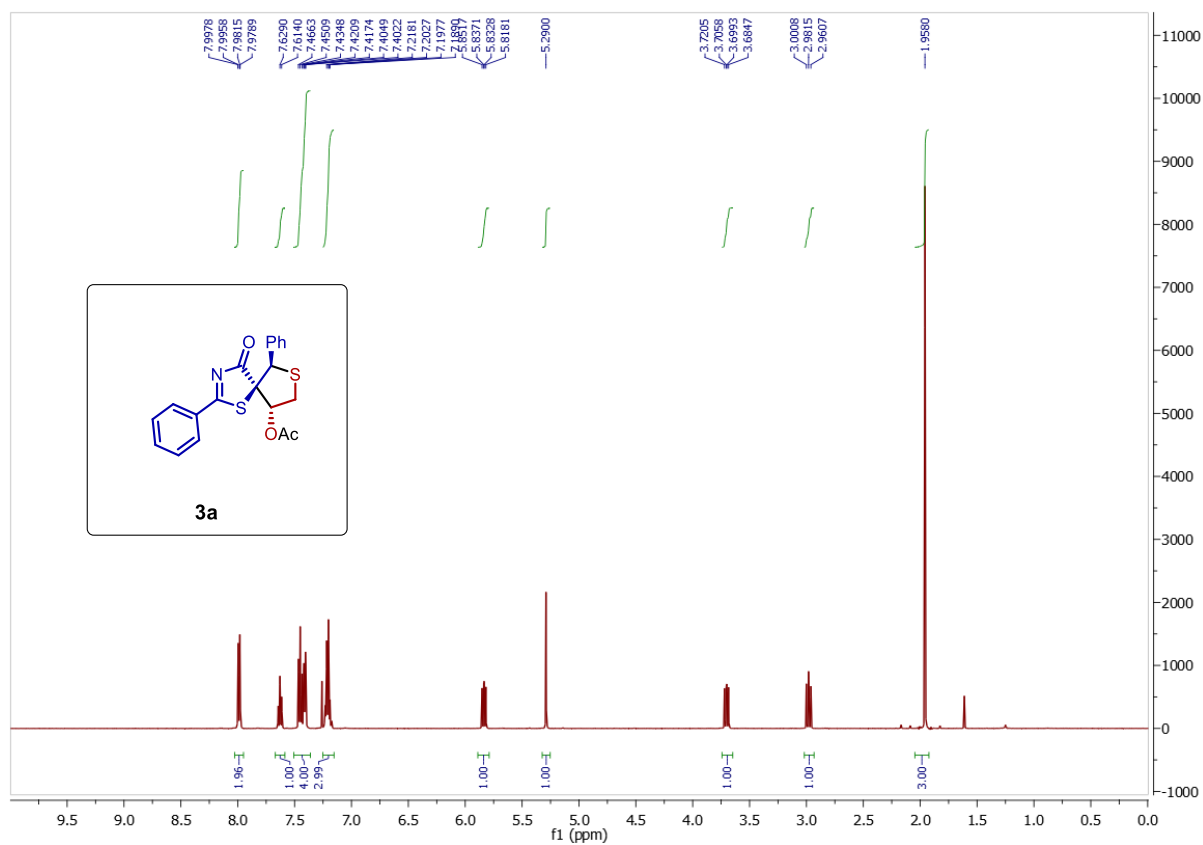
7,7-dioxido-4-oxo-2,6-diphenyl-1,7-dithia-3-azaspiro[4.4]non-2-en-9-yl acetate (5a): White solid,



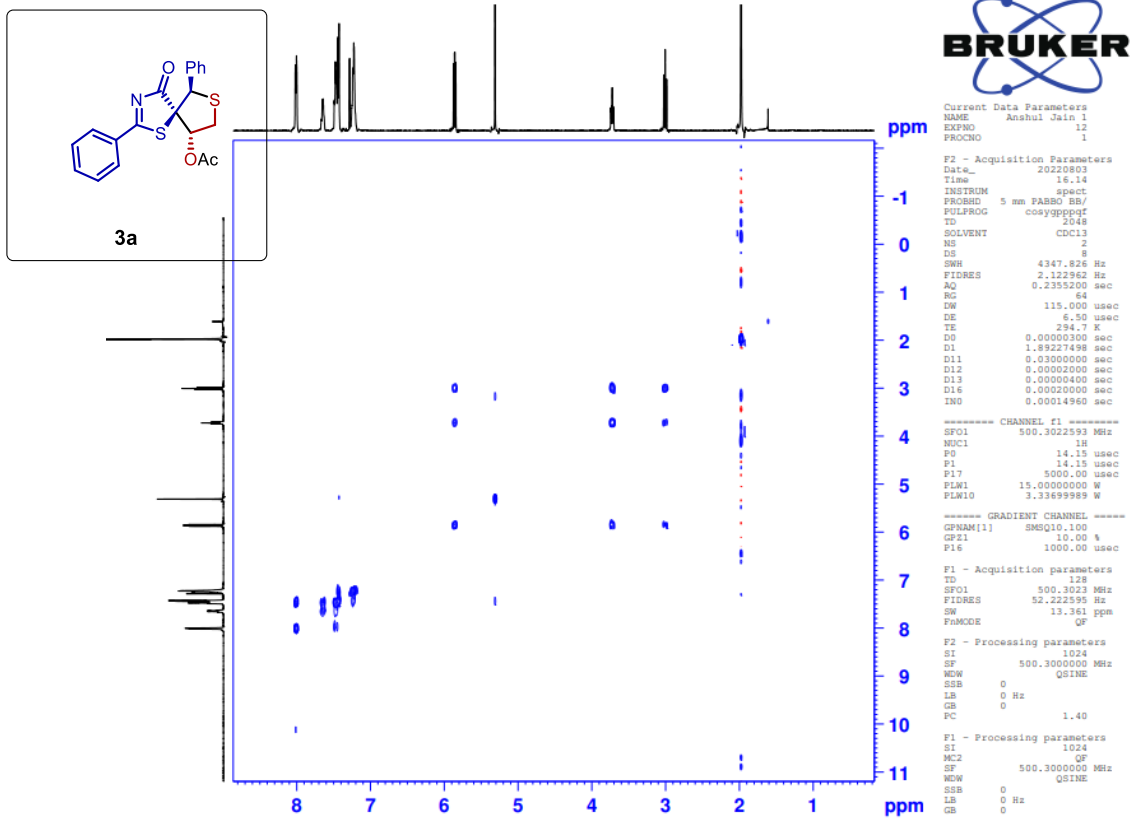
Yield = 85% (141.3 mg); ^1H NMR (500 MHz, CDCl_3) δ 8.06 (dd, J = 8.4, 1.2 Hz, 2H), 7.69 (dd, J = 10.6, 4.3 Hz, 1H), 7.59 – 7.48 (m, 4H), 7.34 – 7.27 (m, 3H), 5.79 (dd, J = 9.1, 7.1 Hz, 1H), 4.86 (s, 1H), 4.15 (dd, J =

14.0, 9.1 Hz, 1H), 3.33 (dd, $J = 14.0, 7.1$ Hz, 1H), 2.02 (s, 3H); ^{13}C NMR (125 MHz, CDCl_3) δ 196.85, 190.03, 169.49, 136.22, 131.39, 131.32, 130.38, 129.37, 129.33, 128.85, 124.56, 73.04, 71.92, 71.32, 55.22, 20.45; IR (ATR): ν 3061, 3018, 2964, 2921, 2849, 1749, 1720, 1683, 1591, 1514, 1485, 1447, 1372, 1329, 1222, 1136 cm^{-1} ; HRMS (ES+) calc. for $\text{C}_{24}\text{H}_{18}\text{NO}_5\text{S}_2$ $[\text{M}+\text{H}]^+$: 416.0621, found : 416.0614; M.P. 182-184 °C.

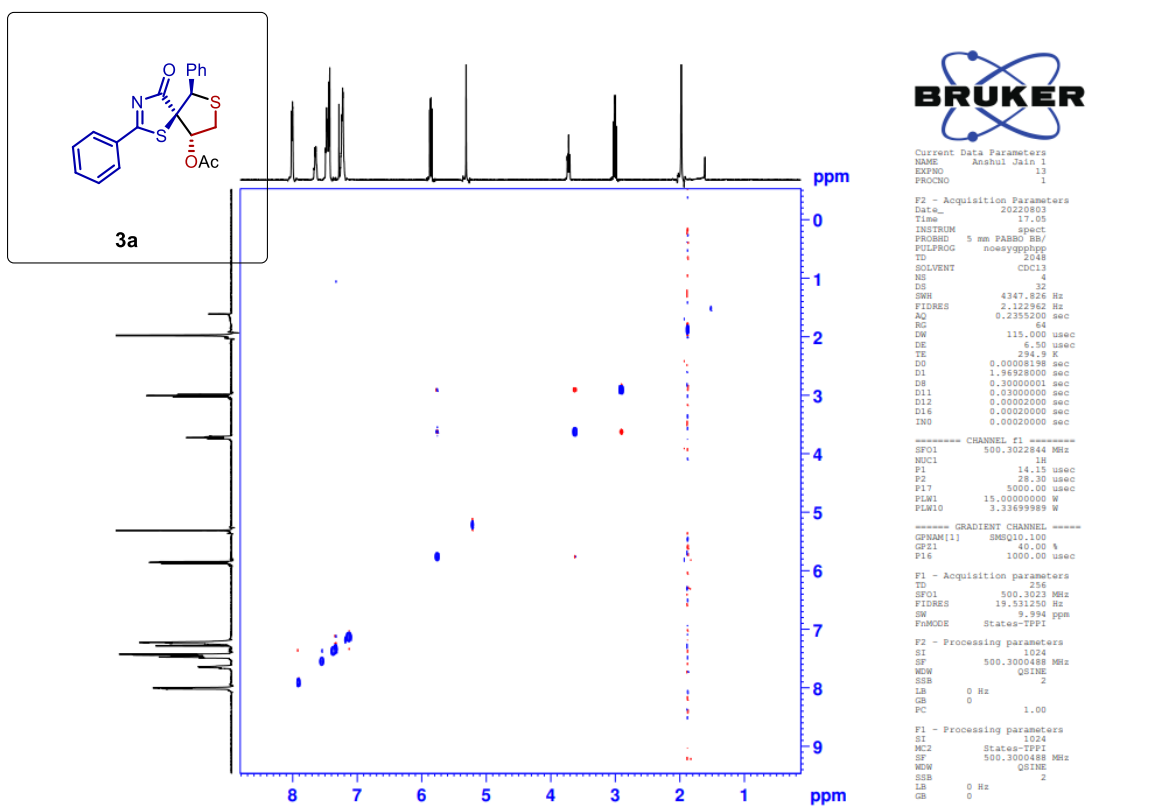
7. ^1H and ^{13}C Spectra



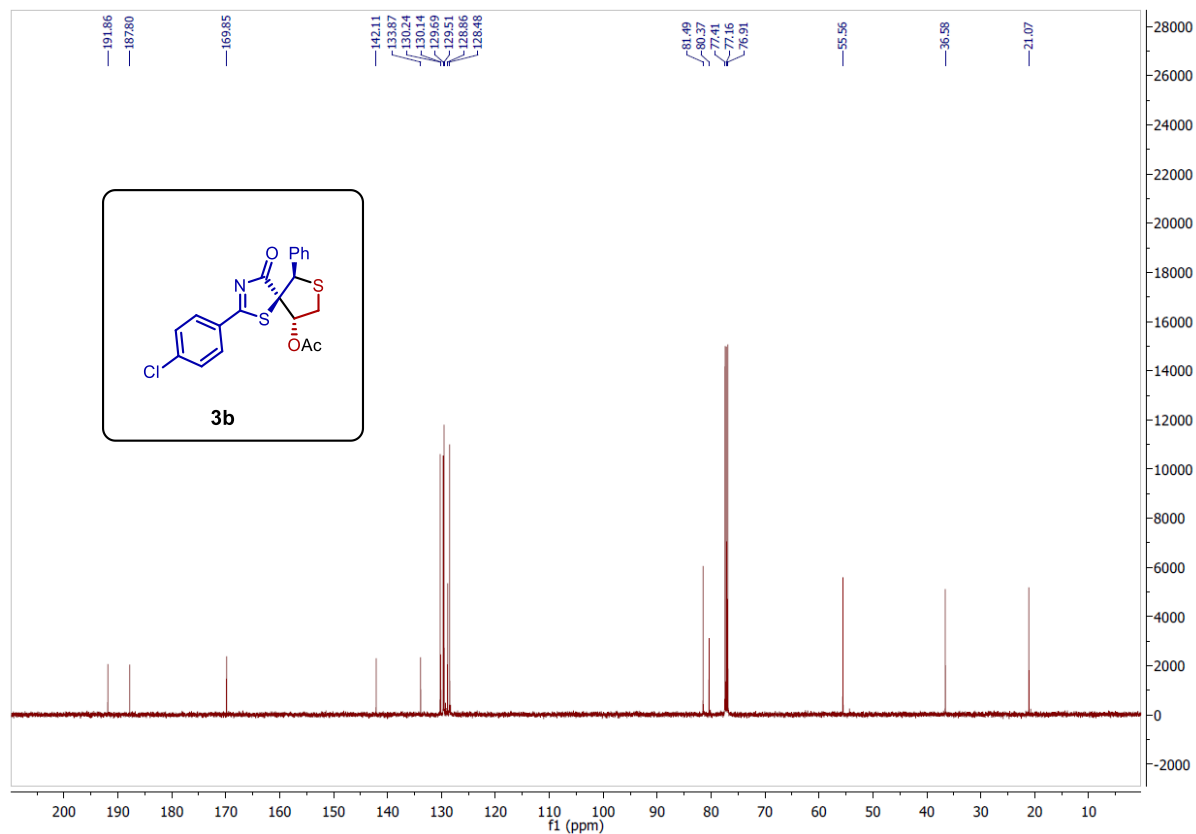
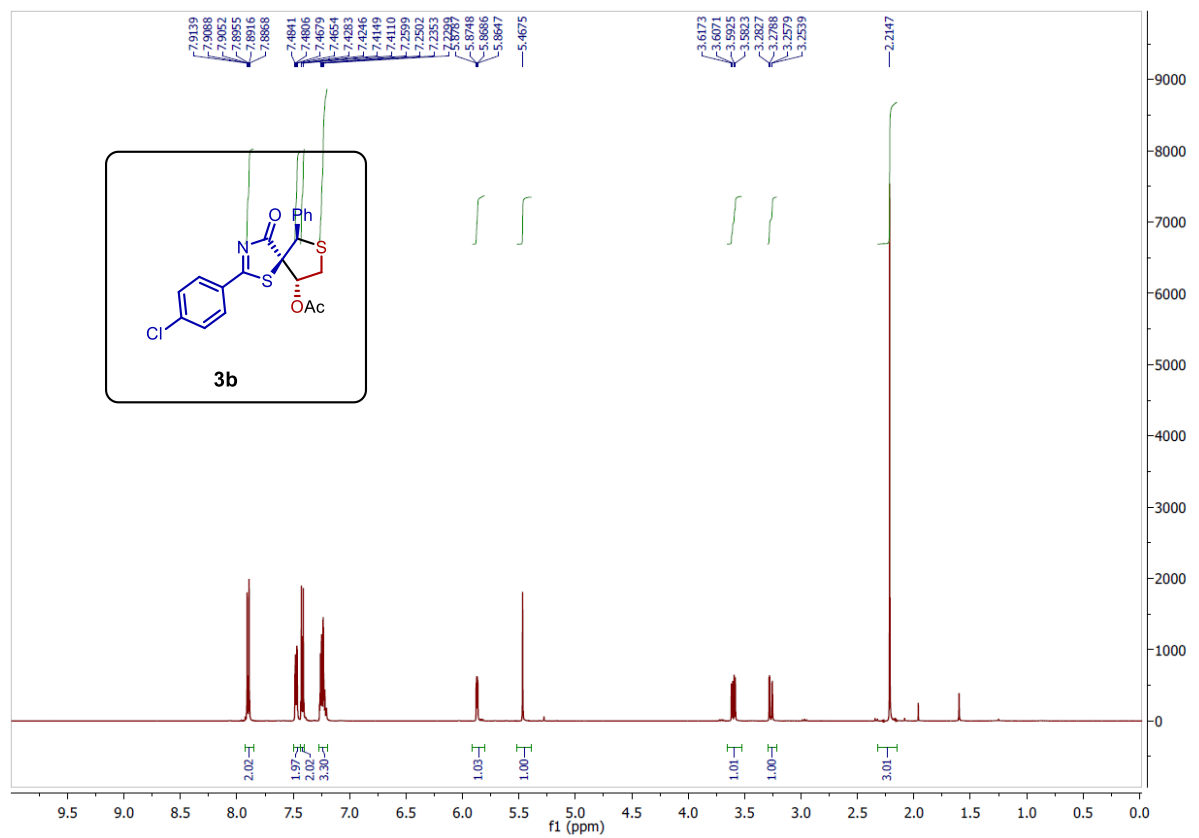
500 MHz ^1H NMR and 125 MHz ^{13}C NMR Spectra of **3a**



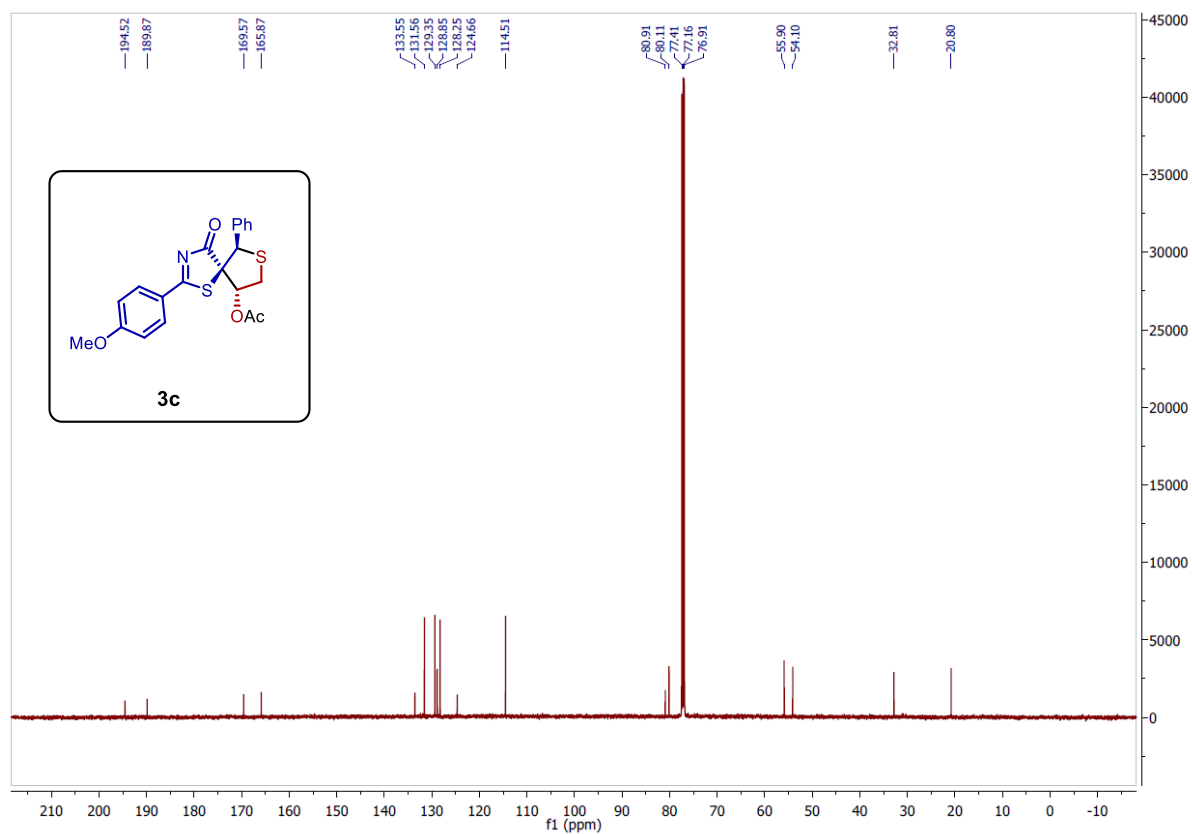
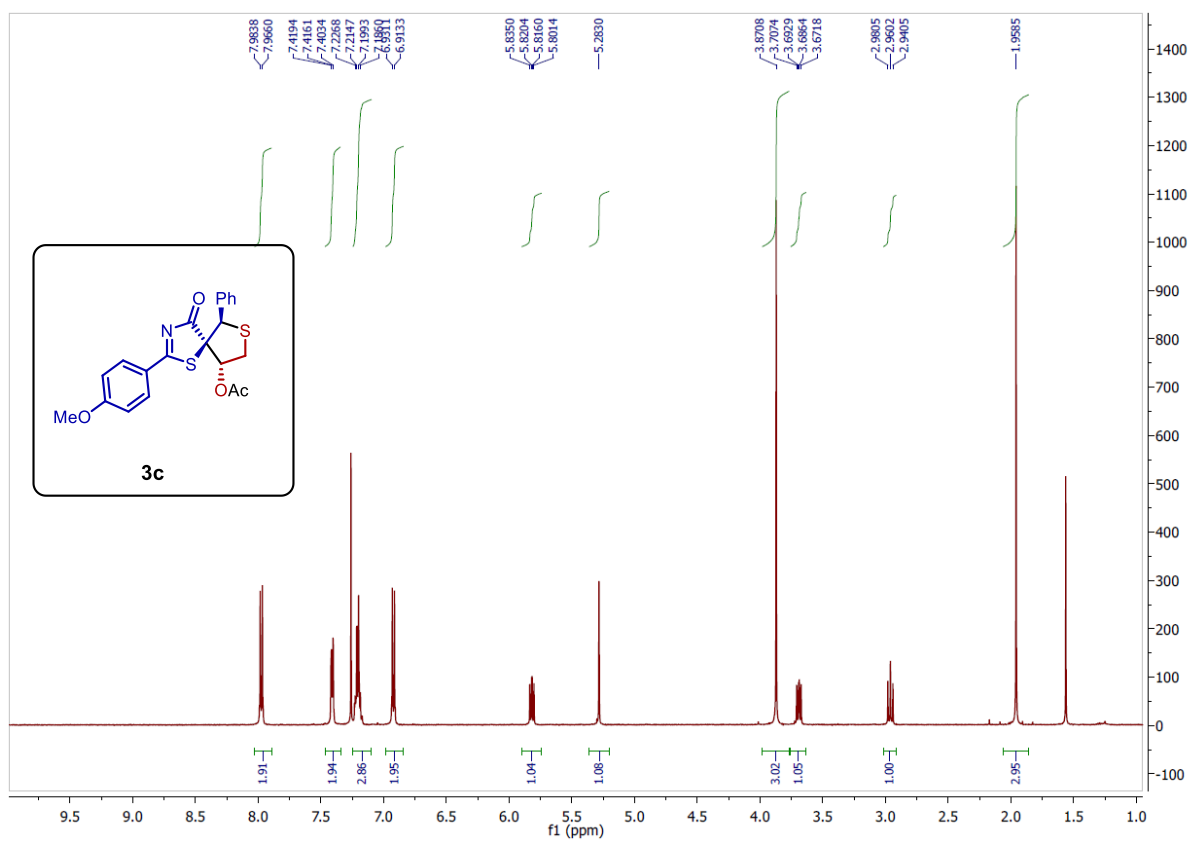
500 MHz ^1H - ^1H COSY Spectra of **3a**



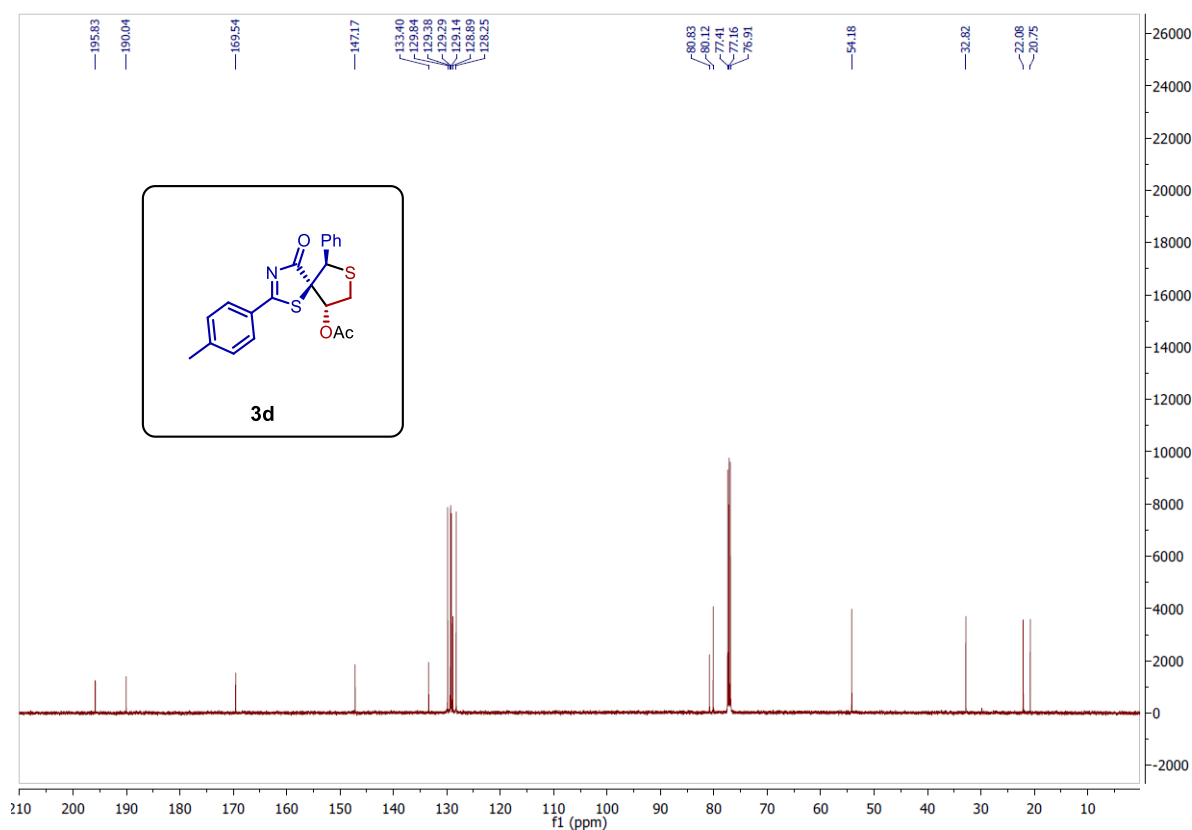
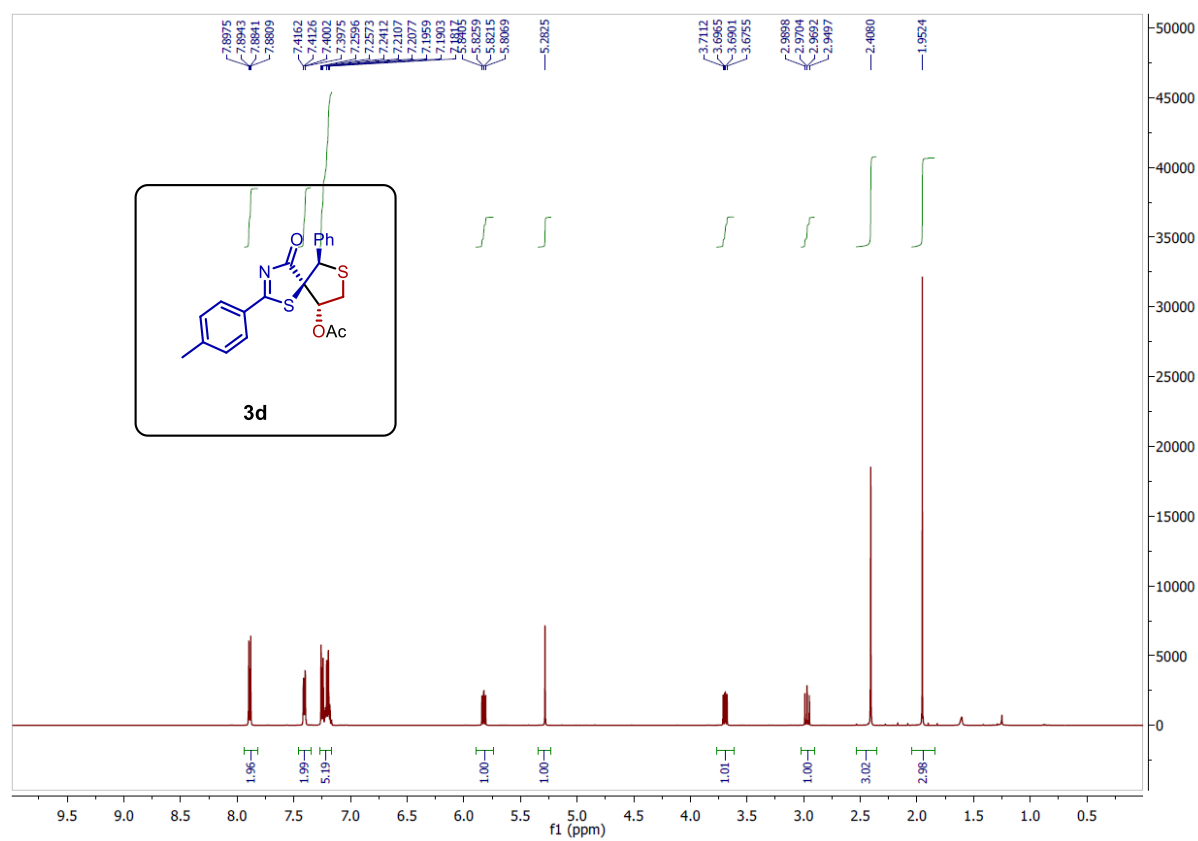
500 MHz ^1H - ^1H NOESY Spectra of **3a**



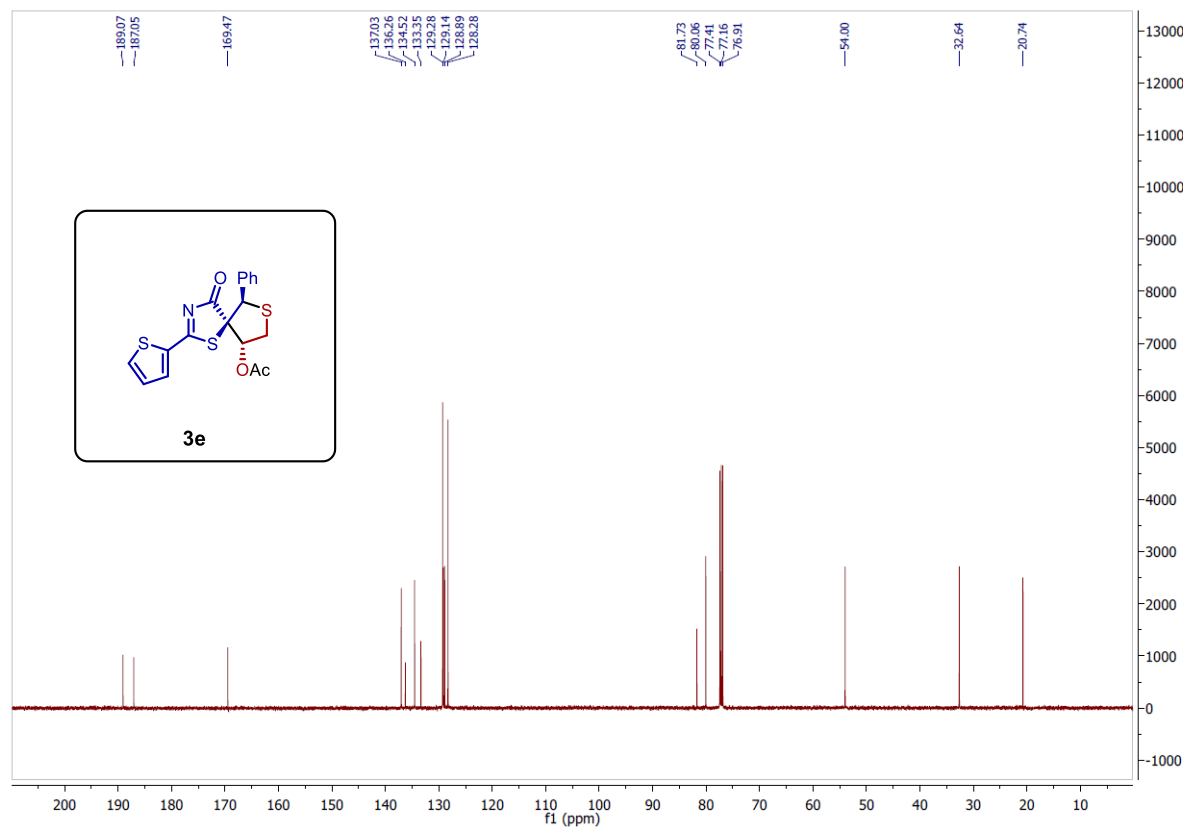
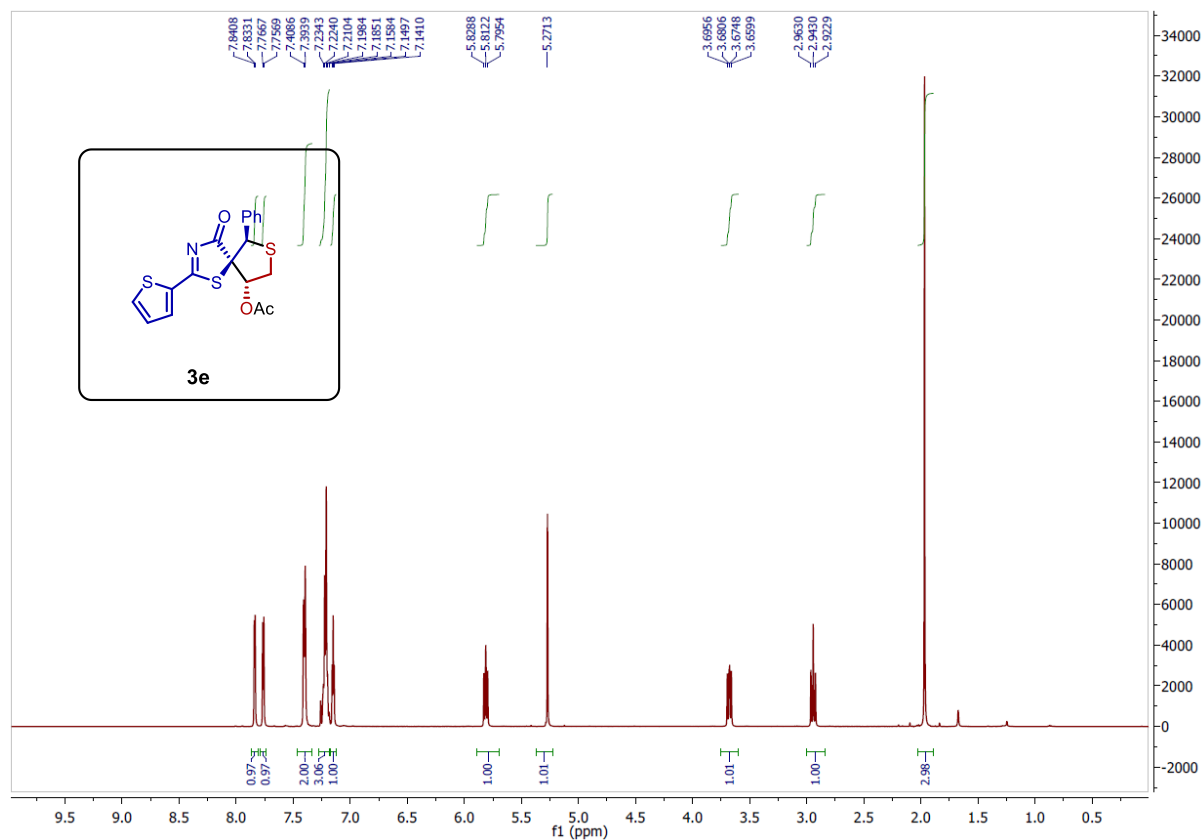
500 MHz ^1H NMR and 125 MHz ^{13}C NMR Spectra of **3b**



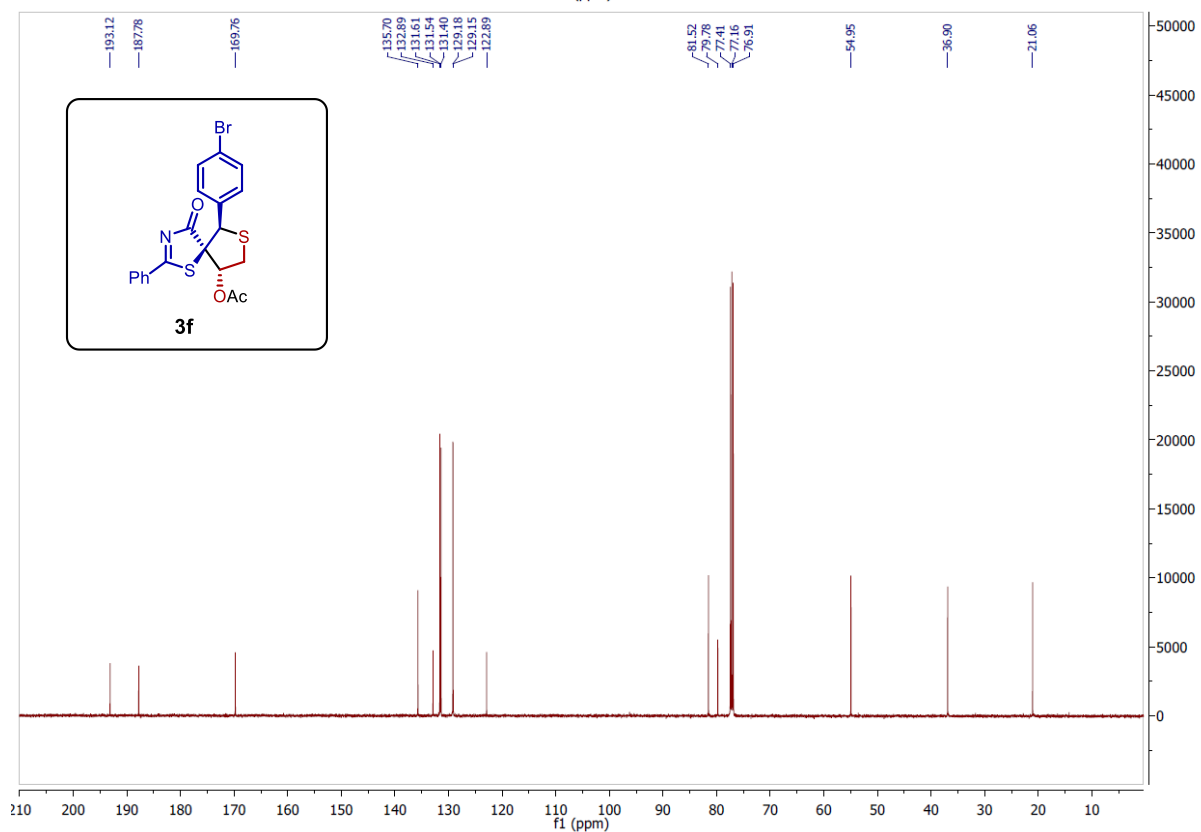
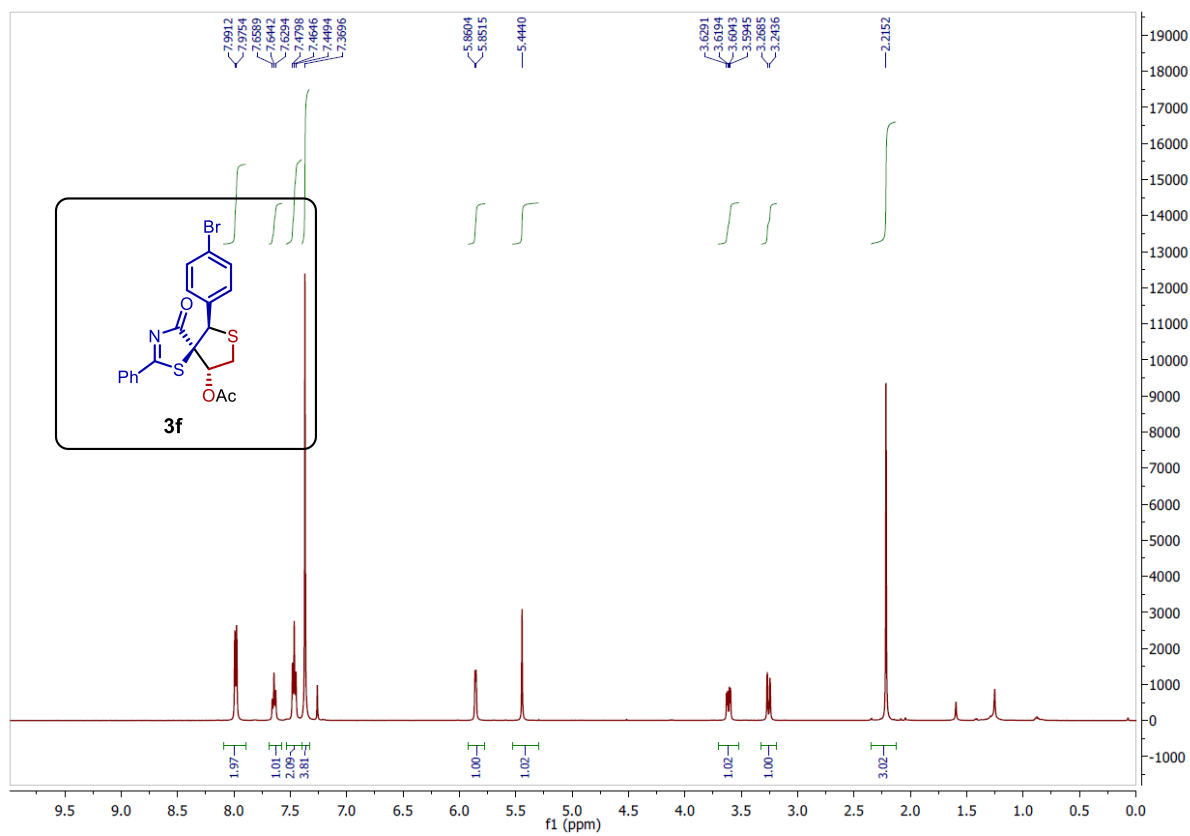
500 MHz ^1H NMR and 125 MHz ^{13}C NMR Spectra of **3c**



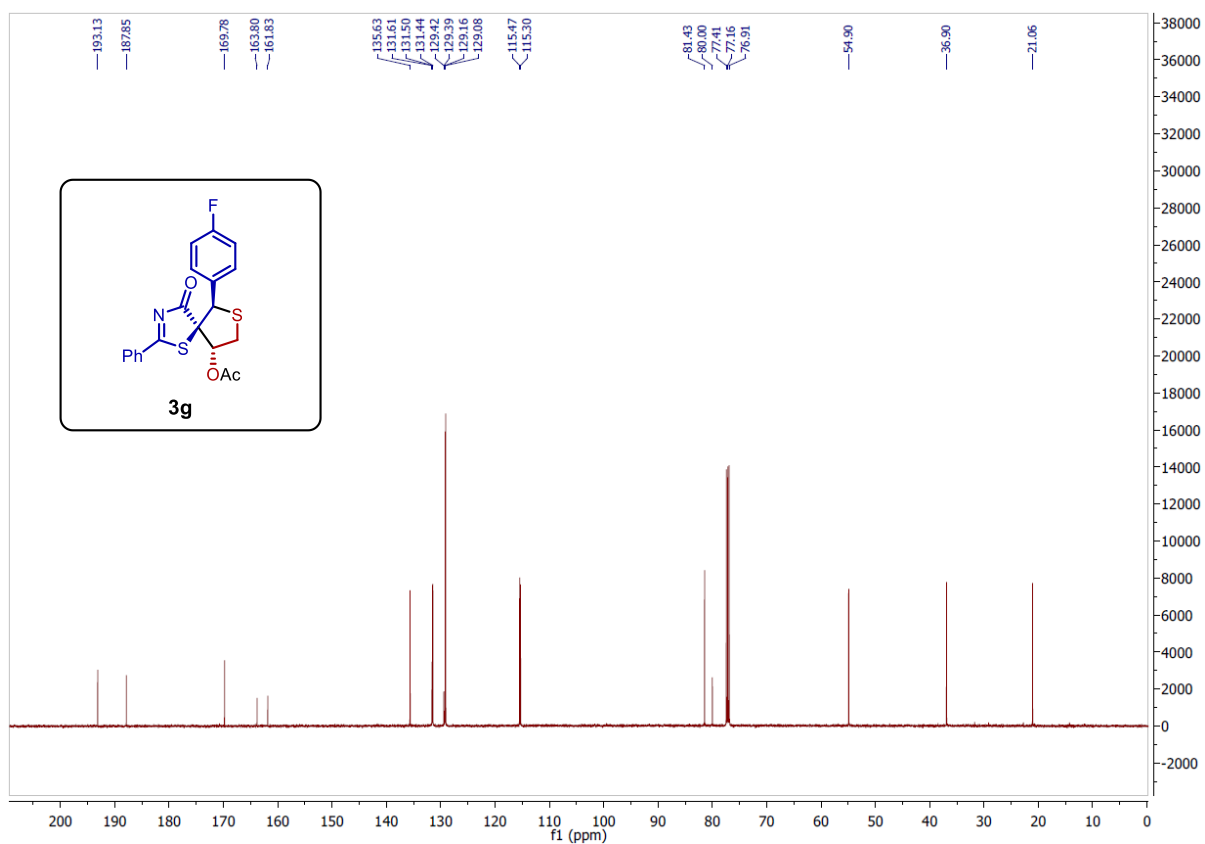
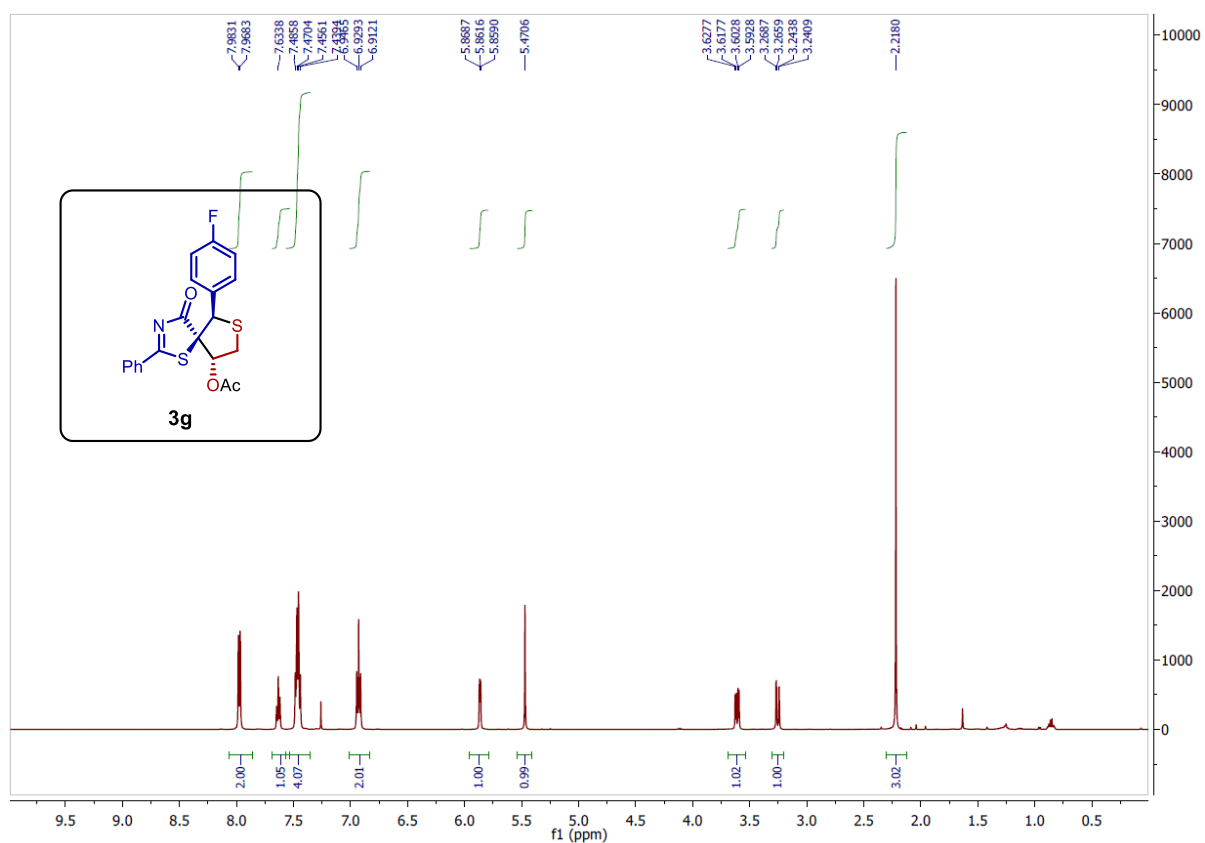
500 MHz ^1H NMR and 125 MHz ^{13}C NMR Spectra of **3d**



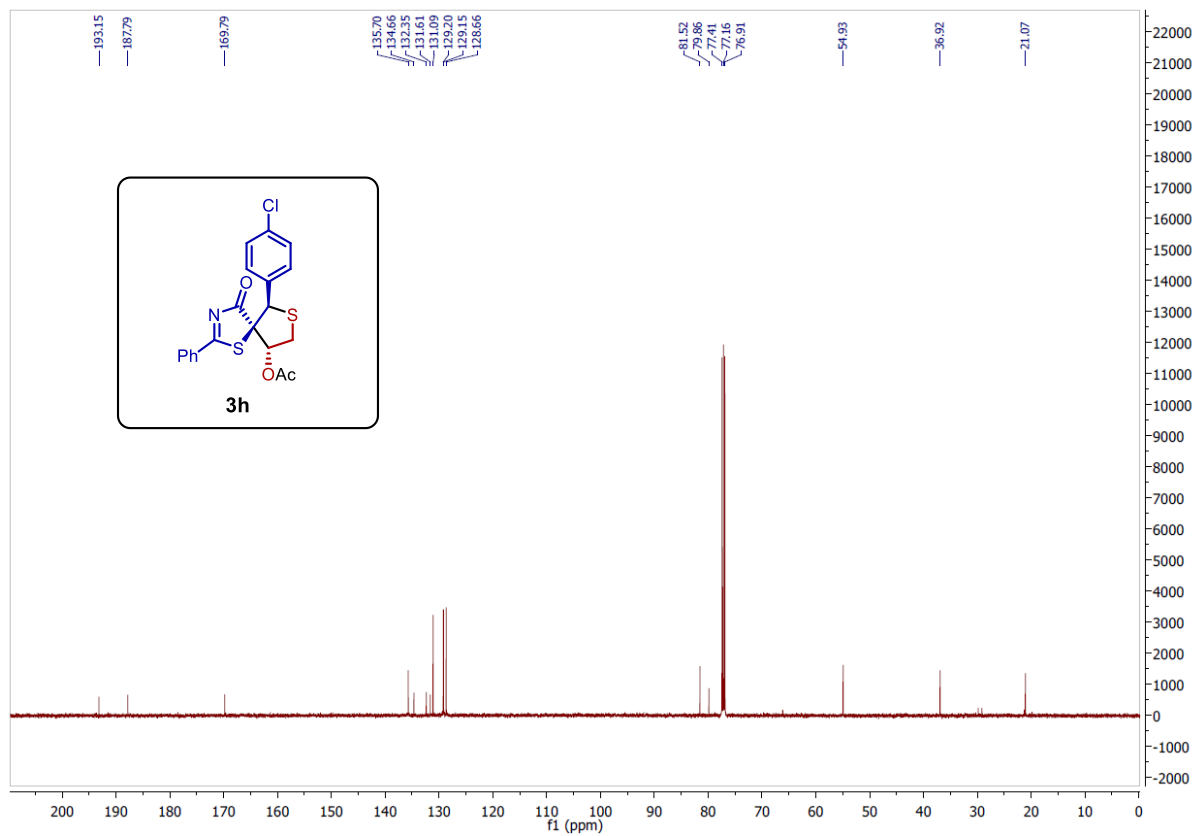
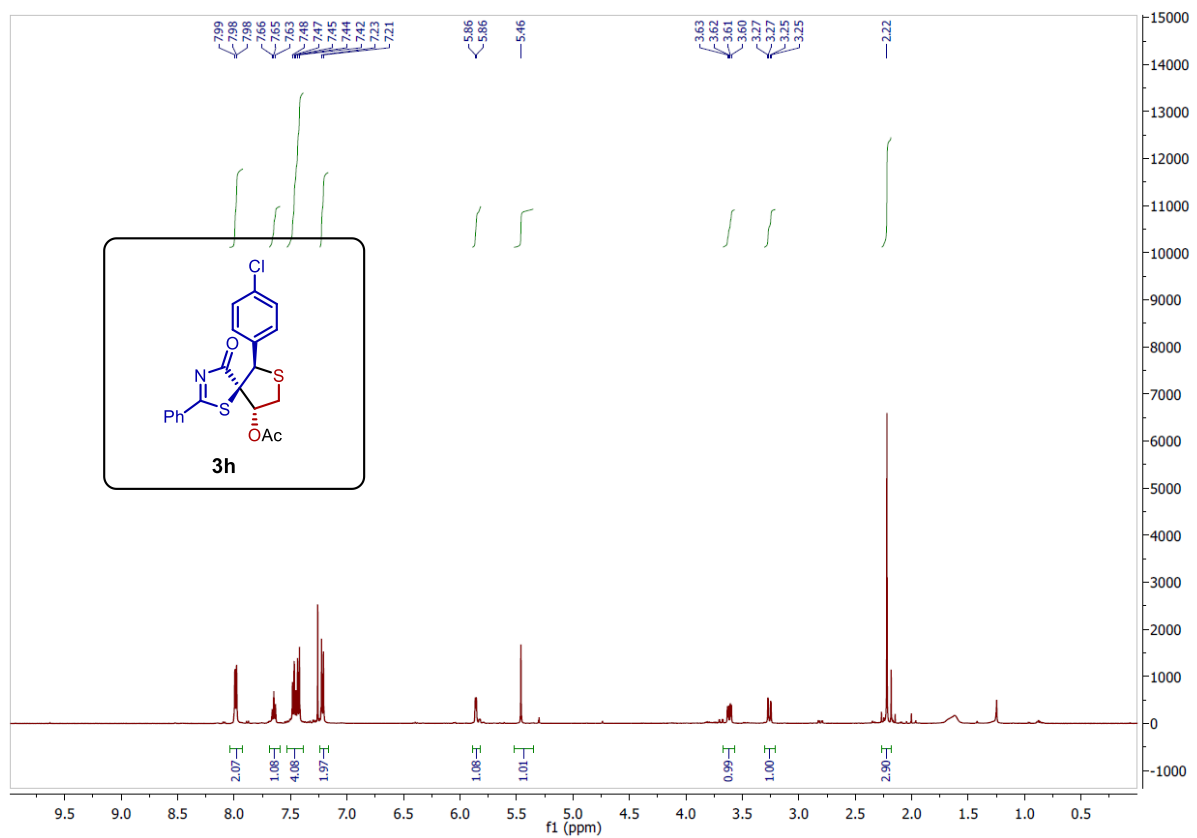
500 MHz ¹H NMR and 125 MHz ¹³C NMR Spectra of **3e**



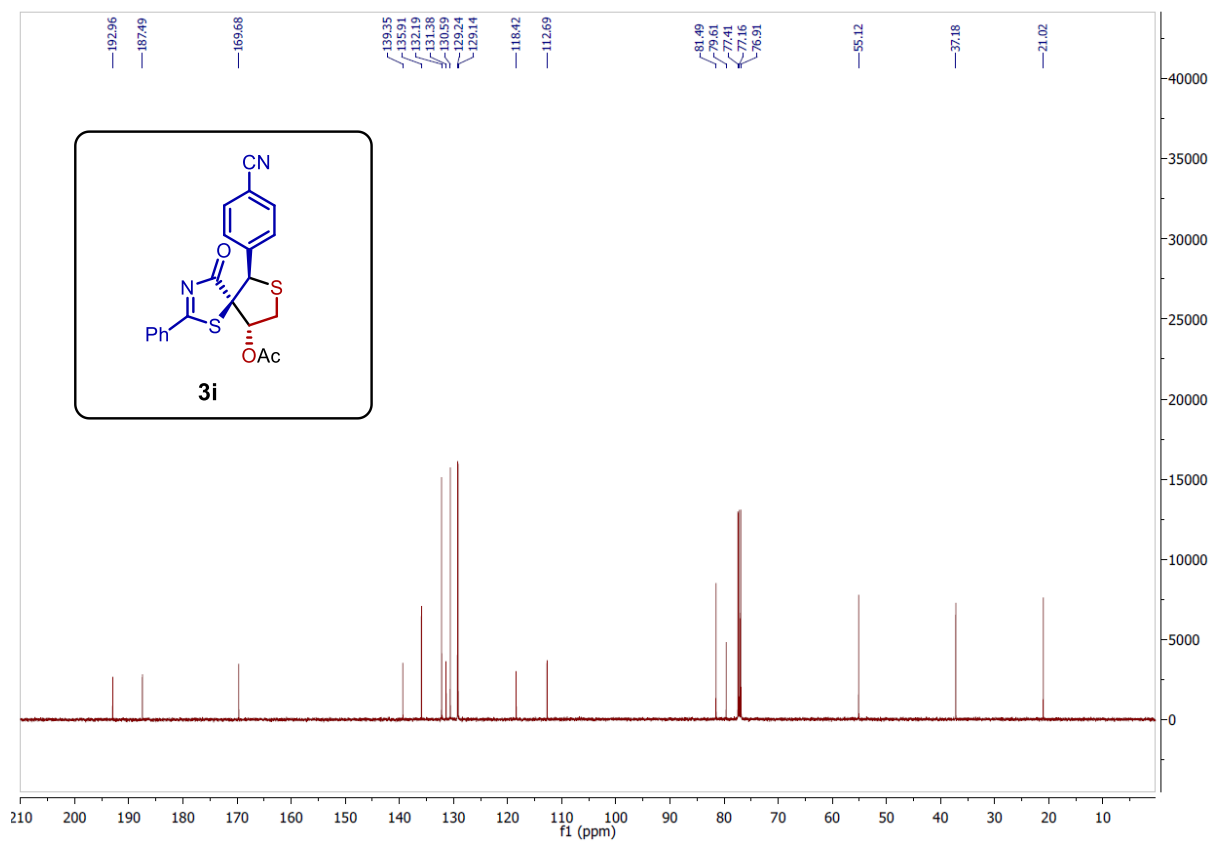
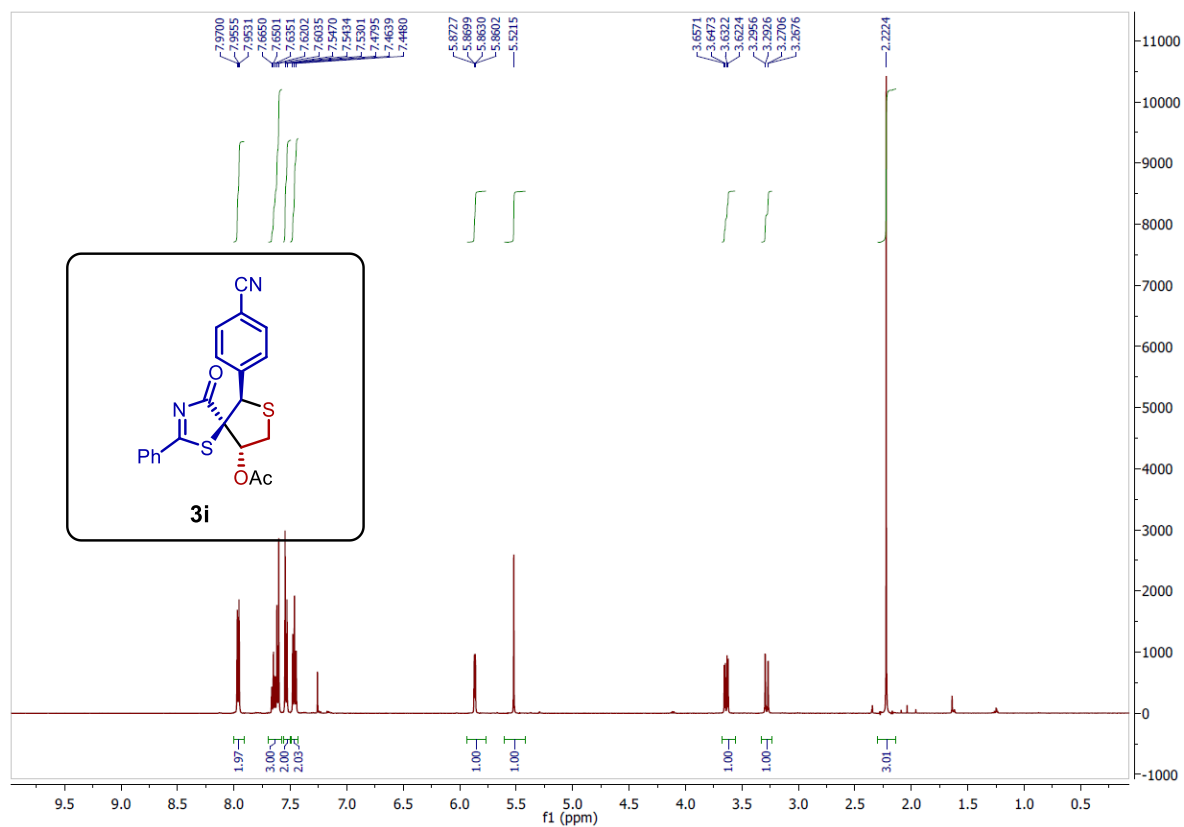
500 MHz ^1H NMR and 125 MHz ^{13}C NMR Spectra of **3f**



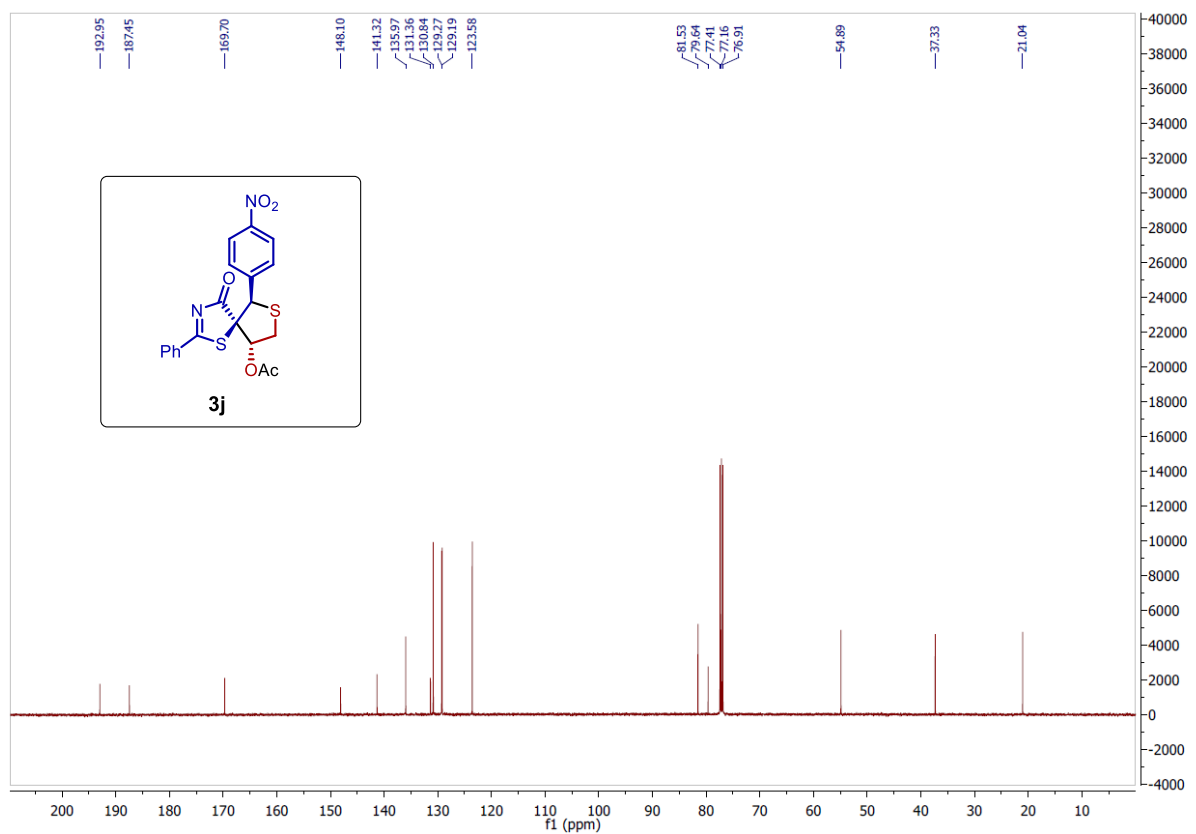
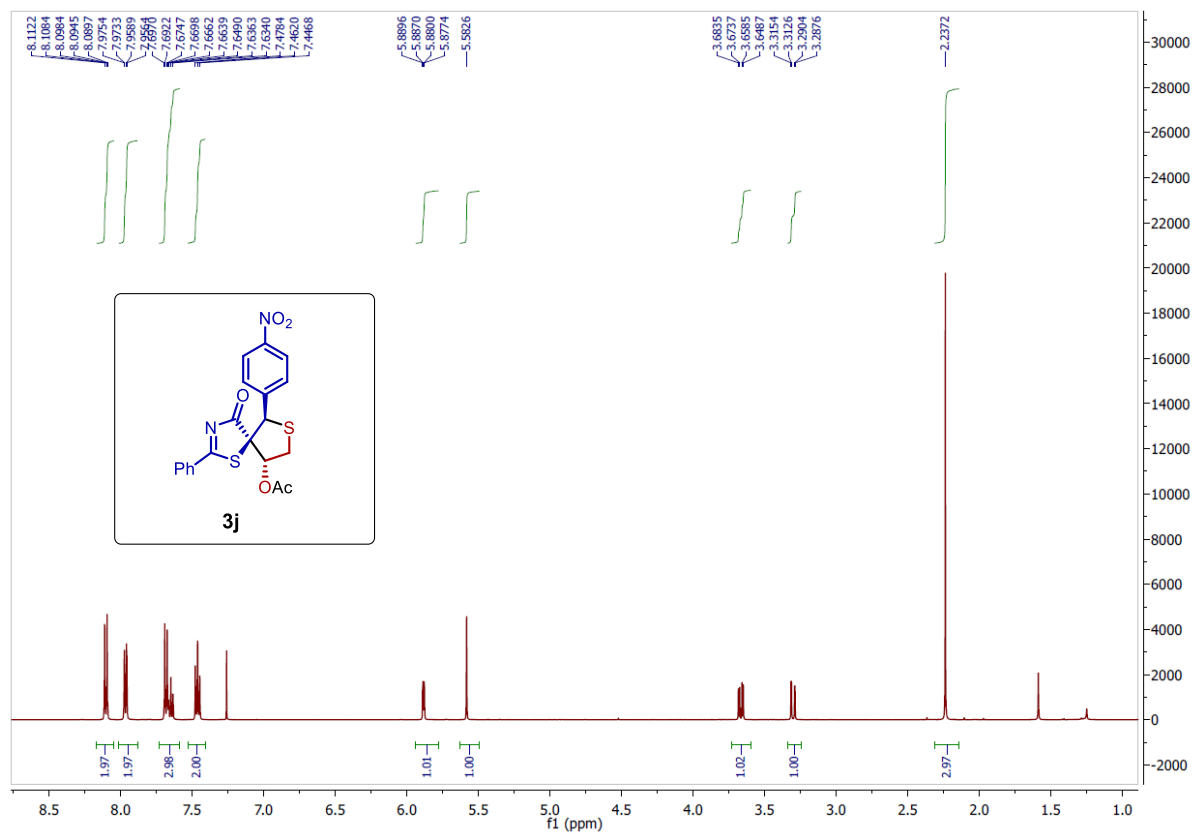
500 MHz ¹H NMR and 125 MHz ¹³C NMR Spectra of **3g**



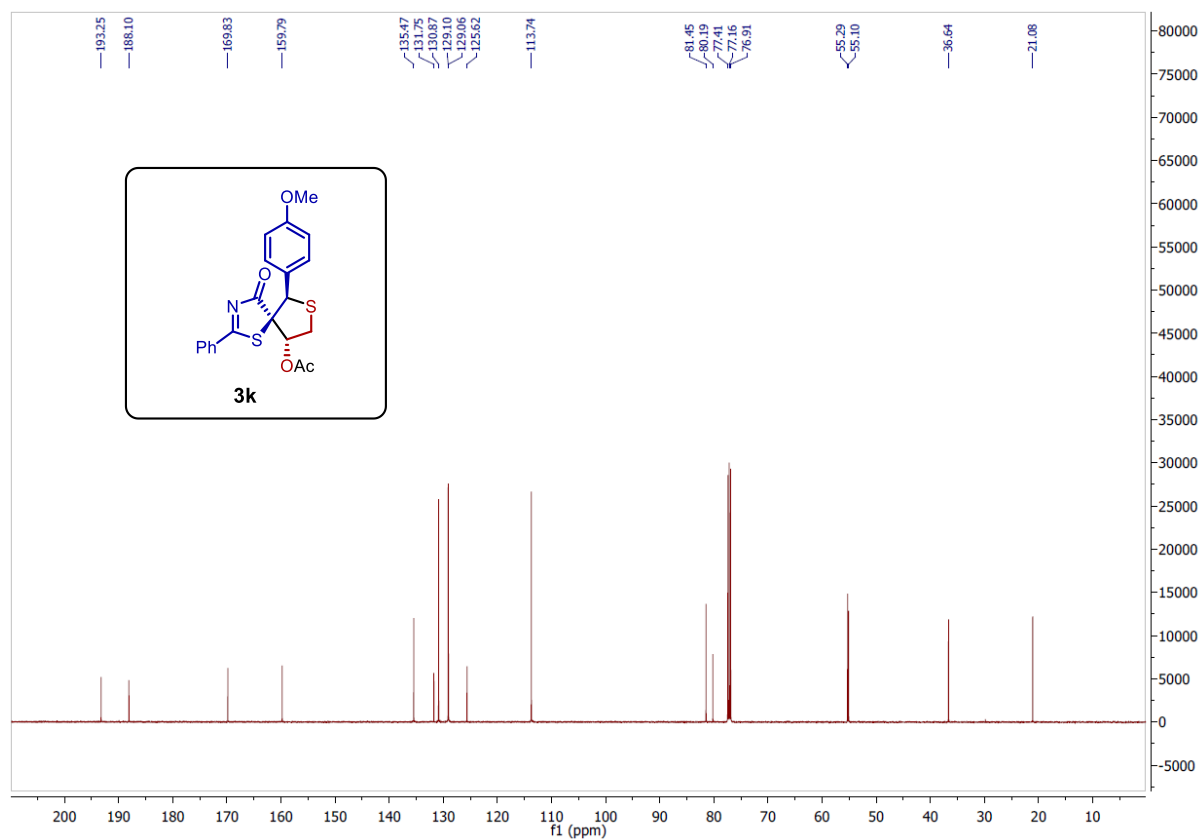
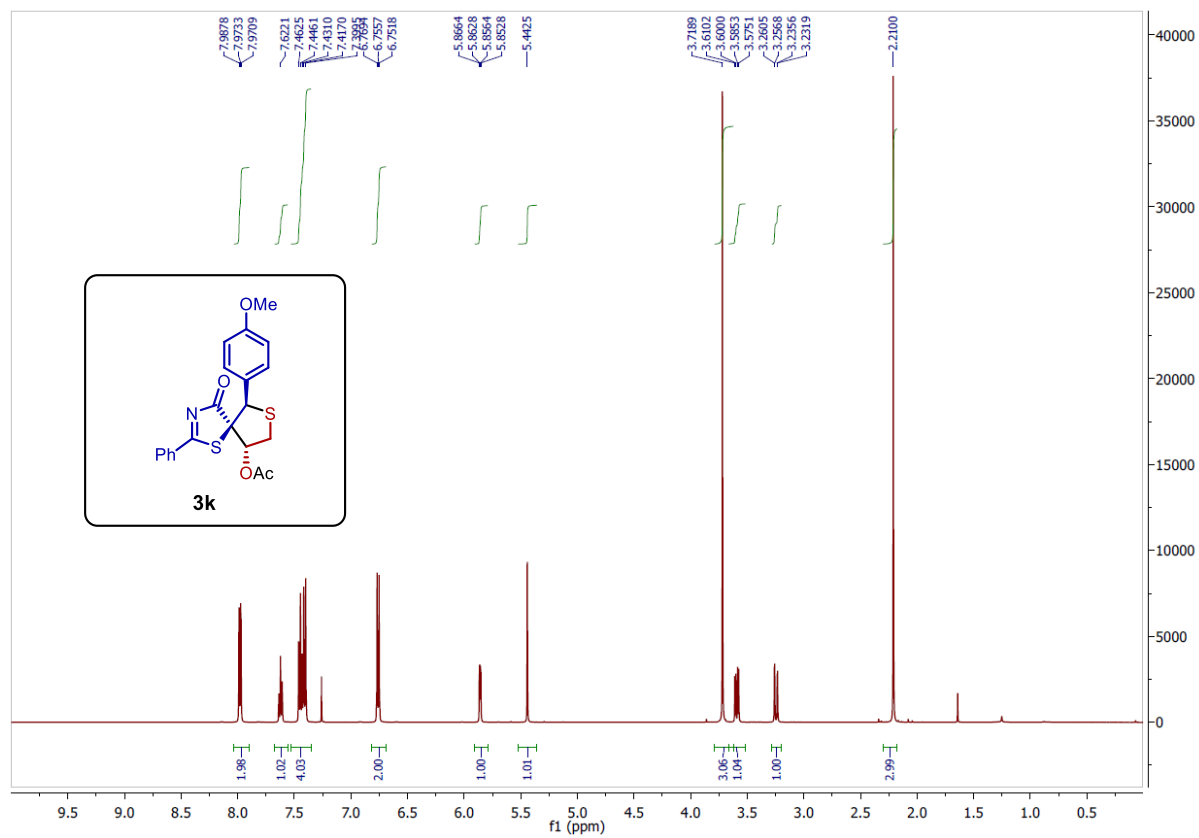
500 MHz ^1H NMR and 125 MHz ^{13}C NMR Spectra of **3h**



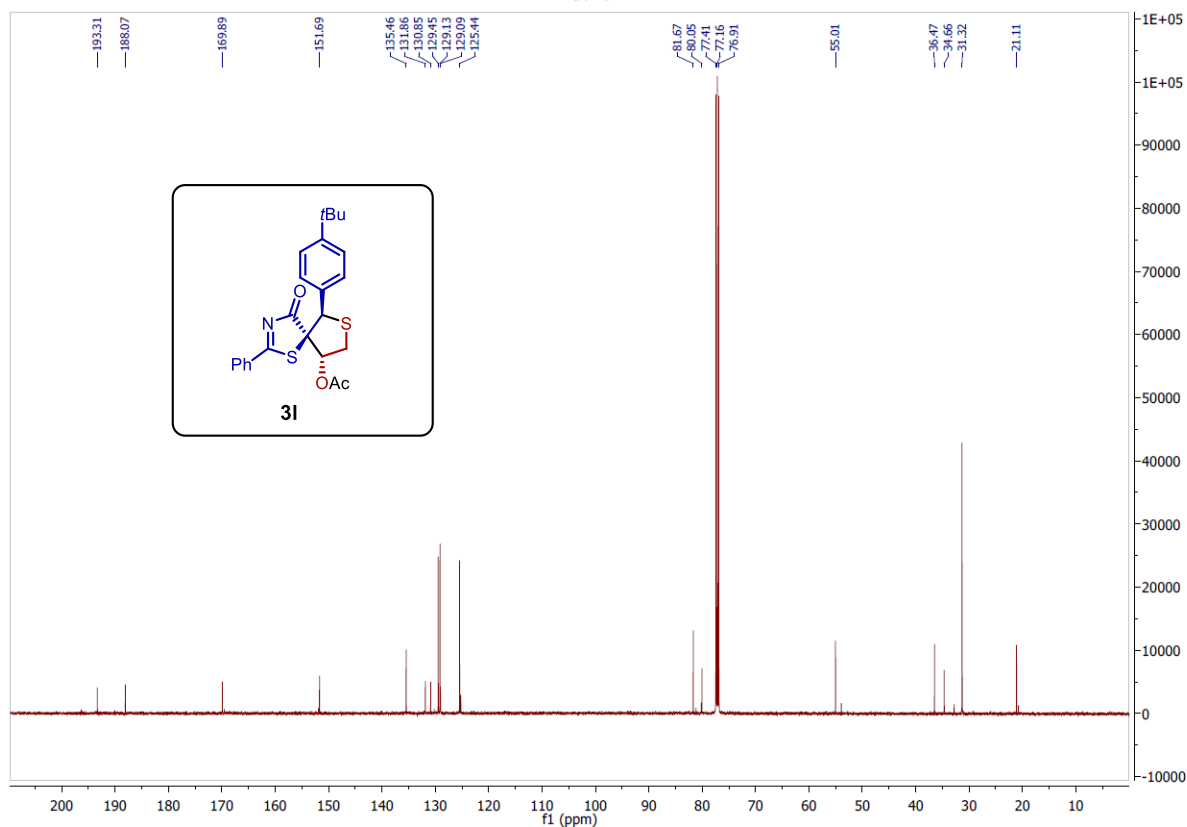
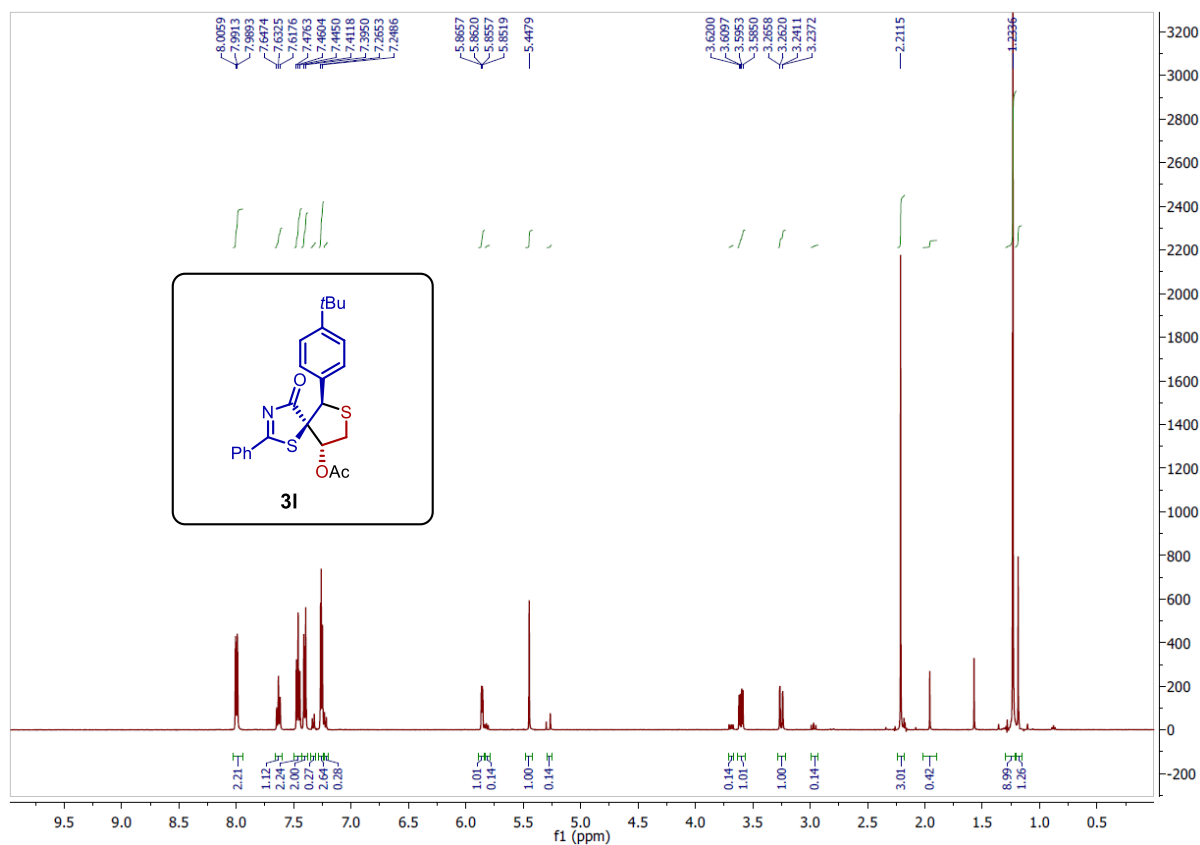
500 MHz ^1H NMR and 125 MHz ^{13}C NMR Spectra of **3i**



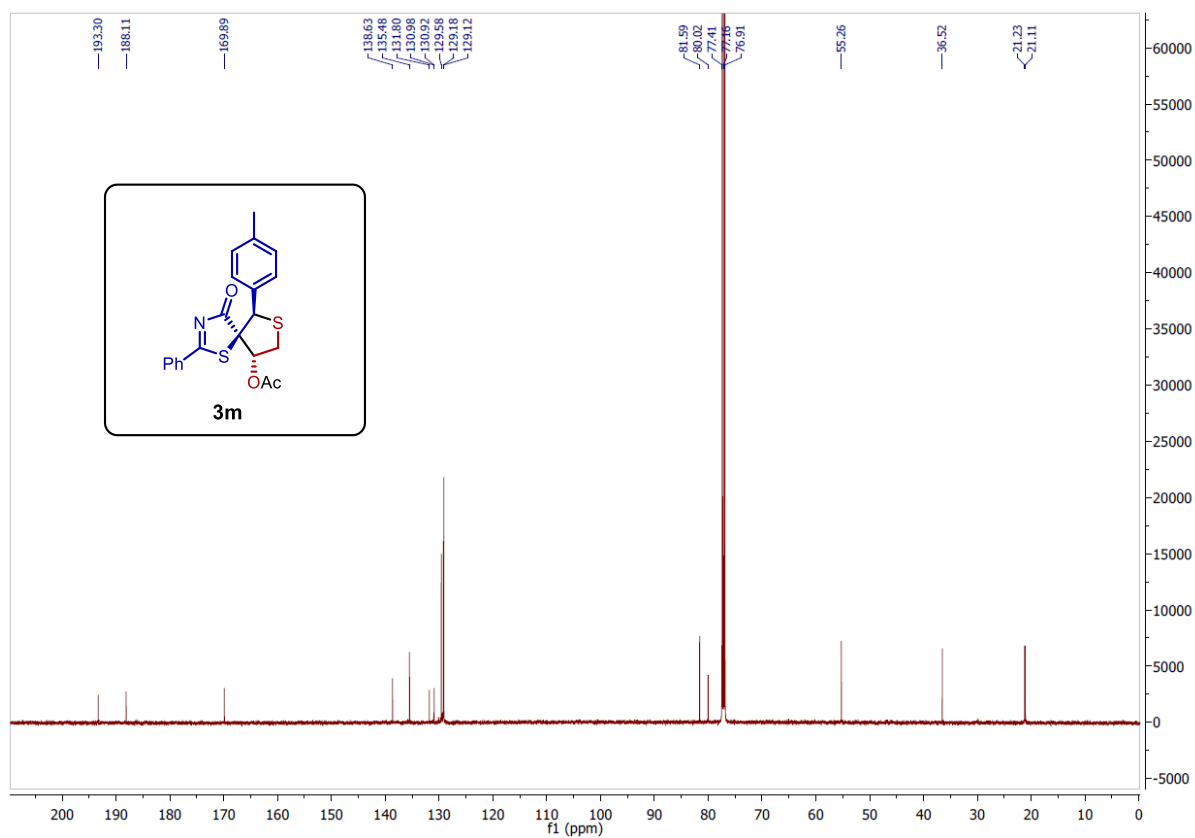
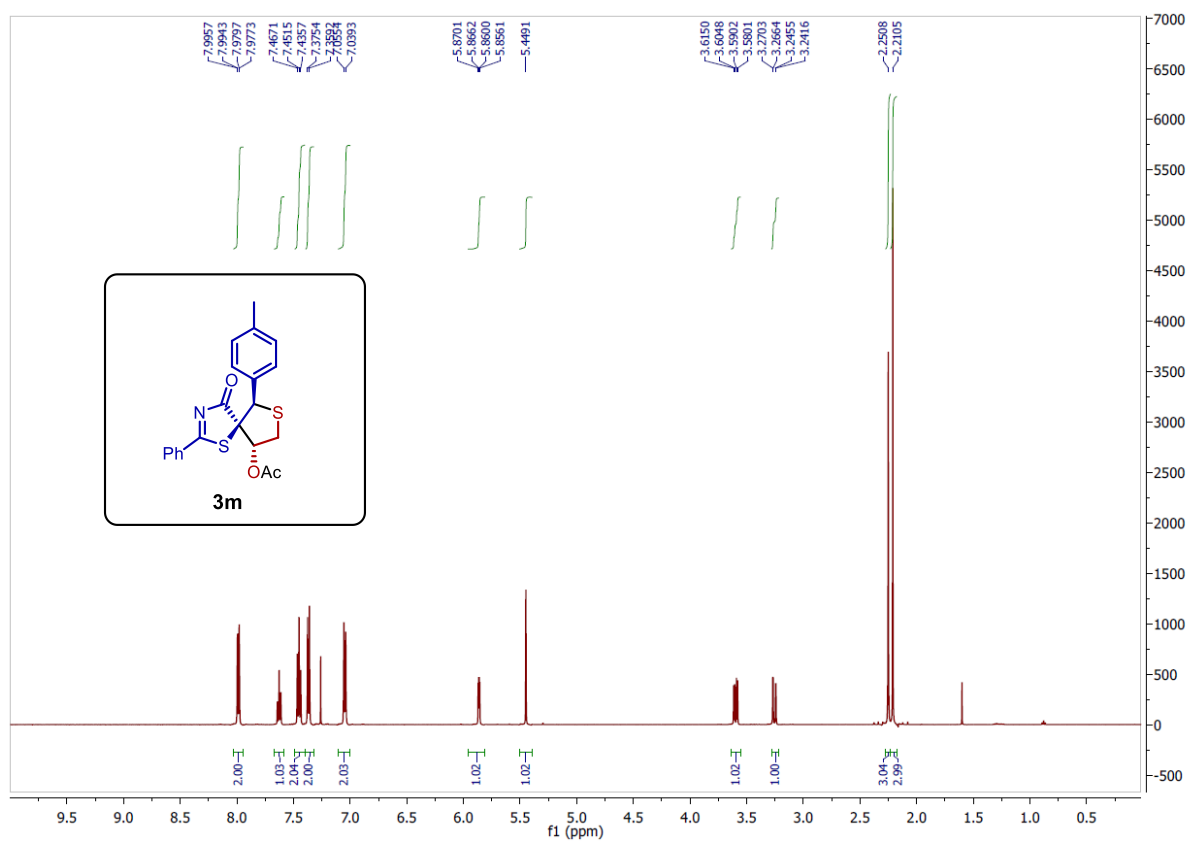
500 MHz ¹H NMR and 125 MHz ¹³C NMR Spectra of **3j**



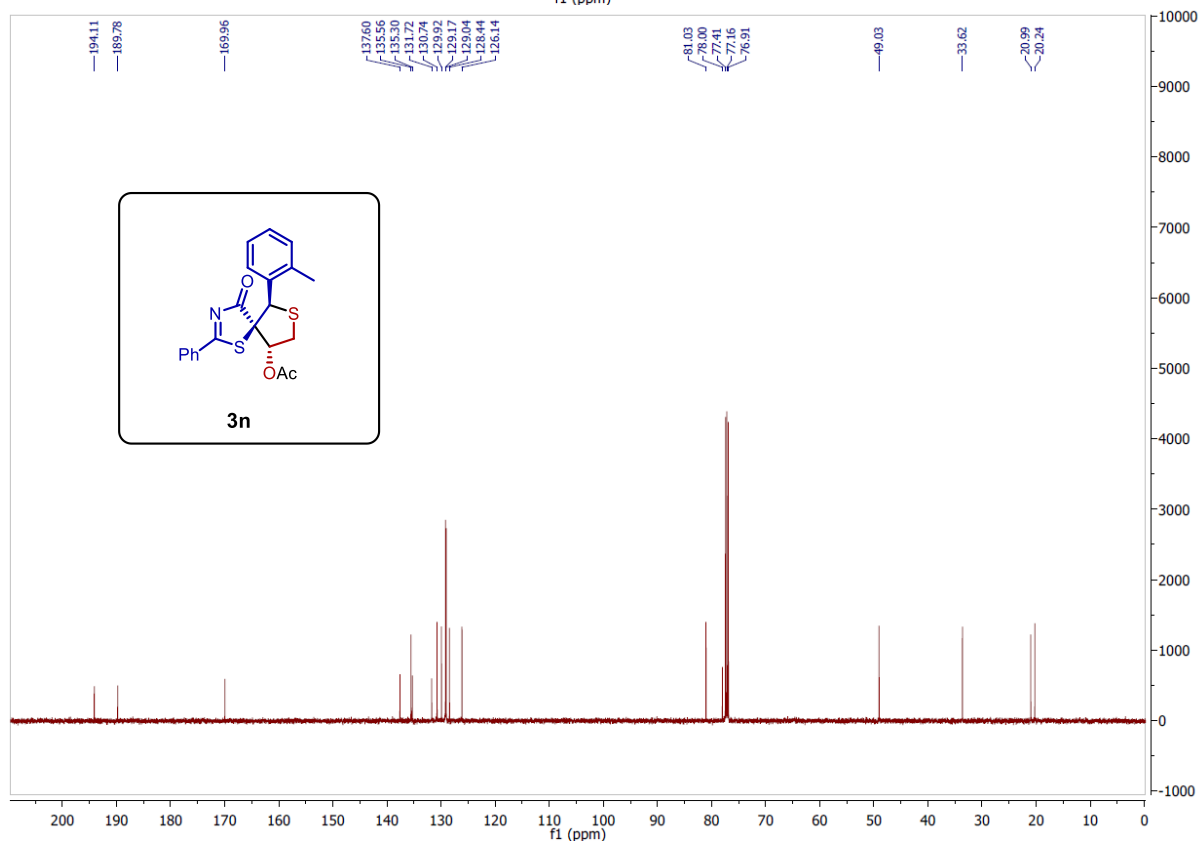
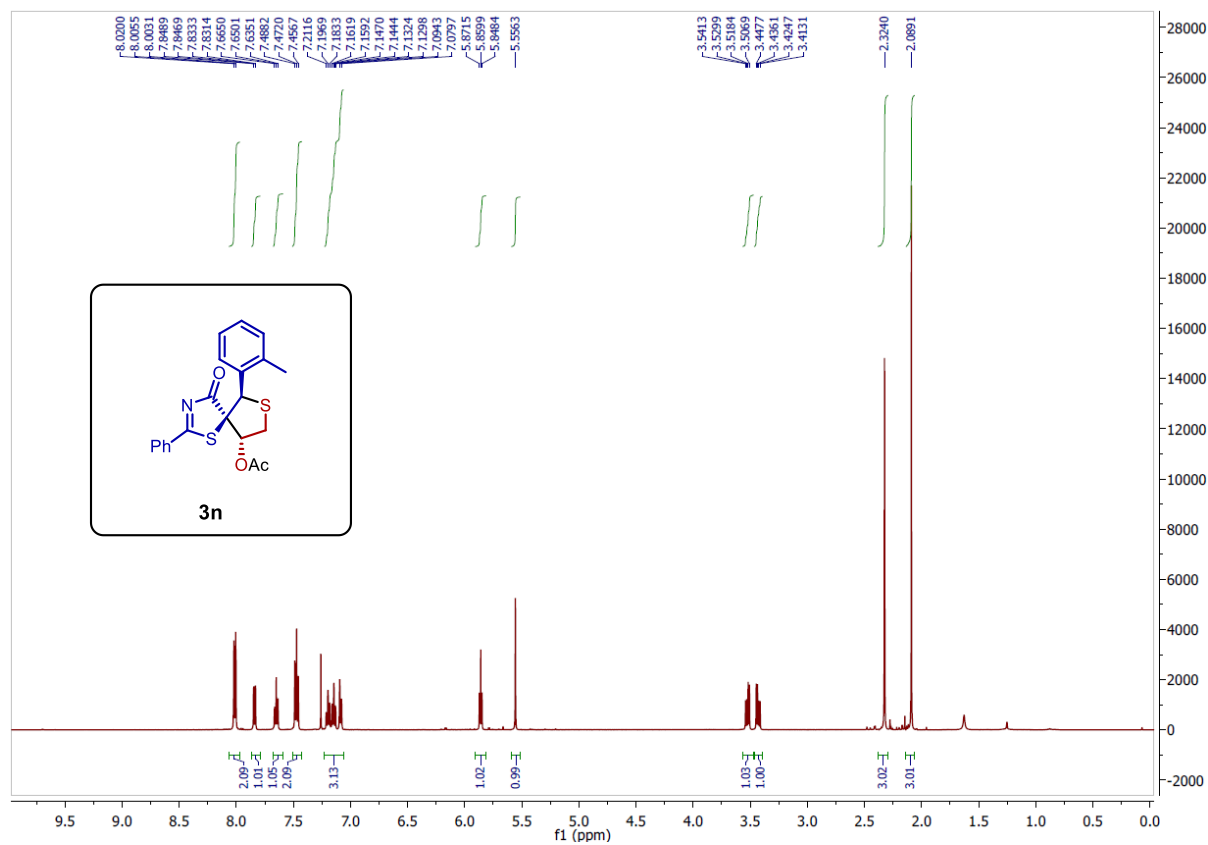
500 MHz ¹H NMR and 125 MHz ¹³C NMR Spectra of **3k**



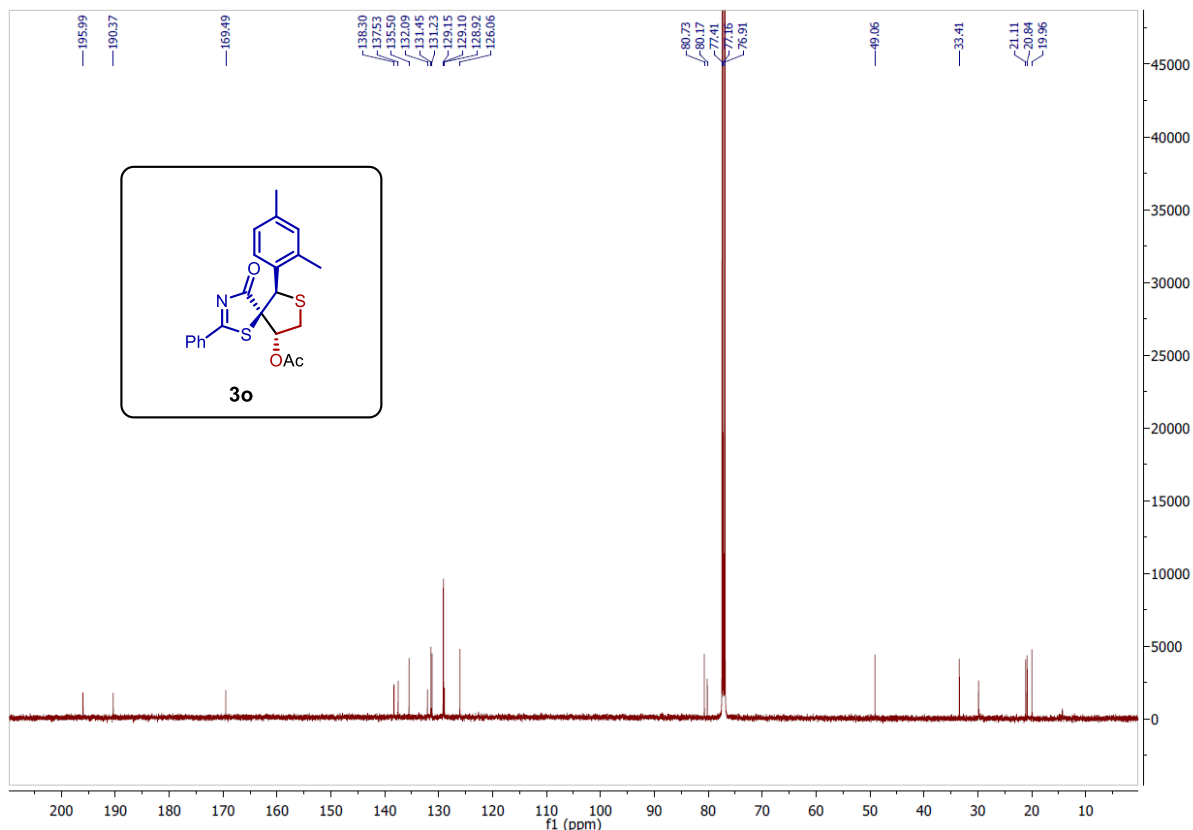
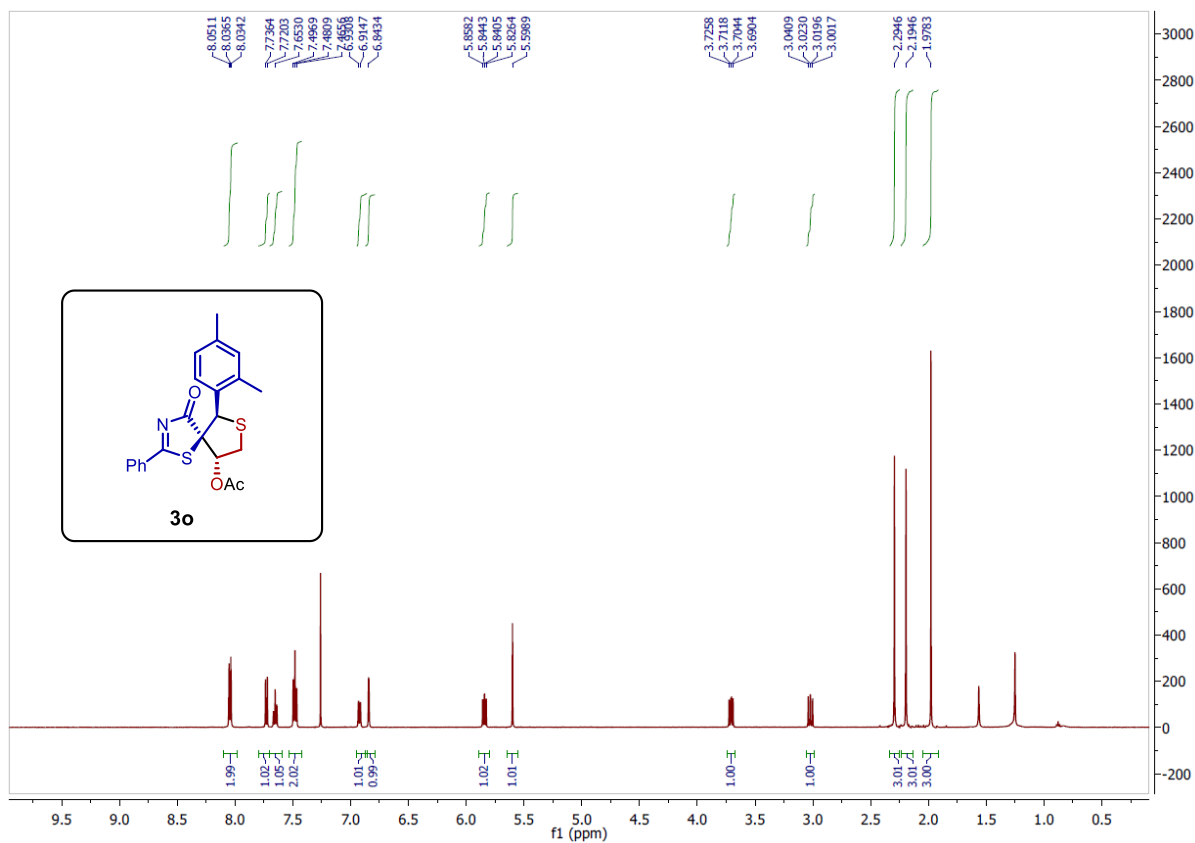
500 MHz ^1H NMR and 125 MHz ^{13}C NMR Spectra of **3I**



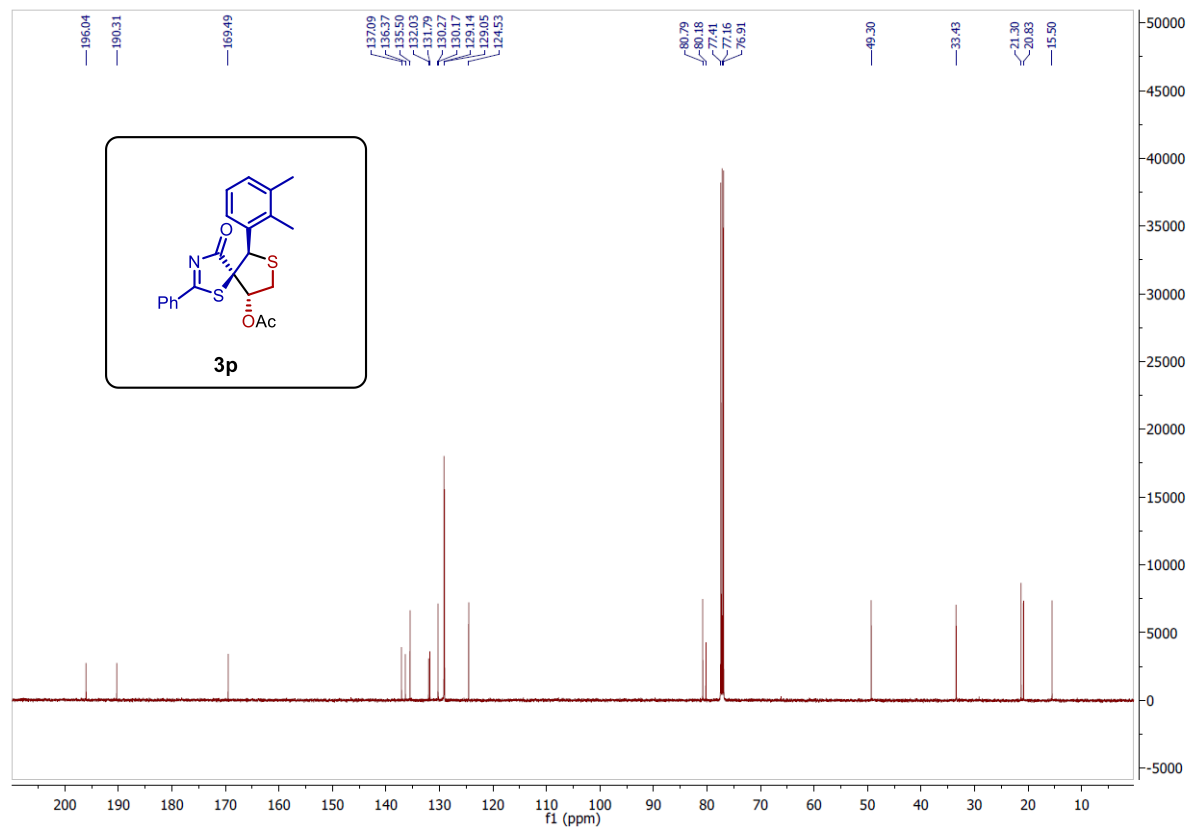
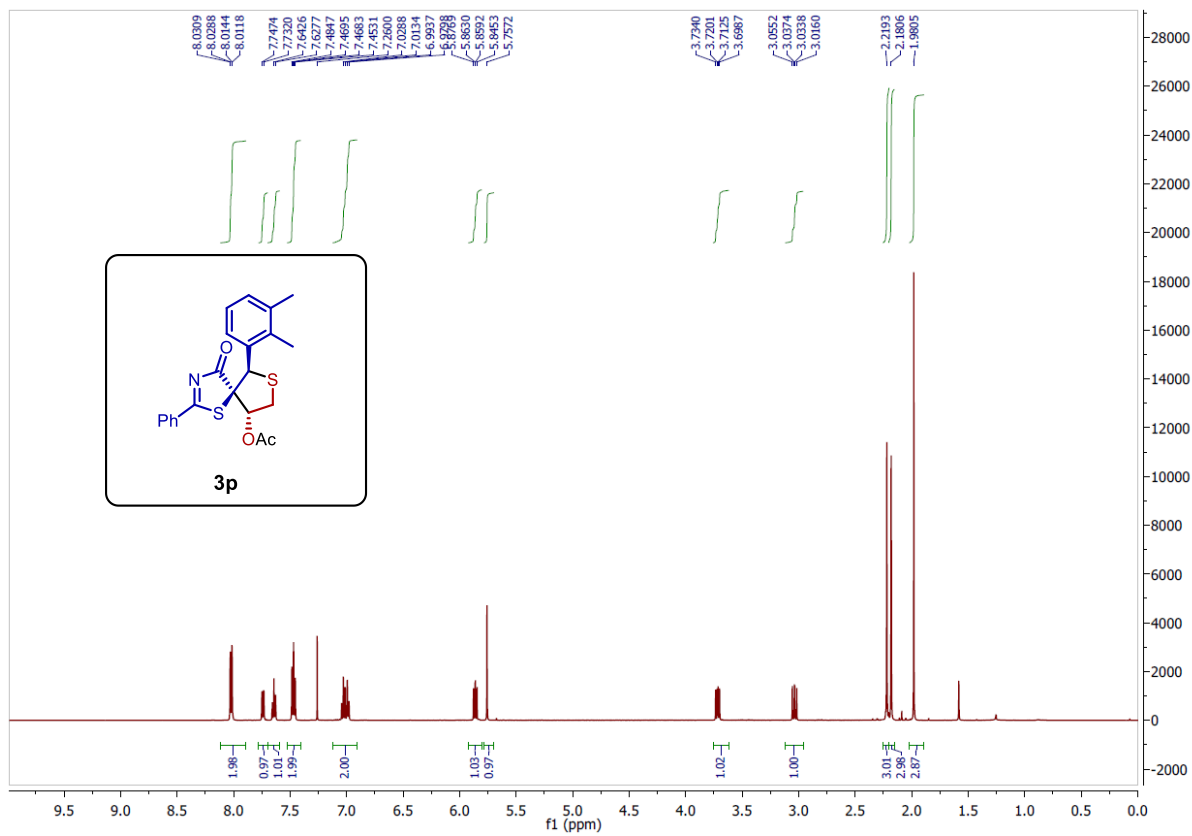
500 MHz ^1H NMR and 125 MHz ^{13}C NMR Spectra of **3m**



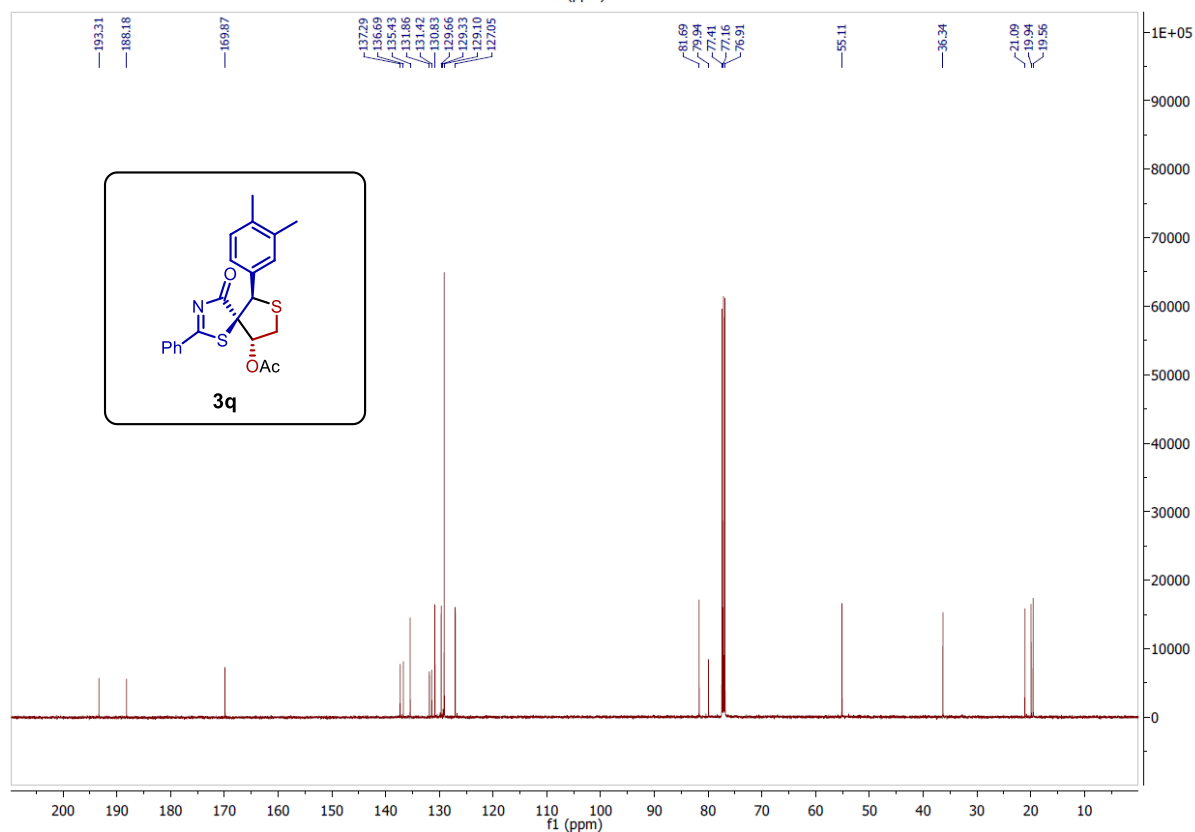
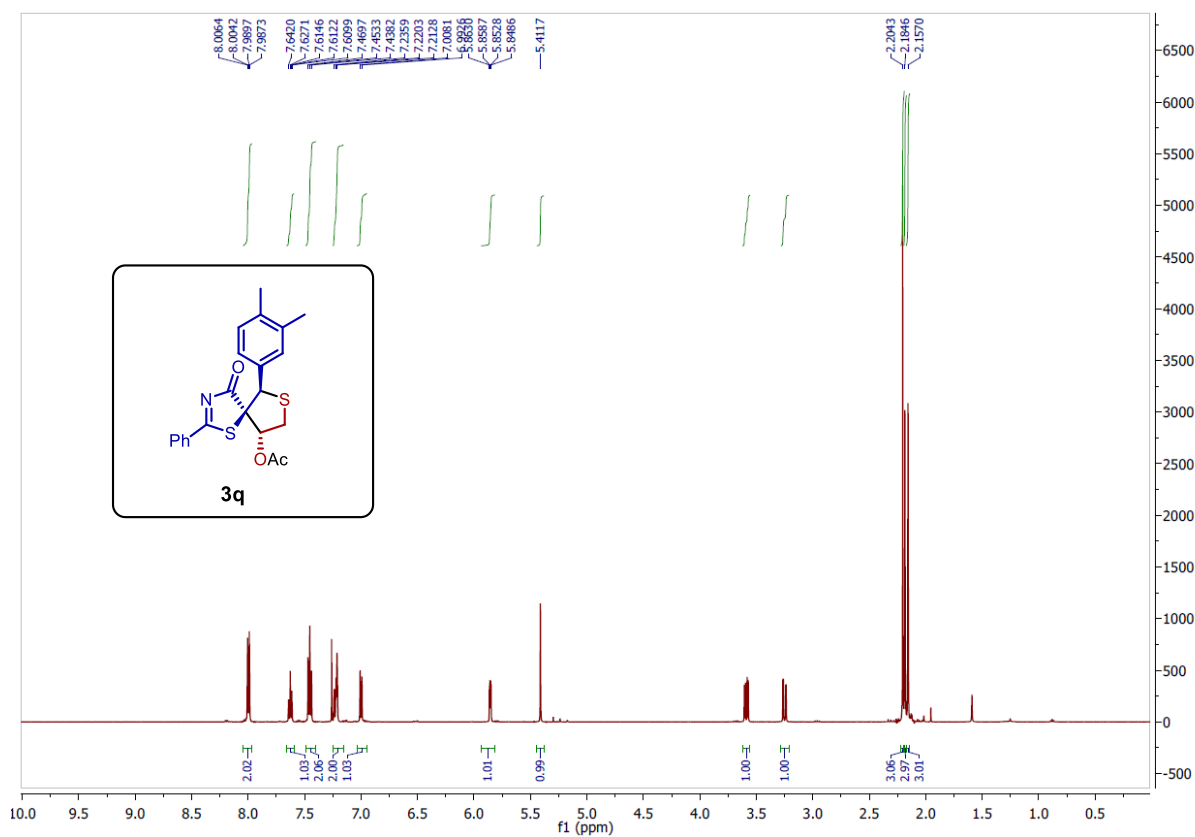
500 MHz ¹H NMR and 125 MHz ¹³C NMR Spectra of **3n**



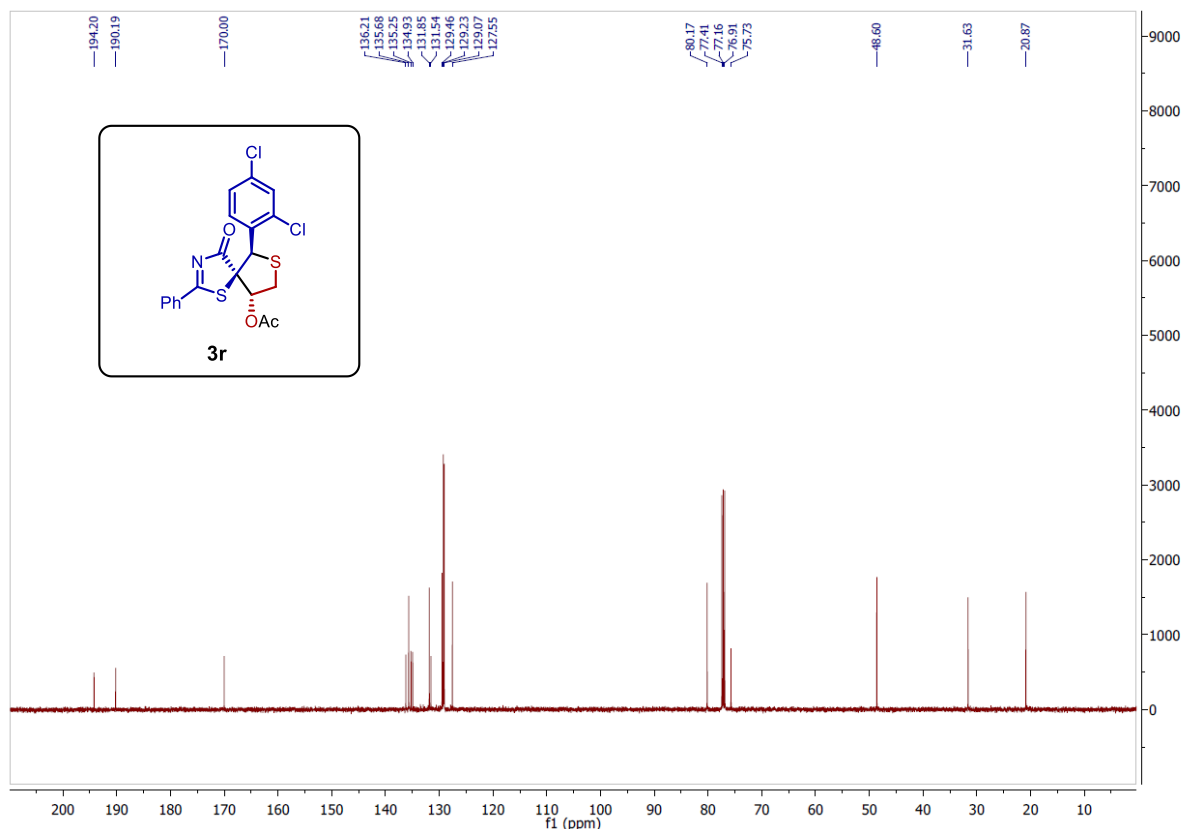
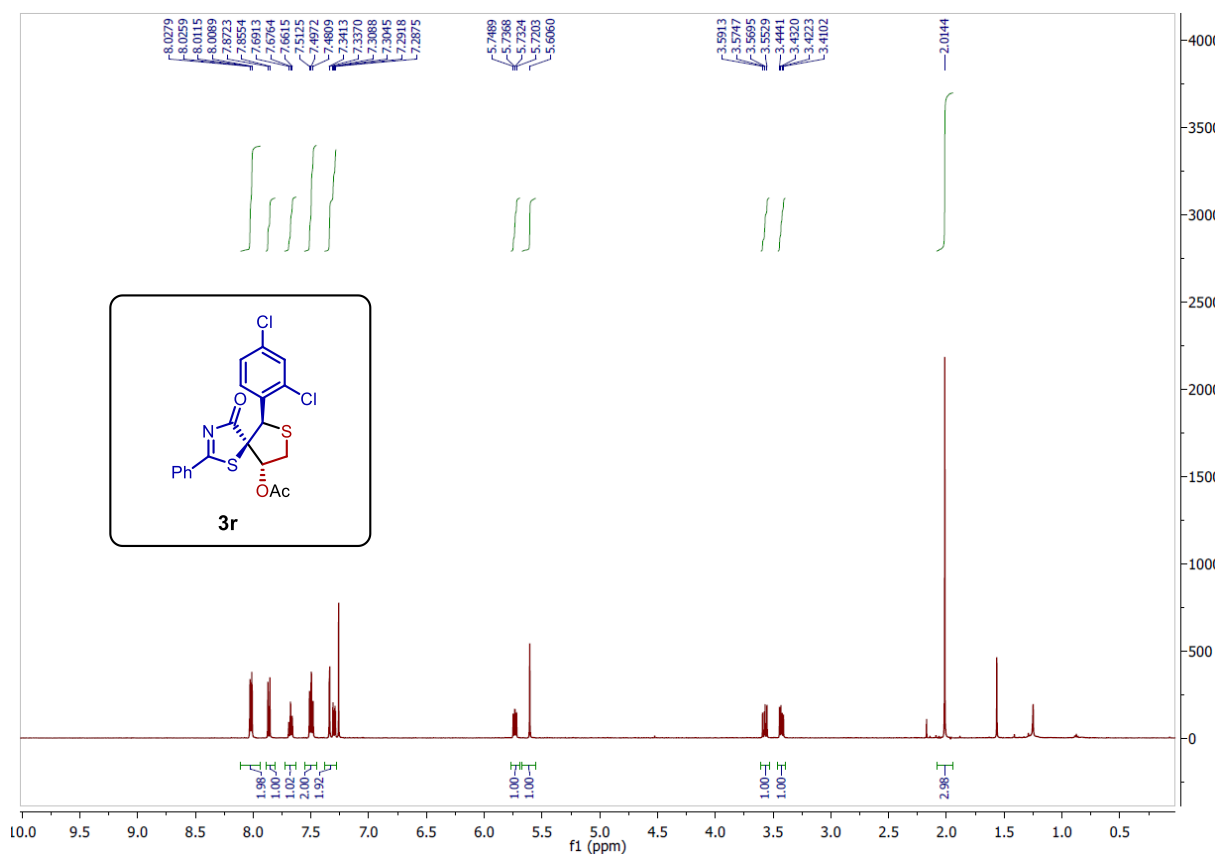
500 MHz ^1H NMR and 125 MHz ^{13}C NMR Spectra of **3o**



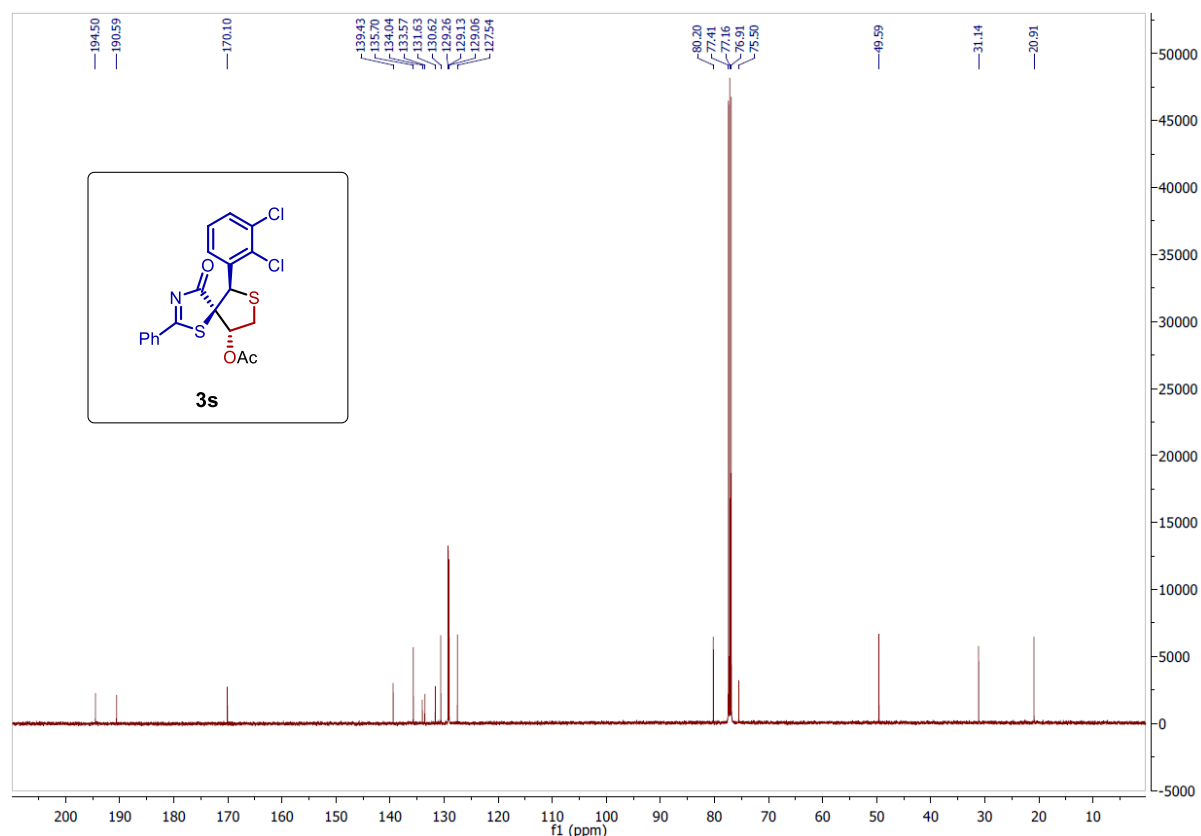
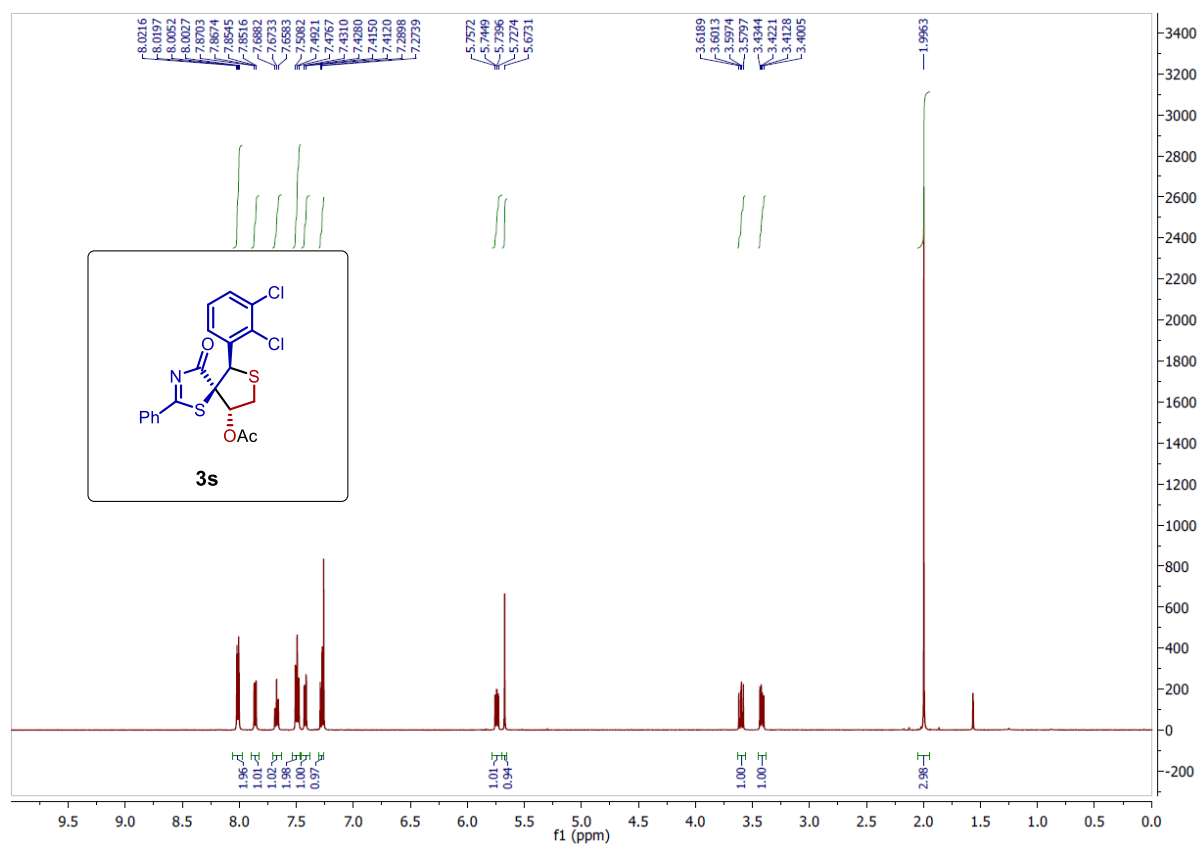
500 MHz ^1H NMR and 125 MHz ^{13}C NMR Spectra of **3p**



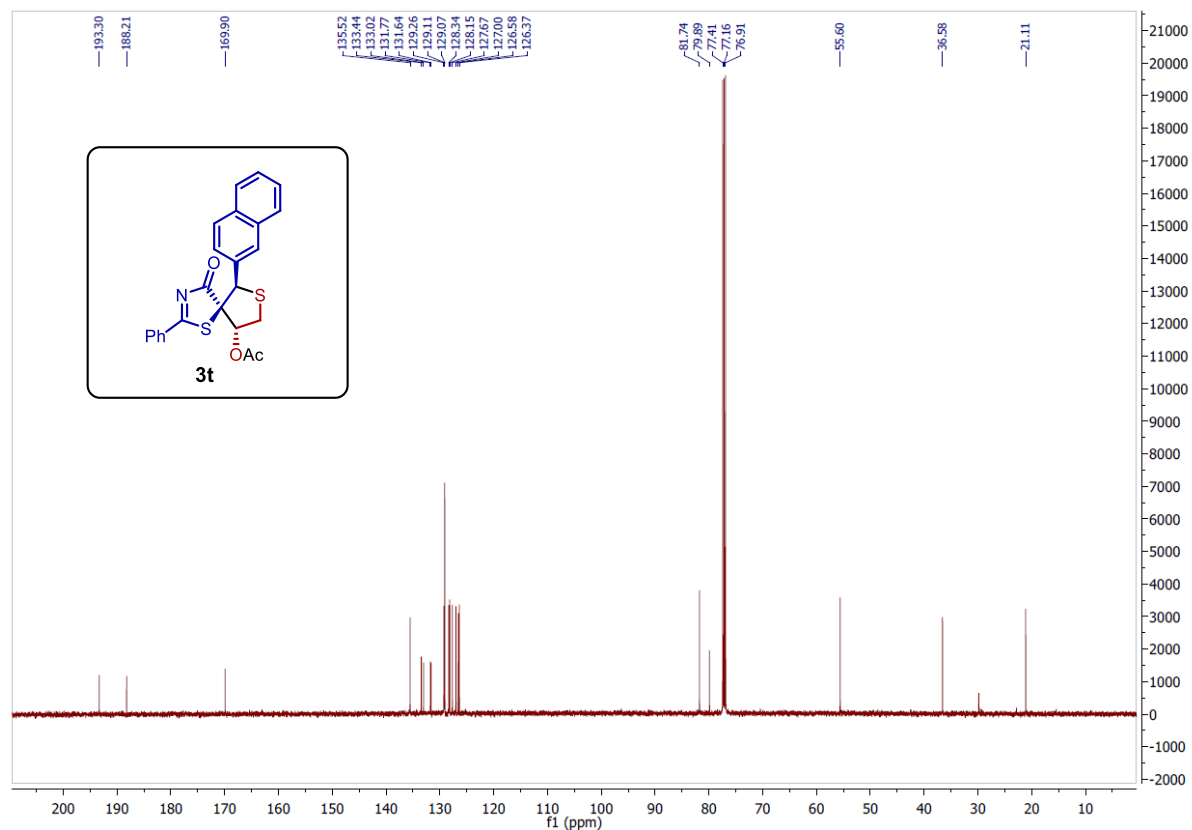
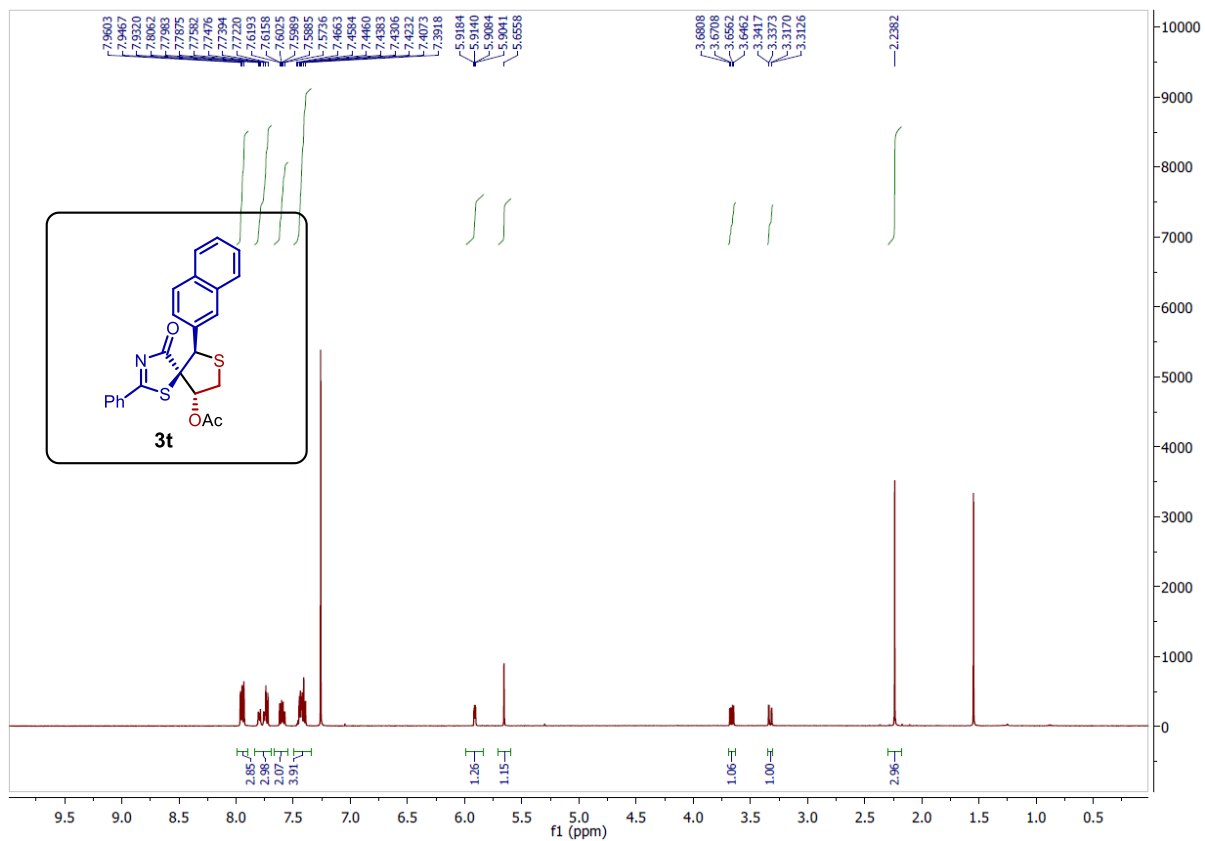
500 MHz ^1H NMR and 125 MHz ^{13}C NMR Spectra of **3q**



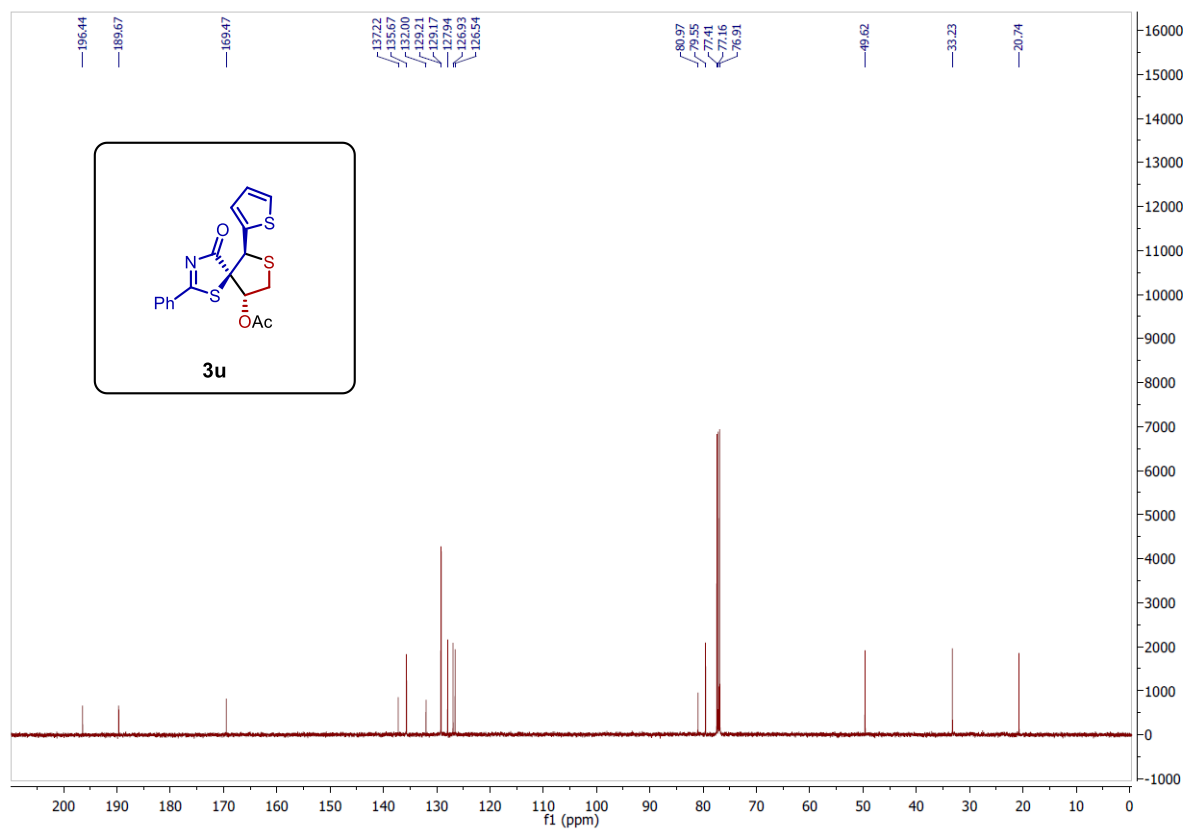
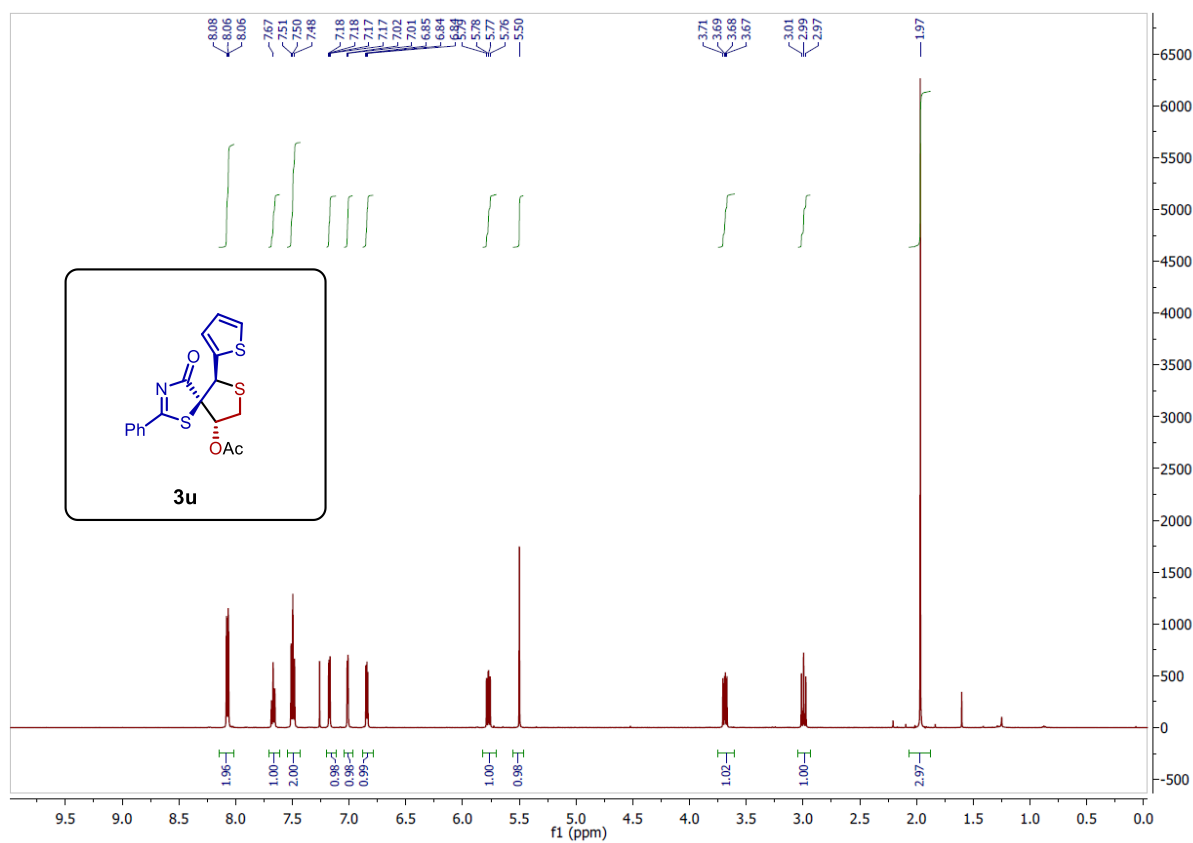
500 MHz ^1H NMR and 125 MHz ^{13}C NMR Spectra of **3r**



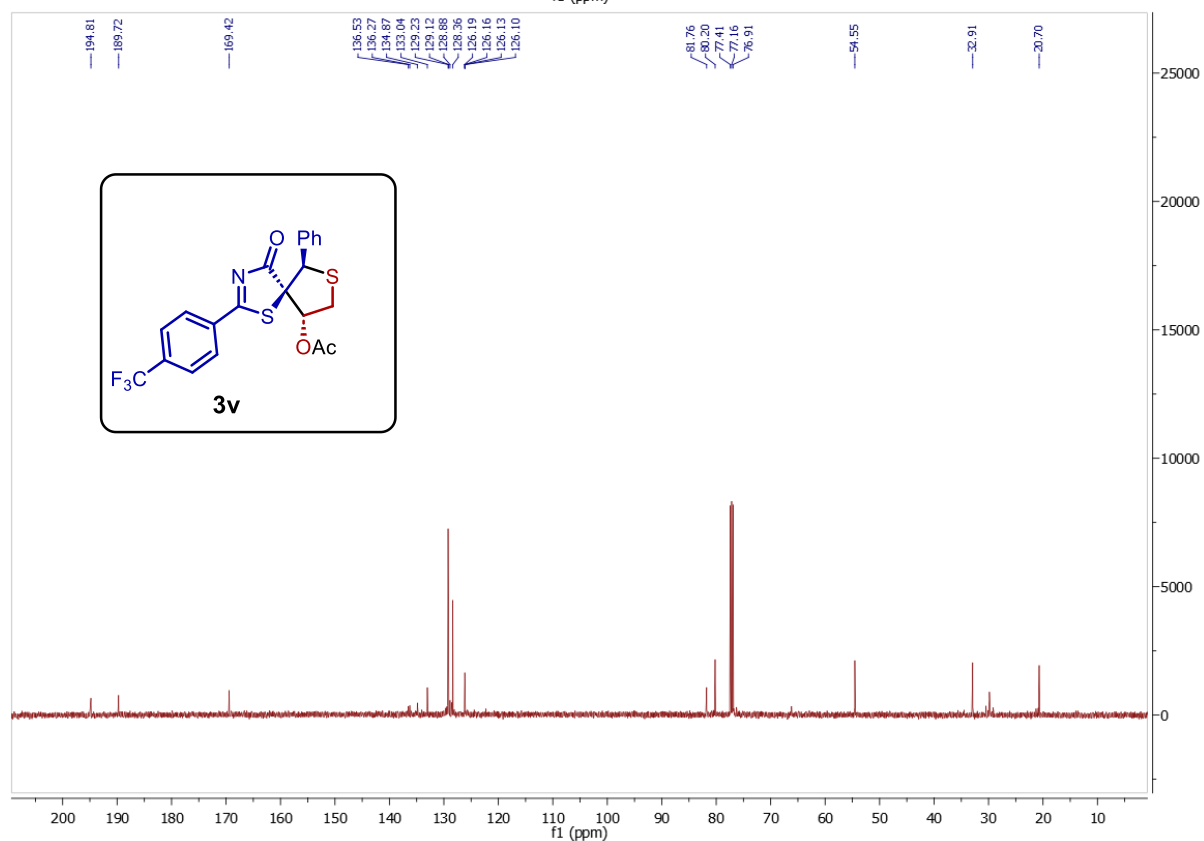
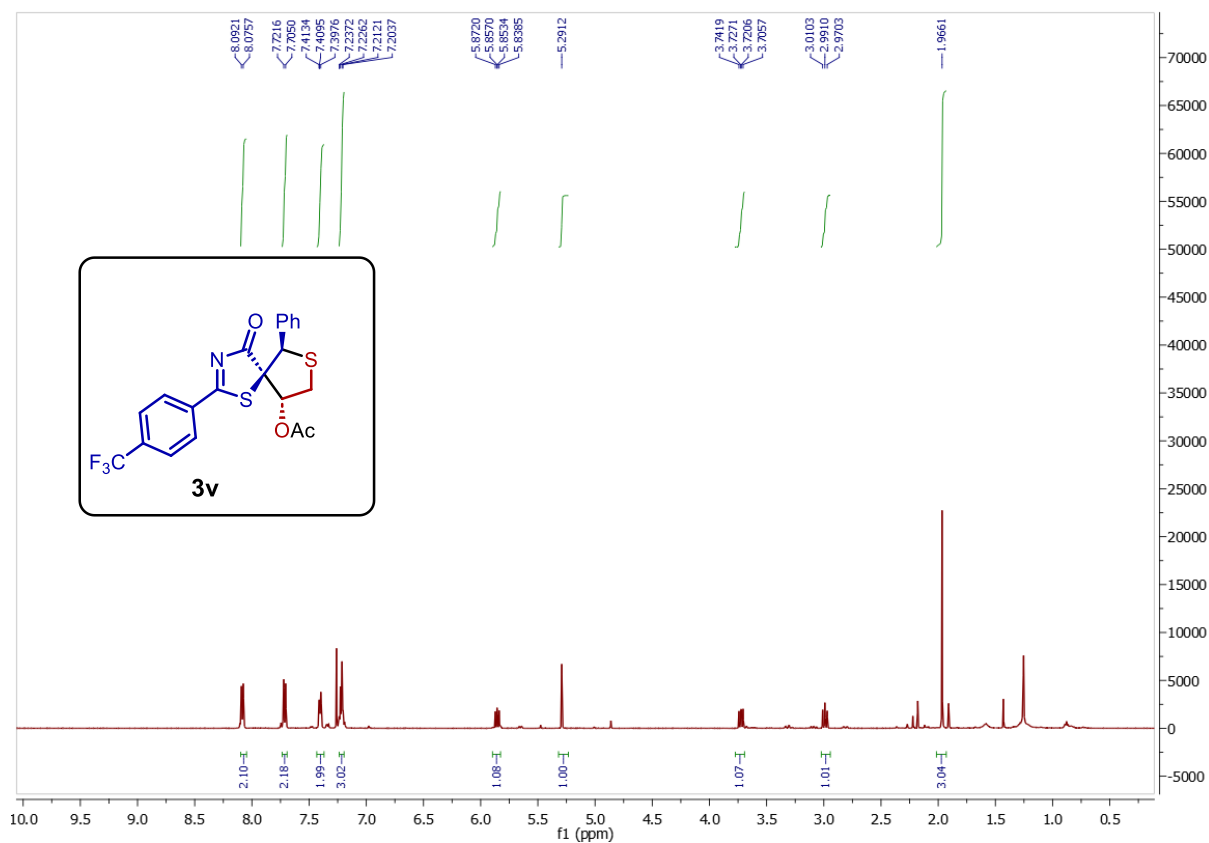
500 MHz ^1H NMR and 125 MHz ^{13}C NMR Spectra of **3s**



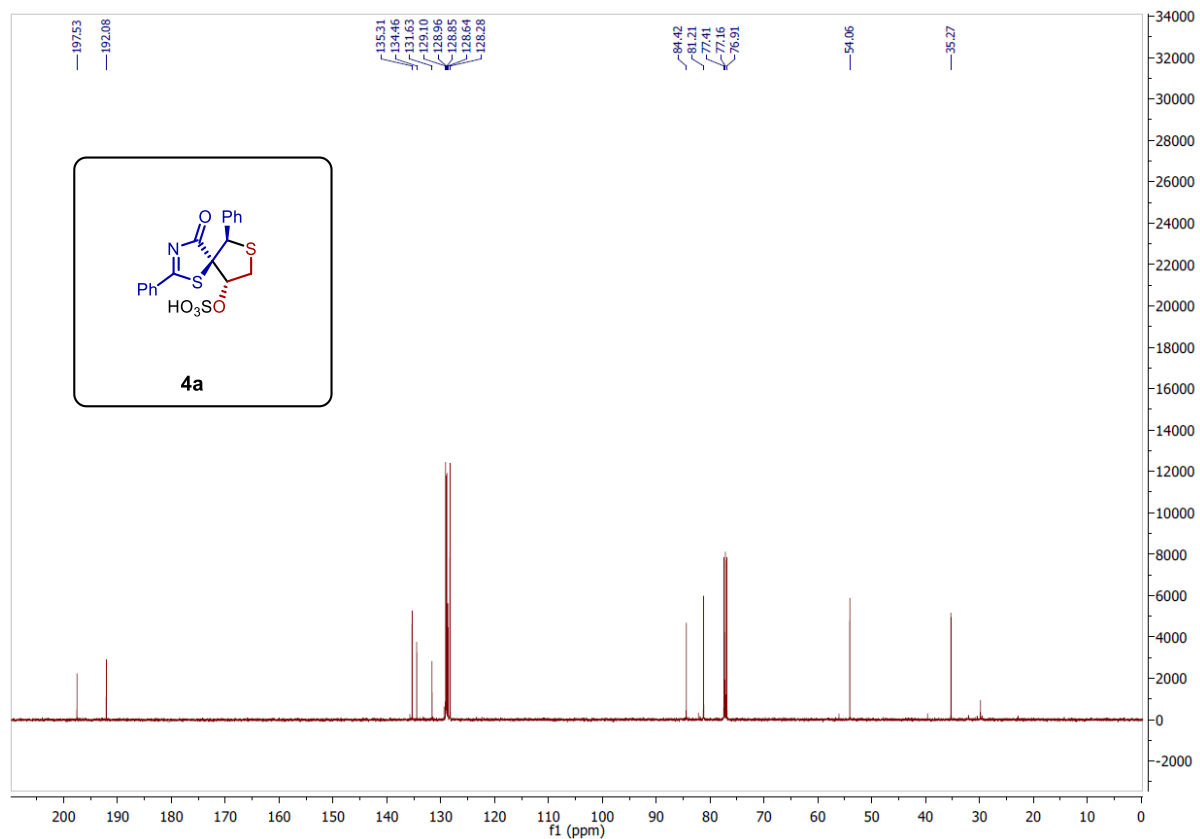
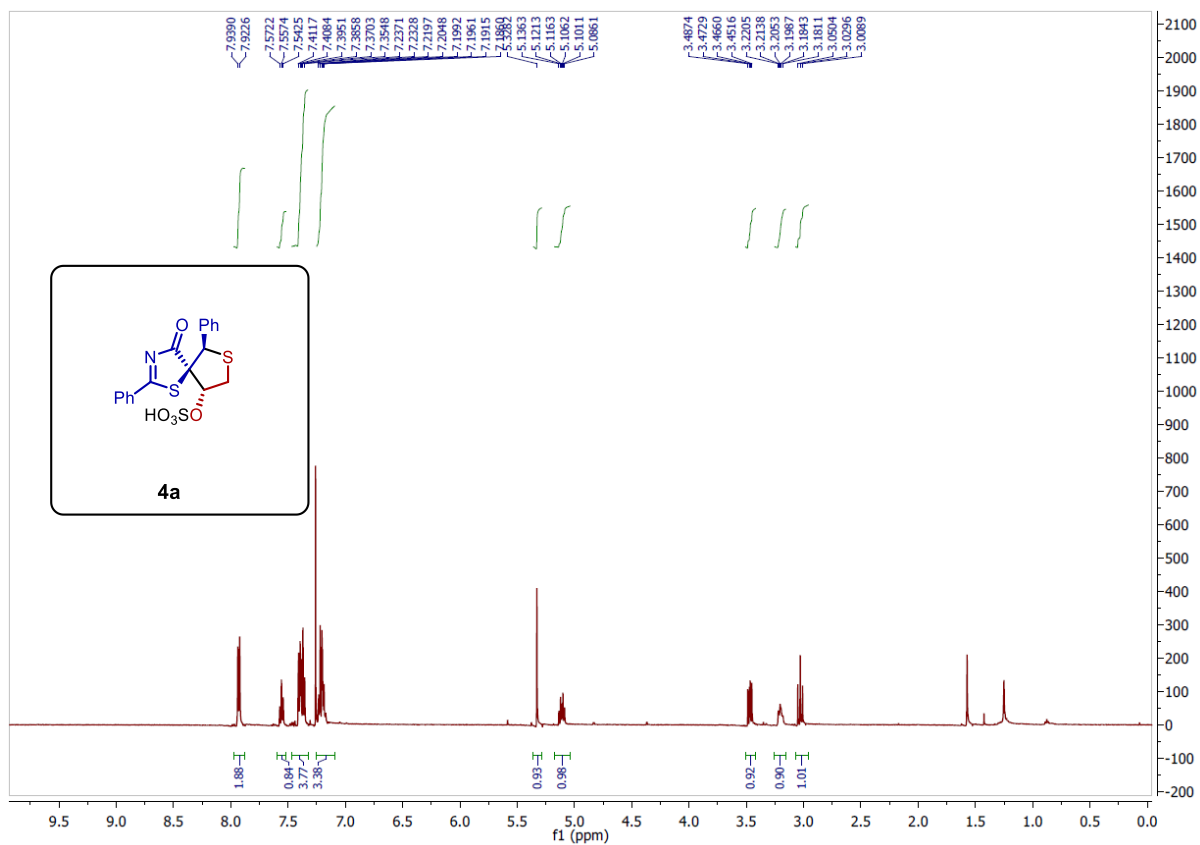
500 MHz ^1H NMR and 125 MHz ^{13}C NMR Spectra of **3t**



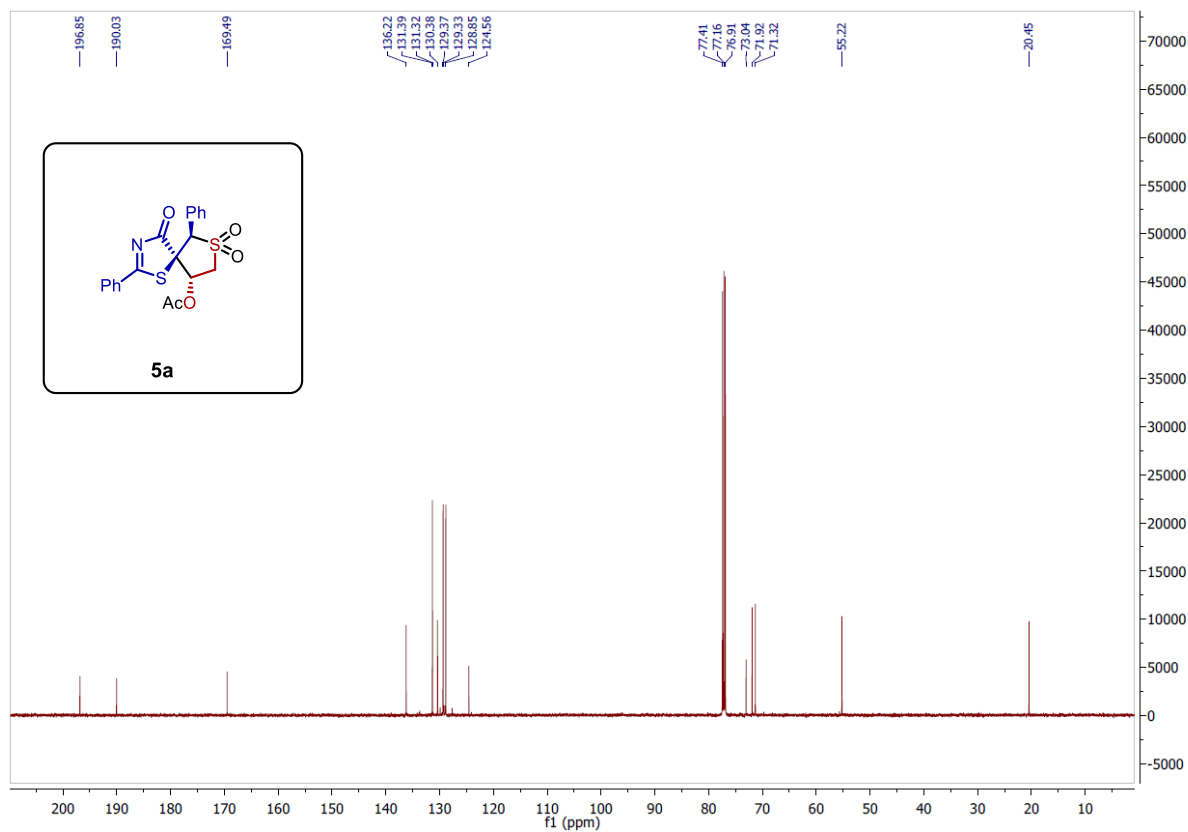
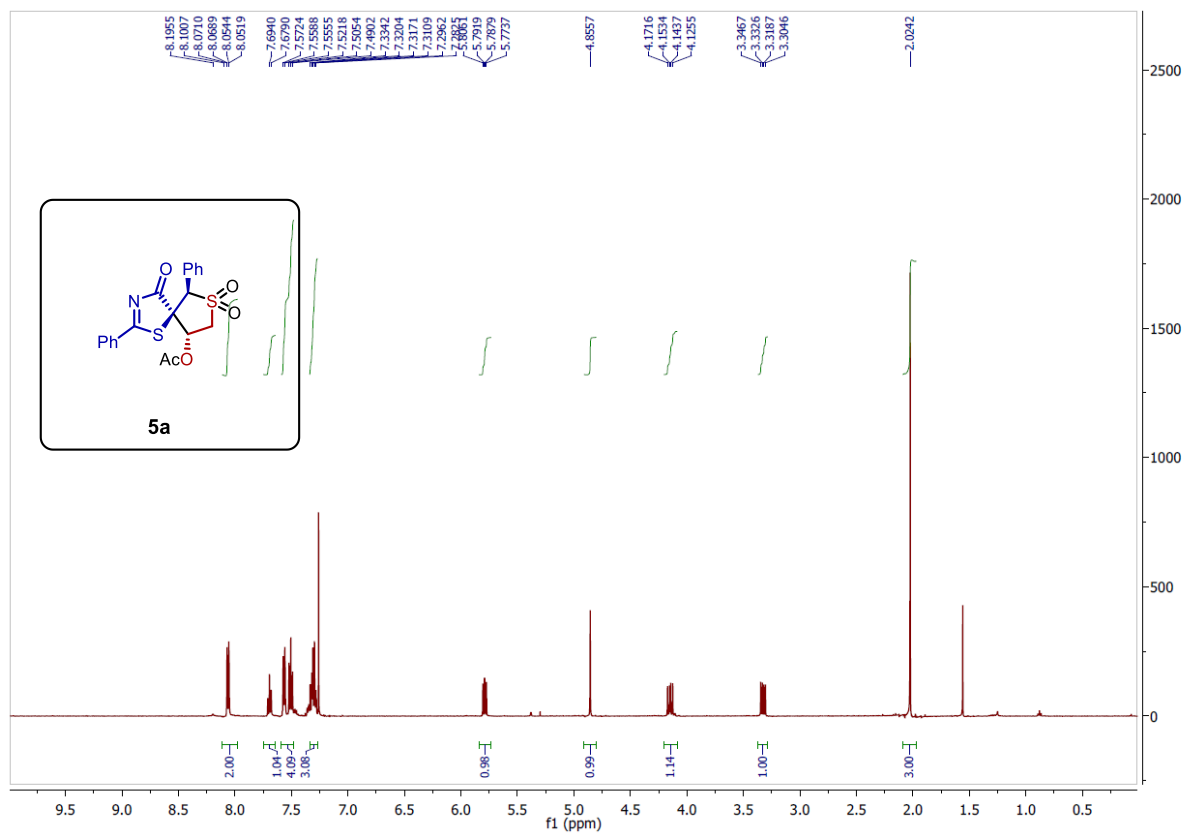
500 MHz ¹H NMR and 125 MHz ¹³C NMR Spectra of **3u**



500 MHz ¹H NMR and 125 MHz ¹³C NMR Spectra of **3v**

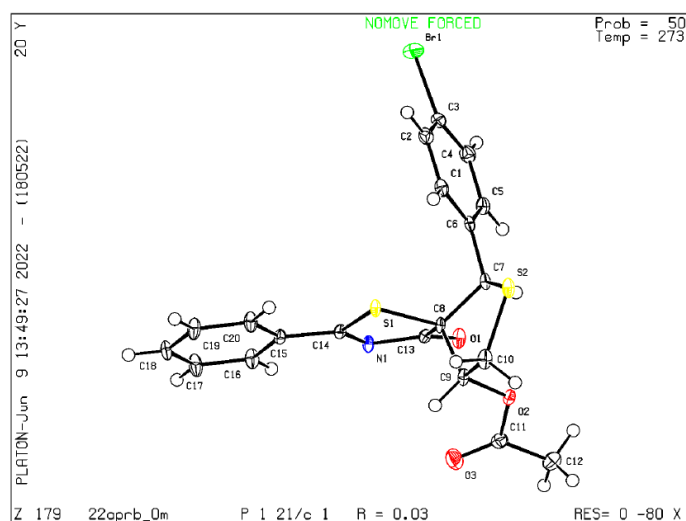


500 MHz ^1H NMR and 125 MHz ^{13}C NMR Spectra of **4a**



500 MHz ^1H NMR and 125 MHz ^{13}C NMR Spectra of **5a**

8. X-ray crystals structure of 3f



ORTEP Diagram of **3f** (CCDC 2178469)

Table S3: Crystal data and structure refinement for **3f**

Identification code	3f
Empirical formula	$C_{20}H_{16}BrNO_3S_2$
Formula weight	462.37
Temperature/K	273.15
Crystal system	monoclinic
Space group	$P2_1/c$
$a/\text{\AA}$	14.0219(3)
$b/\text{\AA}$	7.5128(2)
$c/\text{\AA}$	19.5632(5)
$\alpha/^\circ$	90
$\beta/^\circ$	110.9260(10)
$\gamma/^\circ$	90
Volume/ \AA^3	1924.93(8)
Z	4
$\rho_{\text{calc}}/\text{g cm}^{-3}$	1.595
μ/mm^{-1}	2.373
F(000)	936.0
Crystal size/ mm^3	$0.6 \times 0.3 \times 0.2$
Radiation	MoK α ($\lambda = 0.71073$)
2Θ range for data collection/ $^\circ$	5.864 to 56.614
Index ranges	$-18 \leq h \leq 18, -10 \leq k \leq 10, -26 \leq l \leq 26$
Reflections collected	30510
Independent reflections	4772 [$R_{\text{int}} = 0.0470, R_{\text{sigma}} = 0.0294$]
Data/restraints/parameters	4772/0/245
Goodness-of-fit on F^2	1.087
Final R indexes [$I \geq 2\sigma(I)$]	$R_1 = 0.0287, wR_2 = 0.0707$
Final R indexes [all data]	$R_1 = 0.0344, wR_2 = 0.0738$
Largest diff. peak/hole / $e \text{\AA}^{-3}$	0.33/-0.91

9. Bio-study of spirothiazolono-THTs

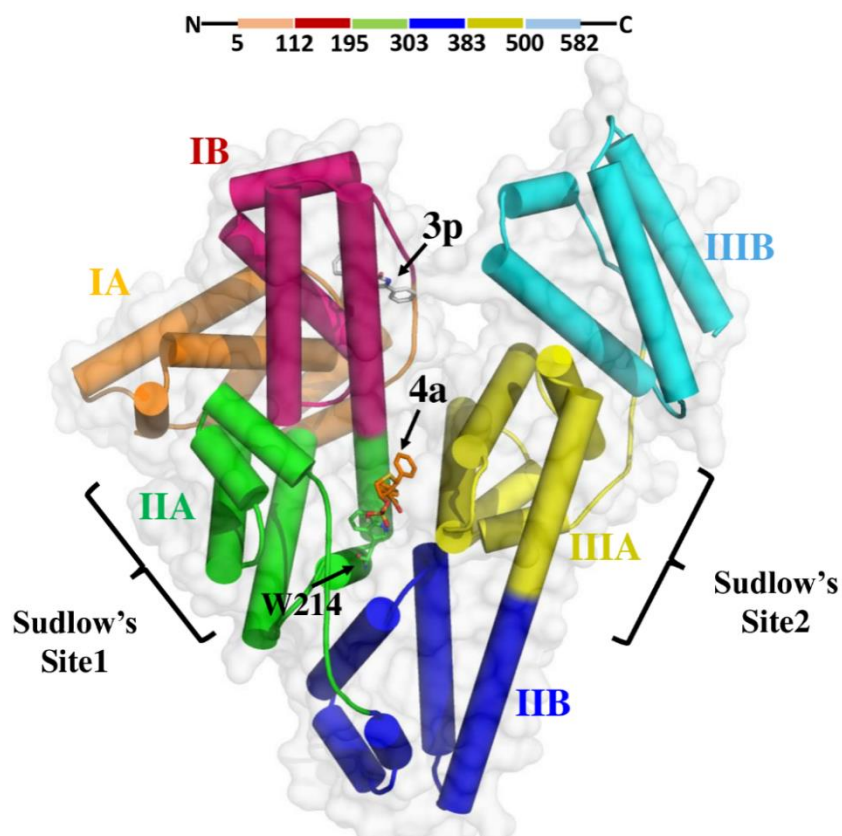


Figure S1: The differentially colour coded 2D domain organization and the 3D structural disposition of previously identified exogenous and endogenous ligand binding sites of HSA with demarcation of two classical drug binding sites (Sudlow's sites). The relative positions of the sTTHT derivative (3p and 4a) binding sites and the position of the tryptophan 214 (W-214) residues have been indicated by black arrows.

Table S4: *In silico*-based interaction profile of sTTHT derivatives with HSA

Name of sTTHT derivative	Calculated Free Energy of Binding (Kcal/Mol)	Predicted Binding affinity to HAS (pKD)
3a	-8.0	3.94
3b	-7.1	4.31
3c	-7.3	4.75
3d	-8.1	4.42
3e	-5.9	4.72
3f	-7.0	3.48
3g	-7.9	4.28
3h	-7.3	4.86
3i	-8.2	4.57
3j	-7.0	4.19
3k	-7.7	4.64
3l	-7.9	5.86
3m	-7.3	4.69
3n	-7.9	4.13
3o	-7.1	4.27
3p	-9.5	5.49
3q	-8.3	4.37
3r	-7.3	4.79
3s	-8.3	4.93
3t	-7.9	4.48
3u	-7.5	4.37
4a	-8.6	4.39
5a	-7.4	4.32

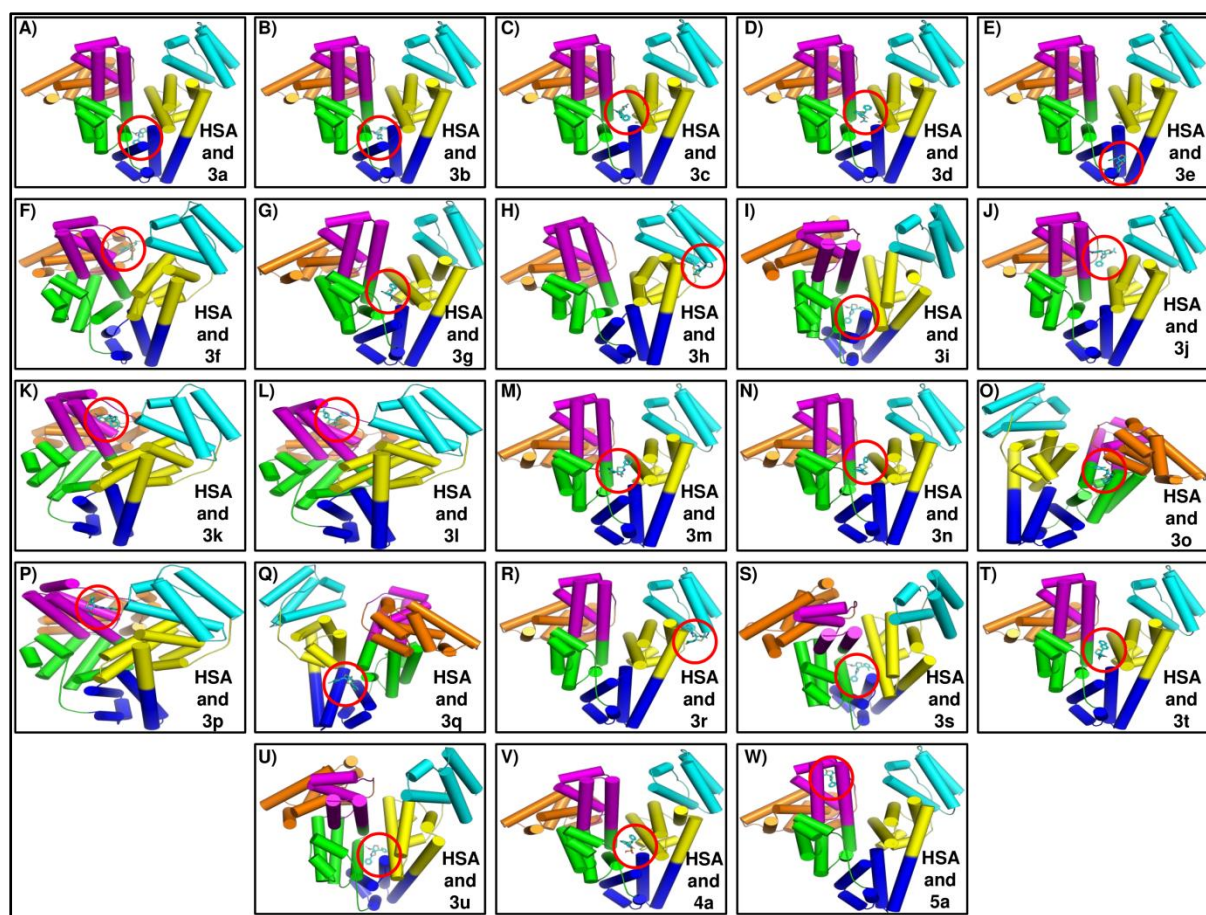


Figure S2: Docked conformation of all the synthesized sTTHT ligands with HSA protein. In each figures the best pose of the docked conformation for the respective ligand is shown in red circle. HSA domains and drug binding sites are same as (colour coded and labelled) indicated in the Figure S1.

Materials and Methods

Molecular docking study and affinity prediction:

Chemdraw from PerkinElmer Informatics was used to generate the two dimensional structures of the all the sTTHT derivatives.² 2D structures were converted into 3D SDF format using Open Babel software.³ Further these ligands were converted into PDB followed by conversion into PDBQT format by using PyMol⁴ and AutoDock Tools 1.5.6.⁵ The HSA protein 3D structure (PDB ID: 1AO6)⁶ was downloaded from Protein data bank RCSB website.⁷ Associated ligands and water molecules were removed using PyMol. The Autodock vina and AutoDock Tools 1.5.7 was used for molecular docking and protein preparation respectively for docking, by addition of Kollman charges and polar hydrogens and saved in PDBQT format. In order to perform blind docking grid box was prepared to cover up whole protein, box size of 1Å with spacing 78x70x82 Å. Post docking, the binding affinity was calculated using the deep learning tool Kdeep⁸ for best pose of the ligands out of nine possible

binding sites. The interaction profile of ligand with protein and binding poses were analyzed by using PyMol and Ligplot.⁹

All atomistic Molecular Dynamics Simulation study

To study the stability of the bound sTTHT ligands with HSA protein we have performed the all-atomistic molecular dynamic simulation (MD simulation) study. Apo- HSA and HSA docked with sTTHT derivatives (**3p** and **4a**) were simulated to understand their relative stability along with the receptor protein (HSA) under the physiologically simulated conditions. All the MD simulation was performed using NAMD 2.14 software.¹⁰ VMD (visual Molecular Dynamics) was used for protein and ligand preparation and results analysis.¹¹ Best pose of the ligand, post docking study by Autodock Tools and protein PDBQT format was used as a complex for simulation file preparation. CHARMM-GUI^{12,13} and its ligand and modeler tools¹³ were used to generate force field and topology files of ligands. The ligand and protein structure complex were solvated with a boundary of 5 Å cubic cell and Langevin dynamics were applied to generate an isothermal –isobaric ensemble environment for simulation. The simulation was performed for 30 ns with a 2 femto second (fs) time step per cycle. The energy minimization of the system was done for 1000 steps and the steps for dcd, xst, and restart frequency were set to 5000 steps and output energy to 50 steps. To study the change in conformation of the alone protein and protein with ligands RMSD profile was analyzed using VMD tools. The data was plotted using origin software.¹⁴

Fluorescence Quenching:

For the fluorescence assay to probe sTTHT interaction with HSA, the purified defatted HSA was procured from Sigma Aldrich and further subjected to gel-filtration chromatography, the peak fraction was collected and analyzed by SDS-PAGE before the commencement of the fluorescence based interaction studies. To validate the *in silico* results of the interaction of sTTHT ligands with the HSA we have performed the *in vitro* fluorescence based titration assay using spectrofluorometer (JASCO FP8300). 150 μM stock solution of purified HSA was prepared in 1X PBS (Phosphate Buffered Saline) (pH 7.4) and its final concentration in the reaction mixture was kept 0.5 μM in all experimental setups. The constant amount of HSA was titrated with increasing concentrations of test sTTHT ligands (derivative **3p** and **4a**). First of all, both the ligands were dissolved in 100% DMSO and final concentration of DMSO in final reaction mixture was kept 1% by diluting with 1X PBS. Varying ligand concentration like 1 μM, 2 μM, 5 μM, 7.5 μM, 10 μM, 12.5 μM, 15 μM and 20 μM were used to titrate the fixed concentration of the purified HSA (0.5 μM). Final reaction mixture contains HSA, varying concentration of ligands, 1% DMSO and 1X PBS up to 3 mL. The reaction mixtures were incubated at room temperature for 20 minutes and then the fluorescence readings were taken. The excitation and emission band width were fixed to 5 nm, the scan speed was 200 nm min⁻¹. The fluorescence emission spectra were recorded from 300 nm to 700 nm while the excitation was fixed at

280 nm. The results of fluorescence spectra were plotted using origin software. The Stern Volmer constants of sTTHT **3p** and sTTHT **4a** binding to HSA have been determined by using the following equations depending on the quenching mechanisms and resulting curves¹⁵

$$\frac{F_0}{F} = 1 + K_{sv}[\text{Ligand}] \text{ (Equation 1: Used for Linear Stern Volmer plot)}$$

$$\frac{F_0}{F} = A e^{K_{sv} [\text{Ligand}]} \text{ (Equation 2: Used for Nonlinear Stern Volmer plot)}$$

In the above-mentioned equations, F and F₀ represent the intrinsic fluorescence intensities of HSA in the absence and the presence of the sTTHT ligands; A is the amplitude and K_{sv} is the Stern Volmer constant.

10. References:

- 1) P. V. Khairnar, Y. H. Su, Y.C. Chen, A. Edukondalu, Y.R. Chen and W. Lin, *Org. Lett.*, 2020, **22**, 6868.
- 2) <https://chemdrawdirect.perkinelmer.cloud/js/sample/index.html>
- 3) N. M. O'Boyle, M. Banck, C. A. James, C. Morley, T. Vandermeersch and G. R. J. Hutchison, *Cheminform.*, 2011, **3**, 33.
- 4) The PyMOL Molecular Graphics System, Version 1.2r3pre, Schrodinger, LLC.
- 5) O. Trott and A. J. Olson, *J. Comput. Chem.*, 2009, **31**, 455.
- 6) S. Sugio, A. Kashima, S. Mochizuki, M. Noda and K. Kobayashi, *Protein Eng.*, 1999, **12**, 439.
- 7) H. M. Berman, J. Westbrook, Z. Feng, G. Gilliland, T. N. Bhat, H. Weissig, I. N. Shindyalov and P. E. Bourne, *Nucleic Acids Res.*, 2000, **28**, 235.
- 8) J. Jimenez, M. Skalic, G. Martinez-Rosell and G. De Fabritiis, *J Chem Inf Model.*, 2018, **58**, 287.
- 9) R. A. Laskowski and M. B. Swindells, *J Chem Inf Model.*, 2011, **51**, 2778.
- 10) J. C. Phillips, D. J. Hardy, J. D. C. Maia, J. E. Stone, J. V. Ribeiro, R. C. Bernardi, R. Buch, G. Fiorin, J. Hénin, W. Jiang, R. McGreevy, M. C. R. Melo, B. K. Radak, R. D. Skeel, A. Singharoy, Y. Wang, B. Roux, A. Aksimentiev, Z. Luthey-Schulten, L. V. Kale, K. Schulten, C. Chipot, and E. Tajkhorshid, *J. Chem. Phys.*, 2020, **153**, 044130.
- 11) W. Humphrey, A. Dalke and K. Schulten, *J. Mol. Graph.*, 1996, **14**, 33.
- 12) S. Jo, T. Kim, V. G. Iyer and W. Im, *J. Comput. Chem.*, 2008, **29**, 1859.
- 13) S. Kim, J. Lee, S. Jo, C. L. Brooks, H. S. Lee and W. Im, *J. Comput. Chem.*, 2017, **38**, 1879.
- 14) Origin, Version 2022. OriginLab Corporation, Northampton, MA, USA.
- 15) J. Carvalho, P. Nottelet, J. L. Mergny, J. A. Queiroz, G. F. Salgado and C. Cruz, *Biochimie*, 2017, **135**, 186.